

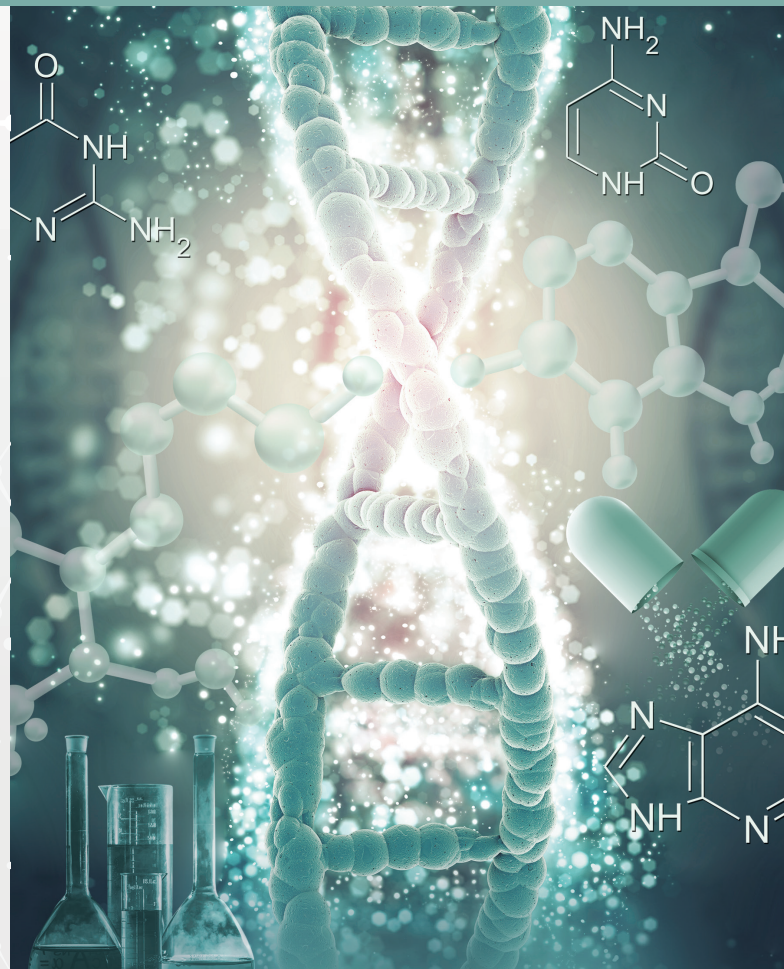
E-ISSN: 2148-6247



# Turkish Journal of PHARMACEUTICAL SCIENCES

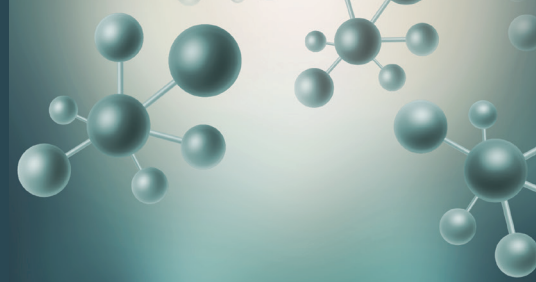
An Official Journal of the Turkish Pharmacists' Association, Academy of Pharmacy

Volume: 20 Issue: 4 August 2023



[www.turkjps.org](http://www.turkjps.org)





# Turkish Journal of PHARMACEUTICAL SCIENCES

## OWNER

Onur Arman ÜNEY on behalf of the Turkish Pharmacists' Association

## Editor-in-Chief

**Prof. İlky Erdoğın Orhan, Ph.D.**

ORCID: <https://orcid.org/0000-0002-7379-5436>

Gazi University, Faculty of Pharmacy, Department of Pharmacognosy, Ankara, TÜRKİYE  
iorhan@gazi.edu.tr

## Associate Editors

**Prof. Bensu Karahaliil, Ph.D.**

ORCID: <https://orcid.org/0000-0003-1625-6337>

Gazi University, Faculty of Pharmacy,  
Department of Pharmaceutical Toxicology, Ankara, TÜRKİYE  
bensu@gazi.edu.tr

**Assoc. Prof. Sinem Aslan Erdem, Ph.D.**

ORCID: <https://orcid.org/0000-0003-1504-1916>

Ankara University, Faculty of Pharmacy, Department of  
Pharmacognosy, Ankara, TÜRKİYE  
saslan@pharmacy.ankara.edu.tr

## Editorial Board

**Prof. Afonso Miguel CAVACO, Ph.D.**

ORCID: [orcid.org/0000-0001-8466-0484](https://orcid.org/0000-0001-8466-0484)

Lisbon University, Faculty of Pharmacy, Department  
of Pharmacy, Pharmacology and Health Technologies,  
Lisboa, PORTUGAL  
acavaco@campus.ul.pt

**Prof. Bezhan CHANKVETADZE, Ph.D.**

ORCID: [orcid.org/0000-0003-2379-9815](https://orcid.org/0000-0003-2379-9815)

Ivane Javakhishvili Tbilisi State University, Institute of  
Physical and Analytical Chemistry, Tbilisi, GEORGIA  
jpb\_a\_bezhan@yahoo.com

**Prof. Blanca LAFFON, Ph.D.**

ORCID: [orcid.org/0000-0001-7649-2599](https://orcid.org/0000-0001-7649-2599)

DICOMOSA group, Advanced Scientific Research  
Center (CICA), Department of Psychology, Area  
Psychobiology, University of A Coruña, Central  
Services of Research Building (ESCI), Campus Elviña  
s/n, A Coruña, SPAIN  
blanca.laffon@udc.es

**Prof. Christine LAFFORGUE, Ph.D.**

ORCID: [orcid.org/0000-0001-7798-2565](https://orcid.org/0000-0001-7798-2565)

Paris Saclay University, Faculty of Pharmacy,  
Department of Dermopharmacology and  
Cosmetology, Paris, FRANCE  
christine.lafforgue@universite-paris-saclay.fr

**Prof. Dietmar FUCHS, Ph.D.**

ORCID: [orcid.org/0000-0003-1627-9563](https://orcid.org/0000-0003-1627-9563)

Innsbruck Medical University, Center for Chemistry  
and Biomedicine, Institute of Biological Chemistry,  
Biocenter, Innsbruck, AUSTRIA  
dietmar.fuchs@i-med.ac.at

**Prof. Francesco EPIFANO, Ph.D.**

ORCID: [0000-0002-0381-7812](https://orcid.org/0000-0002-0381-7812)

Università degli Studi G. d'Annunzio Chieti e Pescara,  
Chieti CH, ITALY  
francesco.epifano@unich.it

**Prof. Fernanda BORGES, Ph.D.**

ORCID: [orcid.org/0000-0003-1050-2402](https://orcid.org/0000-0003-1050-2402)

Porto University, Faculty of Sciences, Department of  
Chemistry and Biochemistry, Porto, PORTUGAL  
fborges@fc.up.pt

**Prof. Göksel ŞENER, Ph.D.**

ORCID: [orcid.org/0000-0001-7444-6193](https://orcid.org/0000-0001-7444-6193)

Fenerbahçe University, Faculty of Pharmacy,  
Department of Pharmacology, İstanbul, TÜRKİYE  
gsener@marmara.edu.tr

**Prof. Gülbin ÖZÇELİKAY, Ph.D.**

ORCID: [orcid.org/0000-0002-1580-5050](https://orcid.org/0000-0002-1580-5050)

Ankara University, Faculty of Pharmacy, Department  
of Pharmacy Management, Ankara, TÜRKİYE  
gozcelikay@ankara.edu.tr

**Prof. Hermann BOLT, Ph.D.**

ORCID: [orcid.org/0000-0002-5271-5871](https://orcid.org/0000-0002-5271-5871)

Dortmund University, Leibniz Research Centre, Institute  
of Occupational Physiology, Dortmund, GERMANY  
bolt@ifado.de

**Prof. Hildebert WAGNER, Ph.D.**

Ludwig-Maximilians University, Center for  
Pharmaceutical Research, Institute of Pharmacy,  
Munich, GERMANY  
H.Wagner@cup.uni-muenchen.de

**Prof. İ İrem ÇANKAYA, Ph.D.**

ORCID: [orcid.org/0000-0001-8531-9130](https://orcid.org/0000-0001-8531-9130)

Hacettepe University, Faculty of Pharmacy, Department  
of Pharmaceutical Botany, Ankara, TÜRKİYE  
itatli@hacettepe.edu.tr

**Prof. K. Arzum ERDEM GÜRSAN, Ph.D.**

ORCID: [orcid.org/0000-0002-4375-8386](https://orcid.org/0000-0002-4375-8386)

Ege University, Faculty of Pharmacy, Department of  
Analytical Chemistry, İzmir, TÜRKİYE  
arzum.erdem@ege.edu.tr

**Prof. Bambang KUSWANDI, Ph.D.**

ORCID: [0000-0002-1983-6110](https://orcid.org/0000-0002-1983-6110)

Chemo and Biosensors Group, Faculty of Pharmacy  
University of Jember, East Java, INDONESIA  
b\_kuswandi.farmasi@unej.ac.id

**Prof. Luciano SASO, Ph.D.**

ORCID: [orcid.org/0000-0003-4530-8706](https://orcid.org/0000-0003-4530-8706)

Sapienze University, Faculty of Pharmacy  
and Medicine, Department of Physiology and  
Pharmacology "Vittorio Erspamer", Rome, ITALY  
luciano.saso@uniroma1.it

**Prof. Maarten J. POSTMA, Ph.D.**

ORCID: [orcid.org/0000-0002-6306-3653](https://orcid.org/0000-0002-6306-3653)

University of Groningen (Netherlands), Department  
of Pharmacy, Unit of Pharmacoepidemiology &  
Pharmacoeconomics, Groningen, HOLLAND  
m.j.postma@rug.nl

**Prof. Meriç KÖKSAL AKKOÇ, Ph.D.**

ORCID: [orcid.org/0000-0001-7662-9364](https://orcid.org/0000-0001-7662-9364)

Yeditepe University, Faculty of Pharmacy, Department  
of Pharmaceutical Chemistry, İstanbul, TÜRKİYE  
merickoksal@yeditepe.edu.tr

**Prof. Mesut SANCAR, Ph.D.**

ORCID: [orcid.org/0000-0002-7445-3235](https://orcid.org/0000-0002-7445-3235)

Marmara University, Faculty of Pharmacy, Department  
of Clinical Pharmacy, İstanbul, TÜRKİYE  
mesut.sancar@marmara.edu.tr

**Assoc. Prof. Nadja Cristhina de SOUZA  
PINTO, Ph.D.**

ORCID: [orcid.org/0000-0003-4206-964X](https://orcid.org/0000-0003-4206-964X)

University of São Paulo, Institute of Chemistry, São  
Paulo, BRAZIL  
nadja@iq.usp.br



# Turkish Journal of PHARMACEUTICAL SCIENCES

## **Assoc. Prof. Neslihan AYGÜN KOCABAŞ, Ph.D. E.R.T.**

ORCID: orcid.org/0000-0000-0000-0000  
Total Research & Technology Feluy Zone  
Industrielle Feluy, Refining & Chemicals, Strategy  
– Development - Research, Toxicology Manager,  
Seneffe, BELGIUM  
neslihan.aygun.kocabas@total.com

## **Prof. Rob VERPOORTE, Ph.D.**

ORCID: orcid.org/0000-0001-6180-1424  
Leiden University, Natural Products Laboratory,  
Leiden, NETHERLANDS  
verpoort@chem.leidenuniv.nl

## **Prof. Robert RAPOPORT, Ph.D.**

ORCID: orcid.org/0000-0001-8554-1014  
Cincinnati University, Faculty of Pharmacy,  
Department of Pharmacology and Cell Biophysics,  
Cincinnati, USA  
robertrapoport@gmail.com

## **Prof. Tayfun UZBAY, Ph.D.**

ORCID: orcid.org/0000-0002-9784-5637  
Üsküdar University, Faculty of Medicine,  
Department of Medical Pharmacology, Istanbul,  
TÜRKİYE  
tayfun.uzbay@uskudar.edu.tr

## **Prof. Wolfgang SADEE, Ph.D.**

ORCID: orcid.org/0000-0003-1894-6374  
Ohio State University, Center for Pharmacogenomics, Ohio,  
USA  
wolfgang.sadee@osumc.edu

## **Douglas Siqueira de Almeida Chaves, Ph.D.**

Federal Rural University of Rio de Janeiro,  
Department of Pharmaceutical Sciences, Rio de  
Janeiro, BRAZIL  
ORCID: 0000-0002-0571-9538

## Advisory Board

## **Prof. Yusuf ÖZTÜRK, Ph.D.**

Anadolu University, Faculty of Pharmacy,  
Department of Pharmacology, Eskişehir, TÜRKİYE  
ORCID: 0000-0002-9488-0891

## **Prof. Tayfun UZBAY, Ph.D.**

Üsküdar University, Faculty of Medicine,  
Department of Medical Pharmacology, Istanbul,  
TÜRKİYE  
ORCID: orcid.org/0000-0002-9784-5637

## **Prof. K. Hüsnü Can BAŞER, Ph.D.**

Anadolu University, Faculty of Pharmacy,  
Department of Pharmacognosy, Eskişehir, TÜRKİYE  
ORCID: 0000-0003-2710-0231

## **Prof. Erdem YEŞİLADA, Ph.D.**

Yeditepe University, Faculty of Pharmacy,  
Department of Pharmacognosy, Istanbul, TÜRKİYE  
ORCID: 0000-0002-1348-6033

## **Prof. Yılmaz ÇAPAN, Ph.D.**

Hacettepe University, Faculty of Pharmacy,  
Department of Pharmaceutical Technology, Ankara,  
TÜRKİYE  
ORCID: 0000-0003-1234-9018

## **Prof. Sibel A. ÖZKAN, Ph.D.**

Ankara University, Faculty of Pharmacy,  
Department of Analytical Chemistry, Ankara,  
TÜRKİYE  
ORCID: 0000-0001-7494-3077

## **Prof. Ekrem SEZİK, Ph.D.**

Istanbul Health and Technology University, Faculty  
of Pharmacy, Department of Pharmacognosy,  
Istanbul, TÜRKİYE  
ORCID: 0000-0002-8284-0948

## **Prof. Gönül ŞAHİN, Ph.D.**

Eastern Mediterranean University, Faculty of  
Pharmacy, Department of Pharmaceutical  
Toxicology, Famagusta, CYPRUS  
ORCID: 0000-0003-3742-6841

## **Prof. Sevda ŞENEL, Ph.D.**

Hacettepe University, Faculty of Pharmacy,  
Department of Pharmaceutical Technology, Ankara,  
TÜRKİYE  
ORCID: 0000-0002-1467-3471

## **Prof. Sevim ROLLAS, Ph.D.**

Marmara University, Faculty of Pharmacy,  
Department of Pharmaceutical Chemistry, Istanbul,  
TÜRKİYE  
ORCID: 0000-0002-4144-6952

## **Prof. Göksel ŞENER, Ph.D.**

Fenerbahçe University, Faculty of Pharmacy,  
Department of Pharmacology, Istanbul, TÜRKİYE  
ORCID: 0000-0001-7444-6193

## **Prof. Erdal BEDİR, Ph.D.**

İzmir Institute of Technology, Department of  
Bioengineering, İzmir, TÜRKİYE  
ORCID: 0000-0003-1262-063X

## **Prof. Nurşen BAŞARAN, Ph.D.**

Hacettepe University, Faculty of Pharmacy,  
Department of Pharmaceutical Toxicology, Ankara,  
TÜRKİYE  
ORCID: 0000-0001-8581-8933

## **Prof. Bensu KARAHALİL, Ph.D.**

Gazi University, Faculty of Pharmacy, Department  
of Pharmaceutical Toxicology, Ankara, TÜRKİYE  
ORCID: 0000-0003-1625-6337

## **Prof. Betül DEMİRCİ, Ph.D.**

Anadolu University, Faculty of Pharmacy,  
Department of Pharmacognosy, Eskişehir, TÜRKİYE  
ORCID: 0000-0003-2343-746X

## **Prof. Bengi USLU, Ph.D.**

Ankara University, Faculty of Pharmacy, Department  
of Analytical Chemistry, Ankara, TÜRKİYE  
ORCID: 0000-0002-7327-4913

## **Prof. Ahmet AYDIN, Ph.D.**

Yeditepe University, Faculty of Pharmacy,  
Department of Pharmaceutical Toxicology, Istanbul,  
TÜRKİYE  
ORCID: 0000-0003-3499-6435

## **Prof. İlkay ERDOĞAN ORHAN, Ph.D.**

Gazi University, Faculty of Pharmacy, Department  
of Pharmacognosy, Ankara, TÜRKİYE  
ORCID: 0000-0002-7379-5436

## **Prof. Ş. Güniz KÜÇÜKGÜZEL, Ph.D.**

Fenerbahçe University Faculty of Pharmacy,  
Department of Pharmaceutical Chemistry, Istanbul,  
TÜRKİYE  
ORCID: 0000-0001-9405-8905

## **Prof. Engin Umut AKKAYA, Ph.D.**

Dalian University of Technology, Department of  
Chemistry, Dalian, CHINA  
ORCID: 0000-0003-4720-7554

## **Prof. Esra AKKOL, Ph.D.**

Gazi University, Faculty of Pharmacy, Department  
of Pharmacognosy, Ankara, TÜRKİYE  
ORCID: 0000-0002-5829-7869

## **Prof. Erem BİLENSOY, Ph.D.**

Hacettepe University, Faculty of Pharmacy,  
Department of Pharmaceutical Technology, Ankara,  
TÜRKİYE  
ORCID: 0000-0003-3911-6388

## **Prof. Uğur TAMER, Ph.D.**

Gazi University, Faculty of Pharmacy, Department  
of Analytical Chemistry, Ankara, TÜRKİYE  
ORCID: 0000-0001-9989-6123

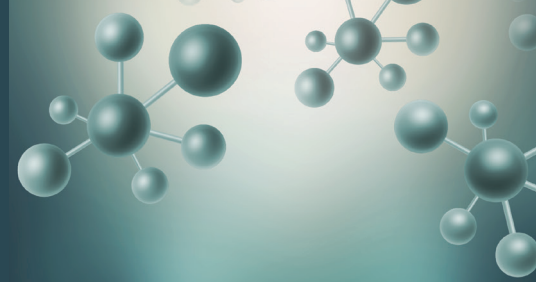
## **Prof. Gülaçtı TOPÇU, Ph.D.**

Bezmialem Vakıf University, Faculty of Pharmacy,  
Department of Pharmacognosy, Istanbul, TÜRKİYE  
ORCID: 0000-0002-7946-6545

## **Prof. Hasan KIRMIZIBEKMEZ, Ph.D.**

Yeditepe University, Faculty of Pharmacy,  
Department of Pharmacognosy, Istanbul, TÜRKİYE  
ORCID: 0000-0002-6118-8225

*\*Members of the Advisory Board consist of the scientists  
who received Science Award presented by TEB Academy  
of Pharmacy in chronological order.*



# Turkish Journal of PHARMACEUTICAL SCIENCES

## AIMS AND SCOPE

The Turkish Journal of Pharmaceutical Sciences is the only scientific periodical publication of the Turkish Pharmacists' Association and has been published since April 2004.

Turkish Journal of Pharmaceutical Sciences journal is regularly published 6 times in a year (February, April, June, August, October, December). The issuing body of the journal is Galenos Yayınevi/Publishing House level. The aim of Turkish Journal of Pharmaceutical Sciences is to publish original research papers of the highest scientific and clinical value at an international level. The target audience includes specialists and professionals in all fields of pharmaceutical sciences.

The editorial policies are based on the "Recommendations for the Conduct, Reporting, Editing, and Publication of Scholarly Work in Medical Journals (ICMJE Recommendations)" by the International Committee of Medical Journal Editors (20, archived at <http://www.icmje.org/>) rules.

### Editorial Independence

Turkish Journal of Pharmaceutical Sciences is an independent journal with independent editors and principles and has no commercial relationship with the commercial product, drug or pharmaceutical company regarding decisions and review processes upon articles.

### ABSTRACTED/INDEXED IN

PubMed  
PubMed Central  
Web of Science-Emerging Sources Citation Index (ESCI)  
SCOPUS SJR  
TÜBİTAK/ULAKBİM TR Dizin  
ProQuest  
Chemical Abstracts Service (CAS)  
EBSCO  
EMBASE  
GALE  
Analytical Abstracts  
International Pharmaceutical Abstracts (IPA)  
Medicinal & Aromatic Plants Abstracts (MAPA)  
British Library  
CSIR INDIA  
GOALI  
Hinari  
OARE  
ARDI  
AGORA  
Türkiye Atıf Dizini  
Türk Medline  
UDL-EDGE  
J- Gate  
Idealonline  
CABI

### OPEN ACCESS POLICY

This journal provides immediate open access to its content on the principle that making research freely available to the public supports a greater global exchange of knowledge.

Open Access Policy is based on the rules of the Budapest Open Access Initiative (BOAI) <http://www.budapestopenaccessinitiative.org/>. By "open access" to peer-reviewed research literature, we mean its free availability on the public internet, permitting any users to read, download, copy, distribute, print, search, or link to the full texts of these articles, crawl them for indexing, pass them as data to software, or use them for any other lawful purpose, without financial, legal, or technical barriers other than those inseparable from gaining access to the internet itself. The only constraint on reproduction and distribution, and the only role for copyright in this domain, should be to give authors control over the integrity of their work and the right to be properly acknowledged and cited.

### CORRESPONDENCE ADDRESS

All correspondence should be directed to the Turkish Journal of Pharmaceutical Sciences Editorial Board

Post Address: Turkish Pharmacists' Association, Mustafa Kemal Mah 2147.Sok No:3 06510 Çankaya/Ankara, TÜRKİYE  
Phone: +90 (312) 409 81 00  
Fax: +90 (312) 409 81 09  
Web Page: <http://turkjps.org>  
E-mail: [turkjps@gmail.com](mailto:turkjps@gmail.com)

### PERMISSIONS

Requests for permission to reproduce published material should be sent to the publisher.

Publisher: Erkan Mor  
Address: Molla Gürani Mah. Kaçamak Sok. 21/1 Fındıkzade, Fatih, İstanbul, Türkiye  
Phone: +90 212 621 99 25  
Fax: +90 212 621 99 27  
Web page: <http://www.galenos.com.tr/en>  
E-mail: [info@galenos.com.tr](mailto:info@galenos.com.tr)

### ISSUING BODY CORRESPONDING ADDRESS

Issuing Body : Galenos Yayınevi  
Address: Molla Gürani Mah. Kaçamak Sk. No: 21/, 34093 İstanbul, Türkiye  
Phone: +90 212 621 99 25 Fax: +90 212 621 99 27  
E-mail: [info@galenos.com.tr](mailto:info@galenos.com.tr)

### MATERIAL DISCLAIMER

The author(s) is (are) responsible for the articles published in the JOURNAL. The editors, editorial board and publisher do not accept any responsibility for the articles.

This work is licensed under a Creative Commons Attribution-NonCommercial-NoDerivatives 4.0 International License.



#### Publisher Contact

Address: Molla Gürani Mah. Kaçamak Sk. No: 21/1  
34093 İstanbul, Türkiye  
Phone: +90 (530) 177 30 97  
E-mail: [info@galenos.com.tr](mailto:info@galenos.com.tr)/[yayin@galenos.com.tr](mailto:yayin@galenos.com.tr)  
Web: [www.galenos.com.tr](http://www.galenos.com.tr) | Publisher Certificate Number: 14521

Publication Date: August 2023

E-ISSN: 2148-6247

International scientific journal published bimonthly.



# Turkish Journal of PHARMACEUTICAL SCIENCES

## INSTRUCTIONS TO AUTHORS

Turkish Journal of Pharmaceutical Sciences journal is published 6 times (February, April, June, August, October, December) per year and publishes the following articles:

- Research articles
- Reviews (only upon the request or consent of the Editorial Board)
- Preliminary results/Short communications/Technical notes/Letters to the Editor in every field of pharmaceutical sciences.

The publication language of the journal is English.

The Turkish Journal of Pharmaceutical Sciences does not charge any article submission or processing charges.

A manuscript will be considered only with the understanding that it is an original contribution that has not been published elsewhere.

The Journal should be abbreviated as "Turk J Pharm Sci" when referenced.

The scientific and ethical liability of the manuscripts belongs to the authors and the copyright of the manuscripts belongs to the Journal. Authors are responsible for the contents of the manuscript and accuracy of the references. All manuscripts submitted for publication must be accompanied by the Copyright Transfer Form [copyright transfer]. Once this form, signed by all the authors, has been submitted, it is understood that neither the manuscript nor the data it contains have been submitted elsewhere or previously published and authors declare the statement of scientific contributions and responsibilities of all authors.

Experimental, clinical and drug studies requiring approval by an ethics committee must be submitted to the JOURNAL with an ethics committee approval report including approval number confirming that the study was conducted in accordance with international agreements and the Declaration of Helsinki (revised 2013) (<http://www.wma.net/en/30publications/10policies/b3/>). The approval of the ethics committee and the fact that informed consent was given by the patients should be indicated in the Materials and Methods section. In experimental animal studies, the authors should indicate that the procedures followed were in accordance with animal rights as per the Guide for the Care and Use of Laboratory Animals (<http://oacu.od.nih.gov/regs/guide/guide.pdf>) and they should obtain animal ethics committee approval.

Authors must provide disclosure/acknowledgment of financial or material support, if any was received, for the current study.

If the article includes any direct or indirect commercial links or if any institution provided material support to the study, authors must state in the cover letter that they have no relationship with the commercial product, drug, pharmaceutical company, etc. concerned; or specify the type of relationship (consultant, other agreements), if any.

Authors must provide a statement on the absence of conflicts of interest among the authors and provide authorship contributions.

All manuscripts submitted to the journal are screened for plagiarism using the 'iThenticate' software. Results indicating plagiarism may result in manuscripts being returned or rejected.

### The Review Process

This is an independent international journal based on double-blind peer-review principles. The manuscript is assigned to the Editor-

in-Chief, who reviews the manuscript and makes an initial decision based on manuscript quality and editorial priorities. Manuscripts that pass initial evaluation are sent for external peer review, and the Editor-in-Chief assigns an Associate Editor. The Associate Editor sends the manuscript to at least two reviewers (internal and/or external reviewers). The Associate Editor recommends a decision based on the reviewers' recommendations and returns the manuscript to the Editor-in-Chief. The Editor-in-Chief makes a final decision based on editorial priorities, manuscript quality, and reviewer recommendations. If there are any conflicting recommendations from reviewers, the Editor-in-Chief can assign a new reviewer.

The scientific board guiding the selection of the papers to be published in the Journal consists of elected experts of the Journal and if necessary, selected from national and international authorities. The Editor-in-Chief, Associate Editors may make minor corrections to accepted manuscripts that do not change the main text of the paper.

In case of any suspicion or claim regarding scientific shortcomings or ethical infringement, the Journal reserves the right to submit the manuscript to the supporting institutions or other authorities for investigation. The Journal accepts the responsibility of initiating action but does not undertake any responsibility for an actual investigation or any power of decision.

The Editorial Policies and General Guidelines for manuscript preparation specified below are based on "Recommendations for the Conduct, Reporting, Editing, and Publication of Scholarly Work in Medical Journals (ICMJE Recommendations)" by the International Committee of Medical Journal Editors (20, archived at <http://www.icmje.org/>).

Preparation of research articles, systematic reviews and meta-analyses must comply with study design guidelines:

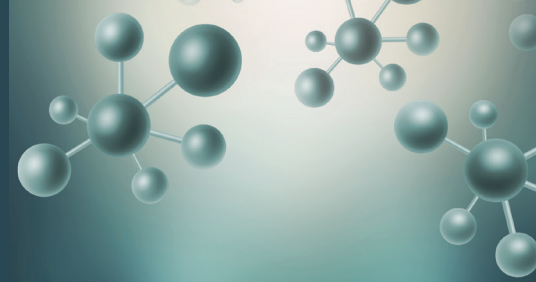
CONSORT statement for randomized controlled trials (Moher D, Schultz KF, Altman D, for the CONSORT Group. The CONSORT statement revised recommendations for improving the quality of reports of parallel group randomized trials. *JAMA* 2001; 285: 1987-91) (<http://www.consort-statement.org/>);

PRISMA statement of preferred reporting items for systematic reviews and meta-analyses (Moher D, Liberati A, Tetzlaff J, Altman DG, The PRISMA Group. Preferred Reporting Items for Systematic Reviews and Meta-Analyses: The PRISMA Statement. *PLoS Med* 2009; 6(7): e1000097.) (<http://www.prisma-statement.org/>);

STARD checklist for the reporting of studies of diagnostic accuracy (Bossuyt PM, Reitsma JB, Bruns DE, Gatsonis CA, Glasziou PP, Irwig LM, et al., for the STARD Group. Towards complete and accurate reporting of studies of diagnostic accuracy: the STARD initiative. *Ann Intern Med* 2003;138:40-4.) (<http://www.stard-statement.org/>);

STROBE statement, a checklist of items that should be included in reports of observational studies (<http://www.strobe-statement.org/>);

MOOSE guidelines for meta-analysis and systemic reviews of observational studies (Stroup DF, Berlin JA, Morton SC, et al. Meta-analysis of observational studies in epidemiology: a proposal for reporting Meta-analysis of observational Studies in Epidemiology (MOOSE) group. *JAMA* 2000; 283: 2008-12).



# Turkish Journal of PHARMACEUTICAL SCIENCES

## INSTRUCTIONS TO AUTHORS

### GENERAL GUIDELINES

Manuscripts can only be submitted electronically through the Journal Agent website (<http://journalagent.com/tjps/>) after creating an account. This system allows online submission and review.

**Format:** Manuscripts should be prepared using Microsoft Word, size A4 with 2.5 cm margins on all sides, 12 pt Arial font and 1.5 line spacing.

**Abbreviations:** Abbreviations should be defined at first mention and used consistently thereafter. Internationally accepted abbreviations should be used; refer to scientific writing guides as necessary.

**Cover letter:** The cover letter should include statements about manuscript type, single-Journal submission affirmation, conflict of interest statement, sources of outside funding, equipment (if applicable), for original research articles.

### ETHICS COMMITTEE APPROVAL

The editorial board and our reviewers systematically ask for ethics committee approval from every research manuscript submitted to the Turkish Journal of Pharmaceutical Sciences. If a submitted manuscript does not have ethical approval, which is necessary for every human or animal experiment as stated in international ethical guidelines, it must be rejected on the first evaluation.

Research involving animals should be conducted with the same rigor as research in humans; the Turkish Journal of Pharmaceutical Sciences asks original approval document to show implements the 3Rs principles. If a study does not have ethics committee approval or authors claim that their study does not need approval, the study is consulted to and evaluated by the editorial board for approval.

### SIMILARITY

The Turkish Journal of Pharmaceutical Sciences is routinely looking for similarity index score from every manuscript submitted before evaluation by the editorial board and reviewers. The journal uses iThenticate plagiarism checker software to verify the originality of written work. There is no acceptable similarity index; but, exceptions are made for similarities less than 15 %.

### REFERENCES

Authors are solely responsible for the accuracy of all references.

**In-text citations:** References should be indicated as a superscript immediately after the period/full stop of the relevant sentence. If the author(s) of a reference is/are indicated at the beginning of the sentence, this reference should be written as a superscript immediately after the author's name. If relevant research has been conducted in Türkiye or by Turkish investigators, these studies should be given priority while citing the literature.

Presentations presented in congresses, unpublished manuscripts, theses, Internet addresses, and personal interviews or experiences should not be indicated as references. If such references are used, they should be indicated in parentheses at the end of the relevant sentence in the text, without reference number and written in full, in order to clarify their nature.

**References section:** References should be numbered consecutively in the order in which they are first mentioned in the text. All authors should be listed regardless of number. The titles of Journals should be abbreviated according to the style used in the Index Medicus.

### Reference Format

**Journal:** Last name(s) of the author(s) and initials, article title, publication title and its original abbreviation, publication date, volume, the inclusive page numbers. Example: Collin JR, Rathbun JE. Involitional entropion: a review with evaluation of a procedure. Arch Ophthalmol. 1978;96:1058-1064.

**Book:** Last name(s) of the author(s) and initials, book title, edition, place of publication, date of publication and inclusive page numbers of the extract cited.

**Example:** Herbert L. The Infectious Diseases (1st ed). Philadelphia; Mosby Harcourt; 1999:11;1-8.

**Book Chapter:** Last name(s) of the author(s) and initials, chapter title, book editors, book title, edition, place of publication, date of publication and inclusive page numbers of the cited piece.

**Example:** O'Brien TP, Green WR. Periocular Infections. In: Feigin RD, Cherry JD, eds. Textbook of Pediatric Infectious Diseases (4th ed). Philadelphia; W.B. Saunders Company;1998:1273-1278.

**Books in which the editor and author are the same person:** Last name(s) of the author(s) and initials, chapter title, book editors, book title, edition, place of publication, date of publication and inclusive page numbers of the cited piece. Example: Solcia E, Capella C, Kloppel G. Tumors of the exocrine pancreas. In: Solcia E, Capella C, Kloppel G, eds. Tumors of the Pancreas. 2nd ed. Washington: Armed Forces Institute of Pathology; 1997:145-210.

### TABLES, GRAPHICS, FIGURES, AND IMAGES

All visual materials together with their legends should be located on separate pages that follow the main text.

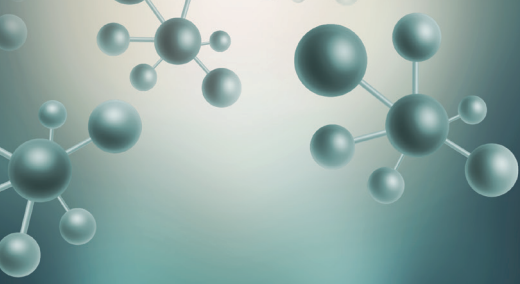
**Images:** Images (pictures) should be numbered and include a brief title. Permission to reproduce pictures that were published elsewhere must be included. All pictures should be of the highest quality possible, in JPEG format, and at a minimum resolution of 300 dpi.

**Tables, Graphics, Figures:** All tables, graphics or figures should be enumerated according to their sequence within the text and a brief descriptive caption should be written. Any abbreviations used should be defined in the accompanying legend. Tables in particular should be explanatory and facilitate readers' understanding of the manuscript, and should not repeat data presented in the main text.

### MANUSCRIPT TYPES

#### Original Articles

Clinical research should comprise clinical observation, new techniques or laboratories studies. Original research articles should include title, structured abstract, key words relevant to the content of the article, introduction, materials and methods, results, discussion, study limitations, conclusion references, tables/figures/images and



# Turkish Journal of PHARMACEUTICAL SCIENCES

## INSTRUCTIONS TO AUTHORS

acknowledgement sections. Title, abstract and key words should be written in both Turkish and English. The manuscript should be formatted in accordance with the above-mentioned guidelines and should not exceed 16 A4 pages.

**Title Page:** This page should include the title of the manuscript, short title, name(s) of the authors and author information. The following descriptions should be stated in the given order:

1. Title of the manuscript (Turkish and English), as concise and explanatory as possible, including no abbreviations, up to 135 characters
2. Short title (Turkish and English), up to 60 characters
3. Name(s) and surname(s) of the author(s) (without abbreviations and academic titles) and affiliations
4. Name, address, e-mail, phone and fax number of the corresponding author
5. The place and date of scientific meeting in which the manuscript was presented and its abstract published in the abstract book, if applicable

**Abstract:** A summary of the manuscript should be written in both Turkish and English. References should not be cited in the abstract. Use of abbreviations should be avoided as much as possible; if any abbreviations are used, they must be taken into consideration independently of the abbreviations used in the text. For original articles, the structured abstract should include the following sub-headings:

**Objectives:** The aim of the study should be clearly stated.

**Materials and Methods:** The study and standard criteria used should be defined; it should also be indicated whether the study is randomized or not, whether it is retrospective or prospective, and the statistical methods applied should be indicated, if applicable.

**Results:** The detailed results of the study should be given and the statistical significance level should be indicated.

**Conclusion:** Should summarize the results of the study, the clinical applicability of the results should be defined, and the favorable and unfavorable aspects should be declared.

**Keywords:** A list of minimum , but no more than 5 key words must follow the abstract. Key words in English should be consistent with "Medical Subject Headings (MESH)" ([www.nlm.nih.gov/mesh/MBrowser.html](http://www.nlm.nih.gov/mesh/MBrowser.html)). Turkish key words should be direct translations of the terms in MESH.

**Original research articles should have the following sections:**

**Introduction:** Should consist of a brief explanation of the topic and indicate the objective of the study, supported by information from the literature.

**Materials and Methods:** The study plan should be clearly described, indicating whether the study is randomized or not, whether it is retrospective or prospective, the number of trials, the characteristics, and the statistical methods used.

**Results:** The results of the study should be stated, with tables/figures given in numerical order; the results should be evaluated according to the statistical analysis methods applied. See General Guidelines for details about the preparation of visual material.

**Discussion:** The study results should be discussed in terms of their favorable and unfavorable aspects and they should be compared with the literature. The conclusion of the study should be highlighted.

**Study Limitations:** Limitations of the study should be discussed. In addition, an evaluation of the implications of the obtained findings/ results for future research should be outlined.

**Conclusion:** The conclusion of the study should be highlighted.

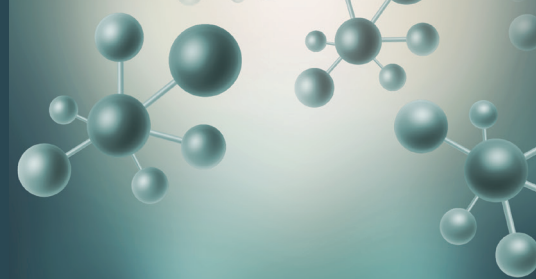
**Acknowledgements:** Any technical or financial support or editorial contributions (statistical analysis, English/Turkish evaluation) towards the study should appear at the end of the article.

**References:** Authors are responsible for the accuracy of the references. See General Guidelines for details about the usage and formatting required.

### Review Articles

Review articles can address any aspect of clinical or laboratory pharmaceuticals. Review articles must provide critical analyses of contemporary evidence and provide directions of or future research. Most review articles are commissioned, but other review submissions are also welcome. Before sending a review, discussion with the editor is recommended.

Reviews articles analyze topics in depth, independently and objectively. The first chapter should include the title in Turkish and English, an unstructured summary and key words. Source of all citations should be indicated. The entire text should not exceed 25 pages (A, formatted as specified above).



## CONTENTS

### Original Articles

- 210 Medication Reconciliation Service in Hospitalized Patients with Infectious Diseases During Coronavirus Disease-2019 Pandemic: An Observational Study  
Cüneyd ENVER, Buket ERTÜRK ŞENGEL, Mesut SANCAR, Volkan KORTEN, Betül OKUYAN
- 218 Validated Stability-Indicating RP-HPLC Method for Daclatasvir in Tablets  
Hemlata M. NIMJE, Smita J. PAWAR, Meenakshi N. DEODHAR
- 226 LC-MS/MS Method Development and Validation for Determination of Favipiravir Pure and Tablet Dosage Forms  
Nandeeshha ITIGIMATH, Hadagali ASHOKA, Basappa C. YALLUR, Manjunatha Devagondanahalli HADAGALI
- 234 Development and Validation of a Spectrofluorimetric Method for the Quantification of Capecitabine in Bulk and Tablets  
Swathi NARAPARAJU, Ambati MUKTI, Durga Panikumar ANUMOLU, Soujanya CHAGANTI
- 240 Role of Chitosan-Loaded Solanine Glycoalkaloid from *Solanum scabrum* Mill. Leaf Extract as Anti-Inflammatory and *In Vitro* Anticancer Agents  
Cletus Anes UKWUBILE, Emmanuel Oise IKPEFAN, Ademola Clement FAMUREWA
- 253 Evaluation of Marketed Rosemary Essential Oils (*Rosmarinus officinalis* L.) in Terms of European Pharmacopoeia 10.0 Criteria  
Timur Hakan BARAK, Elif BÖLÜKBAŞ, Hilal BARDAKCI
- 261 Formulation, Characterization, and Optimization of a Topical Gel Containing Tranexamic Acid to Prevent Superficial Bleeding: *In Vivo* and *In Vitro* Evaluations  
Farideh SHIEHZADEH, Daryosh MOHEBI, Omid CHAVOSHIAN, Sara DANESHMANDI

### Short Communication

- 270 Exploration of Structure-Activity Relationship Using Integrated Structure and Ligand Based Approach: Hydroxamic Acid-Based HDAC Inhibitors and Cytotoxic Agents  
Ekta SHIRBHATE, Jaiprakash PANDEY, Vijay Kumar PATEL, Ravichandran VEERASAMY, Harish RAJAK





# Medication Reconciliation Service in Hospitalized Patients with Infectious Diseases During Coronavirus Disease-2019 Pandemic: An Observational Study

© Cüneyd ENVER<sup>1</sup>, © Buket ERTÜRK ŞENGEL<sup>2</sup>, © Mesut SANCAR<sup>1</sup>, © Volkan KORTEN<sup>2</sup>, © Betül OKUYAN<sup>1\*</sup>

<sup>1</sup>Marmara University, Faculty of Pharmacy, Department of Clinical Pharmacy, İstanbul, Türkiye

<sup>2</sup>Marmara University, Faculty of Medicine, Department of Infectious Diseases and Clinical Microbiology, İstanbul, Türkiye

## ABSTRACT

**Objectives:** To determine the prevalence and type of medication discrepancies and factors associated with unintentional discrepancies and identify the rate of hospital readmission and emergency service visit within 30 days after discharge among hospitalized patients with infectious diseases and receiving clinical pharmacist-led medication reconciliation during the coronavirus disease-2019 (COVID-19) pandemic.

**Materials and Methods:** This observational study was conducted in the internal medicine and infectious diseases wards of a tertiary university hospital between July 2020 and February 2021 among hospitalized adult patients with infectious diseases. Medication reconciliation service (including patient counseling) was provided in person or by telephone. The number and type of medication discrepancies detected during the medication reconciliation services, the acceptance rate of pharmacists' recommendation, and factors associated with having at least one unintentional medication discrepancy at admission were evaluated. At follow-up, hospital readmission and emergency service visit within 30 days after discharge were assessed by telephone.

**Results:** Among 146 patients, 84 (57.5%) had at least one unintentional discrepancy at admission. Only three unintentional discrepancies were determined in three patients at hospital discharge. All the pharmacists' recommendations for medication discrepancies were accepted by the physicians. Having COVID-19 [odds ratio (OR): 2.25, 95% confidence interval (CI): 1.15-4.40;  $p < 0.05$ ], being at a high risk for medication error (OR: 2.01, 95% CI: 1.03-3.92;  $p < 0.05$ ), and higher number of medications used at home (OR: 1.41, 95% CI: 1.23-1.61;  $p < 0.001$ ) were associated with having at least one unintentional discrepancy at admission. The rates of 30 day hospital readmission and admission to the emergency medical service were 12.3% and 15.8%, respectively.

**Conclusion:** Medication reconciliation service provided by in-person or by telephone was useful for detecting and solving unintentional medication discrepancies during the COVID-19 pandemic.

**Key words:** Medication reconciliation, clinical pharmacist, infectious disease medicine, COVID-19, unintentional discrepancy

## INTRODUCTION

Medication reconciliation is "a formal process for creating the most complete and accurate list possible of a patient's current medications and comparing the list to those in the patient

record or medication orders" to avoid medication errors such as duplications and omissions.<sup>1</sup> The medication reconciliation could reduce medication errors and related harms. Providing, recording, and passing along the current and correct medication list of the patient is essential for patient safety, especially

\*Correspondence: betulokuyan@yahoo.com, Phone: +90 216 777 52 00, ORCID-ID: orcid.org/0000-0002-4023-2565

Received: 15.06.2022, Accepted: 06.10.2022



©2023 The Author. Published by Galenos Publishing House on behalf of Turkish Pharmacists' Association.

This is an open access article under the Creative Commons Attribution-NonCommercial-NoDerivatives 4.0 (CC BY-NC-ND) International License.

during the transition of care (including hospital admission and/or discharge).<sup>2</sup>

The medication reconciliation can be provided by various healthcare professionals. However, studies have shown that services such as medication reconciliation and discharge patient consultation led by pharmacists increase patients' knowledge of medication and reduce adverse drug events and medication errors in the transition of care.<sup>3,4</sup> Pharmacists who have diverse knowledge and skills can establish and maintain an effective medication reconciliation process in hospitals and healthcare systems.<sup>5</sup> The medication reconciliation led by an inpatient pharmacist is an effective method for maintaining the patient's post-discharge care.<sup>6</sup> A review published in the Cochrane Library concluded that the impact of pharmacist-involved medication reconciliation services was unclear on medication discrepancies, adverse drug effects, and health values.<sup>7</sup> Medication discrepancy is defined as the differences between medication regimens given in different care settings and often results from lack of documentation and time to create a complete and accurate list of the patients' medication history. Therefore, medication reconciliation is an essential component in ensuring safe patient care by preventing medication discrepancy in any setting.<sup>1,7</sup>

Clinical pharmacists provide medication reconciliation services in patients with various infectious diseases.<sup>8,9</sup> In the infectious disease ward, medication reconciliation reduces the number of undocumented unintentional discrepancies<sup>10</sup> and hospital readmission within a month after discharge.<sup>11</sup>

During the coronavirus disease-2019 (COVID-19) pandemic, clinical pharmacists continued to provide services (including medication reconciliation) with different working models.<sup>12,13</sup> Medication reconciliation service is not provided routinely at hospitals in Türkiye. There are few studies in Türkiye about medication reconciliation services provided in hospitalized older patients at admission<sup>14</sup> and in patients admitted to oncology and internal medicine services.<sup>15</sup>

The aim of the study was to determine the prevalence and type of medication discrepancies and factors associated with unintentional discrepancies and identify the rate of hospital readmission and emergency service visit within 30 days after discharge among hospitalized patients with infectious diseases and receiving clinical pharmacist-led medication reconciliation during the COVID-19 pandemic. The Strengthening the Reporting of Observational Studies in Epidemiology (STROBE) statement was followed to report this observational study.<sup>16</sup>

## MATERIALS AND METHODS

### *Study design and setting*

This observational study was conducted in the internal medicine and infectious diseases wards of a tertiary university hospital between July 2020 and February 2021 among hospitalized adult patients with any infectious diseases (including COVID-19).

### *Study population and recruitment*

All hospitalized adult patients with infectious diseases who chronically used at least one medication before hospital

admission were eligible for this study. All eligible patients were included in the current study without using any specific sampling method. Medication reconciliation services (including gathering the best possible medication history) were provided by clinical pharmacy resident within 48 h after hospital admission in person or by telephone. The patients were excluded from the study, if they were transferred to an intensive care unit or another hospital, stayed in the hospital for less than 24 hours, died, refused the therapy, were unwilling to continue after participating or did not receive medication reconciliation service provided by the clinical pharmacy resident within 48 h after hospital admission.

### *Medication reconciliation*

Neither hospital pharmacists nor clinical pharmacy residents have been involved in medication history taking and medication reconciliation services at this hospital. There was no discharge patient counseling service provided routinely by pharmacists. During this study, medication reconciliation service [both at admission and discharge (including patient counseling service)] was provided in person or by telephone. These services were provided by the clinical pharmacy resident who had theoretical and clinical courses during his education and training for clinical pharmacy services.

Medication reconciliation service flow charts were adapted from previous projects.<sup>17,18</sup> The best possible medication history [including prescribed medications, over-the-counter (OTC) drugs, herbals, and dietary supplements] was taken within 48 h after hospital admission in person and by telephone. At least two resources (such as self-reports of patients and/or caregivers, medication records, and home medicine list) were used for obtaining the best possible medication history.<sup>18</sup>

During medication reconciliation service at hospital admission, a current and accurate medication list was provided by comparing the physicians' orders at admission with their best possible medication history for home medicines. At hospital discharge, medications used in the last 24 h before hospital discharge, the discharge prescription, and the best possible medication history for home medicines were assessed by a clinical pharmacy resident. The medication discrepancies were discussed with the physicians at hospital admission and discharge to provide a current and accurate medication list. At hospital discharge, according to the current and accurate medication list, pill cards (including pictograms),<sup>19</sup> and brochures (including low-molecular-weight heparin prescribed for patients with COVID-19) were provided to the patients by the clinical pharmacy resident. Patient counseling was provided by using the teach-back method.<sup>20</sup>

### *Data collection and variables*

Data including age, sex, education level, having COVID-19, duration of hospital stay, the number of medications used at home, and Charlson comorbidity index<sup>21</sup> were collected at baseline. For evaluating the risk of medication error, statistical consolidation of redundant expression measures (SCOREM) index was calculated<sup>22</sup>. If the total score of SCOREM index was three or greater, the patients were considered as high

risk of medication error. All patients' medications (including prescribed and OTC medications) were recorded. The risk of mortality and unplanned hospital readmission at hospital discharge was calculated using length of stay, acuity of the admission, comorbidity of the patient (LACE) index.<sup>23</sup> If the score of LACE index was 10 points or higher (out of 19), the patients were considered as having a high risk for mortality and unplanned hospital readmission.

Primary outcomes were prevalence, type of medication discrepancies, and factors associated with unintentional medication discrepancies. The number of discrepancies detected during the medication reconciliation service was evaluated and classified according to medication discrepancy taxonomy (MedTax).<sup>24</sup> Resources for obtaining the best possible medication history were recorded. At follow-up, the history of readmission to the hospital or emergency service within 30 days after discharge was assessed by telephone calls.

#### Ethics approval

The study protocol was approved by Marmara University Clinical Trials Ethical Committee (date: June 12, 2020, and number: 09.2020.508). The required permission to conduct this study was obtained from Ministry of Health, The Republic of Türkiye. Informed consent was obtained from patients and/or caregivers.

#### Sample size calculation

As in the study by Cornish et al.<sup>25</sup>, all eligible patients were consecutively included in this study. In a previous study, the rate of patients with at least one unintended medication discrepancy was 47% in internal medicine wards.<sup>26</sup> It was assumed that the rate would be 60% in the study population during the COVID-19 pandemic. The sample size was calculated as 96 with alpha at

0.05 and power of 0.80 to detect the prevalence of unintentional discrepancies.<sup>27</sup>

#### Statistical analysis

Descriptive statistics were presented as number (n) with percentage and median (interquartile range).  $P < 0.05$  was considered statistically significant. According to the findings of the Kolmogorov-Smirnov test, non-parametric statistics were conducted in this study. Fischer's Exact test was used to compare two groups (w/wo COVID-19 and with high or low risks according to LACE index). Univariate logistic regression analysis was performed to determine factors associated with unintentional discrepancies. The odds ratio (OR) [confidence interval (CI) 95%] was presented. Statistical analysis was done using IBM SPSS (Statistical Package for Social Sciences) 11.0 statistics.

## RESULTS

A total of 146 patients, who received medication reconciliation service during hospital admission, were included in the study. Among them, 90 patients (61.6%) received clinical pharmacy resident-led medication reconciliation both at admission and discharge. The flow diagram of the study is displayed in Figure 1. The characteristics of the patients are presented in Table 1.

The most common sources for providing the best possible drug history on admission were the patient's medical record (93.8%), the patient's medication boxes (76.0%), and the patient's self-report (66.4%).

At hospital admission, the median of total discrepancies was 7.0 (5.0-10.0), the median of intentional discrepancies was 6.0 (4.0-9.0), and the median of unintentional discrepancies was 1.0 (0.0-2.0). Among them, 99.3% (n: 145) had at least one intentional

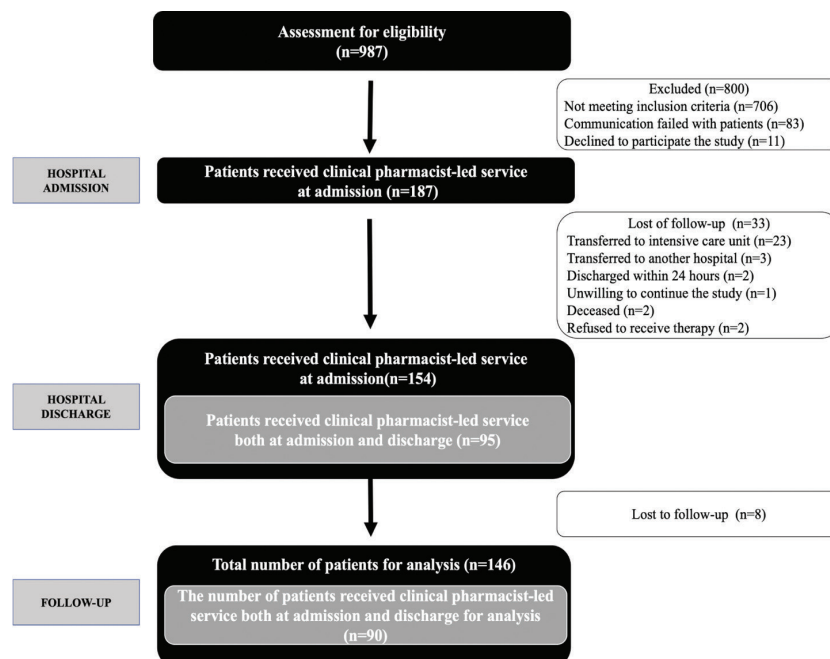


**Figure 1.** STROBE flow diagram of the study

STROBE: Strengthening the Reporting of Observational Studies in Epidemiology

discrepancy and 57.5% (n: 84) had at least one unintentional discrepancy at the hospital admission. At hospital discharge (n: 90), the median of total discrepancies was 3.0 (2.0-5.0) and the median of intentional discrepancies was 3.0 (2.0-4.25). Among them (n: 90), 94.4% (n: 85) had at least one intentional discrepancy and only three unintentional discrepancies were determined in three patients at hospital discharge. The most common unintentional discrepancy was drug omission (n: 142; 74.7%) at admission. All the pharmacists' recommendations for medication discrepancies were accepted by the physicians. The frequency and type of medication discrepancies according to MedTax are presented in Table 2.

Having COVID-19 (OR: 2.25, 95% CI: 1.15-4.40;  $p < 0.05$ ), being at a high risk for medication error according to SCOREM index (OR: 2.01, 95% CI: 1.03-3.92;  $p < 0.05$ ), and a higher number of medications used at home (OR: 1.41, 95% CI: 1.23-1.61;  $p < 0.001$ ) were associated with having at least one unintentional discrepancy. Factors associated with having at least one unintentional discrepancy are presented in Table 3.

Out of 146 patients who received medication reconciliation at admission, 78.8% had a high risk of mortality and unplanned hospital readmission (Table 1). Among these patients (n: 146),

the rates of 30 day hospital readmission and emergency medical service visits were 12.3% and 15.8%, respectively. In 90 patients who received medication reconciliation both at hospital admission and discharge, 80.0% had a high risk of mortality and unplanned hospital readmission (Table 1). Among these patients (n: 90), the rates were 10.0% for 30 day hospital readmission and 14.4% for emergency medical service visit. According to LACE index, patients with high risk had a significantly higher rate of emergency medical service visits within 30 days, when compared with patients with low risk ( $p < 0.05$ ). Patients with infectious diseases other than COVID-19 had a significantly higher rate of hospital readmission within 30 days than patients with COVID-19 ( $p < 0.05$ ). Secondary outcomes during follow-up in patients who received medication reconciliation service are presented in Table 4.

## DISCUSSION

To the best of our knowledge, this is the first study to determine the prevalence and type of medication discrepancies and factors associated with unintentional discrepancies and identify the rate of hospital readmission and emergency service visit within 30 days after discharge among hospitalized patients

**Table 1. Characteristics of patients**

	Total (n: 146) n (%)	CP-led services received both at admission and discharge (n: 90) n (%)
<b>Age median [IQR]</b>	62.0 [54.0-72.0]	62.0 [54.0-72.0]
<b>Sex</b>		
Male	66 (45.2)	38 (42.2)
Female	80 (54.8)	52 (57.8)
<b>Education level*</b>		
<8 y	111 (76.0)	65 (72.2)
≥8 y	35 (24.0)	25 (27.8)
<b>Had COVID-19</b>		
Yes	76 (52.0)	53 (58.9)
No	70 (48.0)	37 (41.1)
<b>The length of stay (day) median [IQR]</b>	10.0 [6.0-15.0]	10.5 [6.75-15.0]
<b>Charlson comorbidity index median [IQR]</b>	3.0 [2.0-4.25]	3.0 [2.0-4.0]
<b>The number of medications used at home median [IQR]</b>	5.0 [3.0-8.0]	5.0 [2.0-7.0]
<b>Patient group according to SCOREM index n (%)</b>		
High risk	71 (48.6)	42 (46.7)
Low risk	75 (51.4)	48 (53.3)
<b>Patient group according to LACE index at discharge n (%)</b>		
Low risk	31 (21.2)	18 (20.0)
High risk	115 (78.8)	72 (80.0)

\*The group was determined according to compulsory education year before 2012 in Türkiye, IQR: Interquartile range, CP: Clinical pharmacy resident, COVID-19: Coronavirus disease-2019, LACE: Length of stay, acuity of the admission, comorbidity of the patient

**Table 2. The frequency and type of medication discrepancies according to medication discrepancy taxonomy**

	Medication reconciliation at admission (n: 146)		Medication reconciliation at discharge (n: 90)	
	Intentional discrepancies	Unintentional discrepancies	Intentional discrepancies	Unintentional discrepancies
	n (%)	n (%)	n (%)	n (%)
<b>Medication mismatched</b>	<b>866 (90.4)</b>	<b>150 (78.9)</b>	<b>269 (87.1)</b>	<b>2 (66.7)</b>
Drug commission or addition	616 (64.3)	6 (3.2)	101 (32.7)	-
Drug omission	218 (22.8)	142 (74.7)	140 (45.3)	1 (33.3)
Therapeutic class substitution	32 (3.3)	2 (1.1)	28 (9.1)	1 (33.3)
<b>Medication partly matched</b>	<b>92 (9.6)</b>	<b>40 (21.1)</b>	<b>40 (12.9)</b>	<b>1 (33.3)</b>
<b>Discrepancy in the name of medication</b>				
Unclear or wrong name	-	3 (1.5)	-	1 (33.3)
Different brand name but the same generic name	14 (1.5)	1 (0.5)	6 (2.0)	-
<b>Discrepancy in the strength and/or frequency and/or number of units of dosage form and/or total daily dose</b>				
Unclear or wrong strength	-	2 (1.1)	-	-
Omission of strength	-	14 (7.4)	-	-
Different strengths and different total daily doses	44 (4.6)	7 (3.7)	24 (7.8)	-
Different strength but the same total daily dose	1 (0.1)	-	1 (0.3)	-
Same strength and the same number of units but different frequency and different total daily dose	4 (0.4)	7 (3.7)	2 (0.6)	-
Same strength but different frequency and different number of units and different total daily dose	4 (0.4)	3 (1.5)	2 (0.6)	-
Same strength but different frequency and different number of units but the same total daily dose	1 (0.1)	-	-	-
<b>Discrepancy in the dosage form/route of administration</b>				
Different dosage form but the same route of administration	3 (0.3)	-	1 (0.3)	-
Different dosage forms and different routes of administration	21 (2.2)	1 (0.5)	4 (1.3)	-
<b>Discrepancy in the time of drug administration</b>				
Different time of administration throughout the day	-	2 (1.1)	-	-
<b>Total</b>	<b>958</b>	<b>190</b>	<b>309</b>	<b>3</b>

**Table 3. Factors associated with having at least one unintentional discrepancy at admission**

	Having at least one unintentional discrepancy at admission (n: 84)		
	OR	CI 95%	p value
<b>Had COVID-19</b>			
Yes	2.25	(1.15-4.40)	0.018
No	Reference		
<b>Patient group according to SCOREM index n (%)</b>			
High risk	2.01	(1.031-3.92)	0.040
Low risk	Reference		
<b>The number of medications used at home</b>	1.41	(1.23-1.61)	<0.001

OR: Odds ratio, CI: Confidence interval, COVID-19: Coronavirus disease-2019

**Table 4. Secondary outcomes during follow-up in patients who received CP-led medication reconciliation service**

	Total (n: 146)	<i>p</i> value	CP-led services both at admission and discharge (n: 90)	<i>p</i> value
<b>30 day hospital readmission n (%)</b>	<b>n: 18 (12.3)</b>		<b>n: 9 (10.0)</b>	
<b>Patient group according to LACE index n (%)</b>				
Low risk	1 (5.6)	NS	1 (11.1)	NS
High risk	17 (94.4)		8 (88.9)	
<b>Had COVID-19</b>				
Yes	5 (27.8)	0.038*	2 (22.2)	0.029*
No	13 (72.2)		7 (77.8)	
<b>30 day emergency medical service visit n (%)</b>	<b>n: 23 (15.8)</b>		<b>n: 13 (14.4)</b>	
<b>Patient group according to LACE index n (%)</b>				
Low risk	1 (4.3)	0.029*	0	-
High risk	22 (95.7)		13 (100)	
<b>Had COVID-19</b>				
Yes	12 (52.2)	NS	7 (59.7)	NS
No	11 (47.8)		6 (40.3)	

\**p*<0.05, COVID-19: Coronavirus disease-2019, NS: Not significant; CP: Clinical pharmacy resident, LACE: Length of stay, acuity of the admission, comorbidity of the patient

with infectious diseases and receiving clinical pharmacist-led medication reconciliation during the COVID-19 pandemic in Türkiye. This service was found useful to detect unintentional discrepancies and all recommendations of the clinical pharmacy resident were accepted by the physicians. More than half of hospitalized patients with infectious diseases had at least one unintentional medication discrepancy at admission. However, the number of patients with at least one unintentional medication discrepancy at discharge was only 3 in patients receiving medication reconciliation both at admission and discharge. Patients with COVID-19 with a high risk for medication errors and higher medications were more likely to have at least one unintentional medication discrepancy at admission during the COVID-19 pandemic.

In Croatia, it was found that 35% of the patients admitted to internal medicine service had at least one unintentional discrepancy.<sup>28</sup> In Italy, one-fourth of patients had at least one unintentional discrepancy at hospital admission and discharge.<sup>29</sup> Cornish et al.<sup>25</sup> determined that half of the patients used four or more medications and had at least one unintentional discrepancy during admission to the internal medicine ward. In China, more than one-fifth of patients had at least one unintentional discrepancy.<sup>30</sup> In the present study, an increased rate of having at least one unintentional discrepancy is likely due to the study population including patients with COVID-19. In line with the finding of the present study, previous studies<sup>28,30,31</sup> exhibited a high number of medications as a factor related to unintentional discrepancy at admission. Like the present study, the most common reason for the unintentional discrepancy was the omission of medication in these studies.<sup>25,28-31</sup>

In this study, the number of unintentional discrepancies was more than half at the hospital admission. On the other hand, only three unintentional discrepancies were detected by the clinical pharmacy resident. Cadman et al.<sup>32</sup> demonstrated a reduction in the number of unintentional discrepancies at discharge after providing medication reconciliation at admission.

#### Study limitations

This study had some limitations, which was conducted in a single center, which limited the generalizability of the findings. Actual or potential harms, including medication errors related to these discrepancies, could not be evaluated with this study protocol. The average time spent providing medication reconciliation was not recorded and assessed because of non-feasibility during the COVID-19 pandemic. Although it was suggested to provide medication reconciliation service within 24 h,<sup>17</sup> medication reconciliation was provided within 48 h during the COVID-19 pandemic. This could impact the effectiveness of this service.

Further studies will evaluate the impact of medication reconciliation services in hospitalized patients with infectious diseases. Implementing this service (in person or by telephone) could decrease the number of unintentional discrepancies in hospitalized patients with COVID-19 and/or high risk of medication errors. This study was conducted during the COVID-19 pandemic by one clinical pharmacy resident. This impact on the rate of patients receiving clinical pharmacy resident-led medication reconciliation both at admission and discharge medication reconciliation at discharge.

## CONCLUSION

Medication reconciliation service provided in person or by telephone was useful for detecting and solving unintentional medication discrepancies during the COVID-19 pandemic.

### Ethics

**Ethics Committee Approval:** The study protocol was approved by the Marmara University Clinical Trials Ethical Committee (date: June 12, 2020, and number: 09.2020.508). The required permission to conduct this study was obtained from Ministry of Health, The Republic of Türkiye.

**Informed Consent:** Informed consent was obtained from patients and/or caregivers.

**Peer-review:** Externally peer-reviewed.

### Authorship Contributions

Concept: B.O., C.E., B.E.Ş., M.S., V.K., Design: B.O., C.E., B.E.Ş., M.S., V.K., Data Collection or Processing: B.O., C.E., B.E.Ş., Analysis or Interpretation: B.O., C.E., B.E.Ş., M.S., V.K., Literature Search: B.O., C.E., B.E.Ş., Writing: B.O., C.E., B.E.Ş., M.S., V.K.

**Conflict of Interest:** No conflict of interest was declared by the authors.

**Financial Disclosure:** The authors declared that this study received no financial support.

## REFERENCES

- Barnsteiner JH. Medication Reconciliation. In: Hughes RG, eds. Patient safety and quality: an evidence-based handbook for nurses. Rockville (MD): Agency for Healthcare Research and Quality (US); chapter 38; 2008. Available from: <https://www.ncbi.nlm.nih.gov/books/NBK2648/>
- Splawski J, Minger H. Value of the pharmacist in the medication reconciliation process. *P T*. 2016;41:176-178.
- Mekonnen AB, McLachlan AJ, Brien JA. Effectiveness of pharmacist-led medication reconciliation programmes on clinical outcomes at hospital transitions: a systematic review and meta-analysis. *BMJ Open*. 2016;6:e010003.
- Phatak A, Prusi R, Ward B, Hansen LO, Williams MV, Vetter E, Chapman N, Postelnick M. Impact of pharmacist involvement in the transitional care of high-risk patients through medication reconciliation, medication education, and postdischarge call-backs (IPITCH Study). *J Hosp Med*. 2016;11:39-44.
- Developed through the ASHP Council on Pharmacy Practice and approved by the ASHP Board of Directors on April 13, 2012, and by the ASHP House of Delegates on June 10, 2012. ASHP statement on the pharmacist's role in medication reconciliation. *Am J Health Syst Pharm*. 2013;70:453-456.
- Kerstenetzky L, Heimerl KM, Hartkopf KJ, Hager DR. Inpatient pharmacists' patient referrals to a transitions-of-care pharmacist: evaluation of an automated referral process. *J Am Pharm Assoc (2003)*. 2018;58:540-546.
- Redmond P, Grimes TC, McDonnell R, Boland F, Hughes C, Fahey T. Impact of medication reconciliation for improving transitions of care. *Cochrane Database Syst Rev*. 2018;8:CD010791.
- Coghlan M, O'Leary A, Melanophy G, Bergin C, Norris S. Pharmacist-led pre-treatment assessment, management and outcomes in a hepatitis C treatment patient cohort. *Int J Clin Pharm*. 2019;41:1227-1238.
- Barnes E, Zhao J, Giumenta A, Johnson M. The effect of an integrated health system specialty pharmacy on HIV antiretroviral therapy adherence, viral suppression, and CD4 count in an outpatient infectious disease clinic. *J Manag Care Spec Pharm*. 2020;26:95-102.
- Bravo P, Martinez L, Metzger S, Da Costa Noble E, Meckenstock R, Greder-Belan A, Parnet L, Samdjee F, Azan S. Conciliation médicamenteuse d'entrée en service de médecine interne: retour d'expérience après un an de pratique [Medication reconciliation in a department of internal medicine and infectious and tropical diseases: feedback after one year practice]. *Rev Med Interne*. 2019;40:291-296. French.
- Bouchand F, Leplay C, Guimaraes R, Fontenay S, Fellous L, Dinh A, Deconinck L, Sénard O, Matt M, Michelin H, Perronne C, Salomon J, Villart M, Izedaren F, Pottier S, Barbot F, Orlikowski D, Vaugier I, Davido B. Impact of a medication reconciliation care bundle at hospital discharge on continuity of care: a randomised controlled trial. *Int J Clin Pract*. 2021;75:e14282.
- Paudyal V, Cadogan C, Fialová D, Henman MC, Hazen A, Okuyan B, Lutters M, Stewart D. Provision of clinical pharmacy services during the COVID-19 pandemic: experiences of pharmacists from 16 European countries. *Res Social Adm Pharm*. 2021;17:1507-1517.
- Li H, Zheng S, Liu F, Liu W, Zhao R. Fighting against COVID-19: innovative strategies for clinical pharmacists. *Res Social Adm Pharm*. 2021;17:1813-1818.
- Selcuk A, Sancar M, Okuyan B, Demirtunc R, Izzettin FV. The potential role of clinical pharmacists in elderly patients during hospital admission. *Pharmazie*. 2015;70:559-562.
- Sancar M, Demir Özker P, Er E, Turan B, Okuyan B. The implementation of a pharmacist driven medication reconciliation program at the admission to hospital. *Clin Exp Health Sci*. 2014;4:226-231.
- von Elm E, Altman DG, Egger M, Pocock SJ, Gøtzsche PC, Vandenbroucke JP; STROBE Initiative. The Strengthening the Reporting of Observational Studies in Epidemiology (STROBE) statement: guidelines for reporting observational studies. *J Clin Epidemiol*. 2008;61:344-349.
- WHO The High 5s Project - Medication Reconciliation Implementation Guide. Accessed Date 27 April 2022. Available from: [https://www.who.int/initiatives/high-5s-standard-operating-procedures\\_](https://www.who.int/initiatives/high-5s-standard-operating-procedures_)
- Canadian Patient Safety Institute, ISMP Canada Medication Reconciliation in Acute Care 2017. Accessed Date: 27 April 2022. Available from: <https://www.ismp-canada.org/download/MedRec/MedRec-AcuteCare-GSK-EN.pdf>
- Okuyan B, Ozcan V, Balta E, Durak-Albayrak O, Turker M, Sancar M, Yavuz BB, Uner S, Ozcebe H. The impact of community pharmacists on older adults in Turkey. *J Am Pharm Assoc (2003)*. 2021;61:e83-e92.
- Agency for Healthcare Research and Quality. Health Literacy Universal Precautions Toolkit, 2<sup>nd</sup> edition. Accessed Date: 27 April 2022. Available from: <https://www.ahrq.gov/health-literacy/improve/precautions/tool5.html>
- Charlson ME, Pompei P, Ales KL, MacKenzie CR. A new method of classifying prognostic comorbidity in longitudinal studies: development and validation. *J Chronic Dis*. 1987;40:373-383.
- Audurier Y, Roubille C, Manna F, Zerkowski L, Faucanie M, Macioce V, Castet-Nicolas A, Jalabert A, Villiet M, Fesler P, Lohan-Descamps

- L, Breuker C. Development and validation of a score to assess risk of medication errors detected during medication reconciliation process at admission in internal medicine unit: SCOREM study. *Int J Clin Pract.* 2021;75:e13663.
23. van Walraven C, Dhalla IA, Bell C, Etchells E, Stiell IG, Zarnke K, Austin PC, Forster AJ. Derivation and validation of an index to predict early death or unplanned readmission after discharge from hospital to the community. *CMAJ.* 2010;182:551-557.
24. Almasreh E, Moles R, Chen TF. The medication discrepancy taxonomy (MedTax): the development and validation of a classification system for medication discrepancies identified through medication reconciliation. *Res Social Adm Pharm.* 2020;16:142-148.
25. Cornish PL, Knowles SR, Marchesano R, Tam V, Shadowitz S, Juurlink DN, Etchells EE. Unintended medication discrepancies at the time of hospital admission. *Arch Intern Med.* 2005;165:424-429.
26. Salameh L, Abu Farha R, Basheti I. Identification of medication discrepancies during hospital admission in Jordan: prevalence and risk factors. *Saudi Pharm J.* 2018;26:125-132.
27. Abu Farha R, Abu Hammour K, Al-Jamei S, AlQudah R, Zawiah M. The prevalence and clinical seriousness of medication discrepancies identified upon hospital admission of pediatric patients. *BMC Health Serv Res.* 2018;18:966.
28. Marinović I, Marušić S, Mucalo I, Mesarić J, Bačić Vrca V. Clinical pharmacist-led program on medication reconciliation implementation at hospital admission: experience of a single university hospital in Croatia. *Croat Med J.* 2016;57:572-581.
29. Dei Tos M, Canova C, Dalla Zuanna T. Evaluation of the medication reconciliation process and classification of discrepancies at hospital admission and discharge in Italy. *Int J Clin Pharm.* 2020;42:1061-1072.
30. Guo Q, Guo H, Song J, Yin D, Song Y, Wang S, Li X, Duan J. The role of clinical pharmacist trainees in medication reconciliation process at hospital admission. *Int J Clin Pharm.* 2020;42:796-804.
31. Masse M, Yelnik C, Labreuche J, André L, Bakhache E, Décaudin B, Drumez E, Odou P, Dambrine M, Lambert M. Risk factors associated with unintentional medication discrepancies at admission in an internal medicine department. *Intern Emerg Med.* 2021;16:2213-2220.
32. Cadman B, Wright D, Bale A, Barton G, Desborough J, Hammad EA, Holland R, Howe H, Nunney I, Irvine L. Pharmacist provided medicines reconciliation within 24 hours of admission and on discharge: a randomised controlled pilot study. *BMJ Open.* 2017;7:e013647.





# Validated Stability-Indicating RP-HPLC Method for Daclatasvir in Tablets

Hemlata M. NIMJE<sup>1\*</sup> Smita J. PAWAR<sup>1</sup>, Meenakshi N. DEODHAR<sup>2</sup>

<sup>1</sup>Pune District Education Association's Seth Govind Raghunath Sable College of Pharmacy, Department of Pharmaceutical Chemistry, Pune, India

<sup>2</sup>Lokmanya Tilak Institute Pharmaceutical Sciences, Department of Pharmaceutical Chemistry, Pune, India

## ABSTRACT

**Objectives:** The current study goal was to create a precise, sensitive, and validated reverse phase-high performance liquid chromatography (RP-HPLC) method for assessing the direct-acting antiviral daclatasvir (DCV) as well as to evaluate the stability of DCV in both drug and tablet formulations. The current investigation was to display stability indicating methods under different stress conditions, including hydrolysis (acidic, basic, and neutral), oxidation, and photolysis.

**Materials and Methods:** All experiments were performed on HPLC Agilent 1100 with a stainless steel Hypersil C<sub>18</sub> column having a particle size of 5 μm and a dimension of 4.6 x 250 mm. The mobile phase chosen was acetonitrile: 0.05% o-phosphoric acid (50:50 v/v) in isocratic mode with 0.7 mL/min flow rate and wavelength 315 nm was selected for detection.

**Results:** This method was validated for linearity and range, accuracy, precision, limit of detection, limit of quantification, and robustness in accordance with International Council for Harmonisation (ICH) requirements. The results were satisfactory. It was observed that retention time (t<sub>R</sub>) was 3.760 ± 0.01 min. In acidic conditions, DCV degradans show t<sub>R</sub> at 3.863, 4.121, and 4.783 min and tandem mass spectrometry (MS/MS) spectra scans had m/z 339.1, 561.2 fragment ions. In basic condition, DCV degradans show t<sub>R</sub> at 5.188, 5.469 min and MS/MS spectra scans having m/z 294.1, 339.1, 505.2, 527.2 fragment ions. In oxidation conditions, DCV degradans shows t<sub>R</sub> at 4.038 min and MS/MS spectra scans having m/z 301.1 and 339.1 fragment ions were observed.

**Conclusion:** All the mass fragments exhibited additional degradation observed for different stress conditions. This will help to identify the structure of the degradant and its pathways. No degradation was observed in neutral and photolytic conditions.

**Key words:** Daclatasvir, RP-HPLC, tablets, validation, stability-indicating method

## INTRODUCTION

Millions of people suffer from hepatitis C virus (HCV) infections. Daclatasvir (DCV) permits once-daily oral treatment, has been shown in *in vitro* experiments to have a very potent antiviral activity against several HCV genotypes.<sup>1,2</sup> Since, direct acting antivirals (DAAs) for HCV have become available, any possible medication interactions between antiretrovirals and DAAs must be assessed before co-therapy.<sup>3</sup> Cirrhosis and hepatocellular cancer have been linked to chronic HCV in various parts of the world.<sup>4</sup> DCV is an effective, new, and non-selective structural protein inhibitor, formerly known as BMS-790052.<sup>5</sup> NS5A, the multifunctional protein which is a crucial part of the

HCV replication complex, is inhibited by DCV. It inhibits viral RNA replication and virion development. Data from computer models and *in vitro* investigations point to an interaction between DCV and the protein's N-terminus in domain 1 that may result in structural alterations that reduce NS5A activity.<sup>6-8</sup> Chemically, DCV is methyl ((1S)-1-(((2S)-2-[5-(4'-(2-((2S)-1-((2S)-2-((methoxycarbonyl)amino)-3-methylbutanoyl)-2-pyrrolidinyl)-1H-imidazol-5-yl)-4-biphenyl)-1H-imidazol-2-yl)-1-pyrrolidinyl)carbonyl)-2-methylpropyl) carbamate (Figure 1). The molecular formula of DCV is C<sub>40</sub>H<sub>50</sub>N<sub>8</sub>O<sub>6</sub> and the molecular weight is 738.89 g/mol.<sup>9</sup> Nimje and Deodhar<sup>10,11</sup> developed stability indicating methods for DCV by high-performance

\*Correspondence: hemanimje@gmail.com, Phone: +91 9689953100, ORCID-ID: orcid.org/0000-0002-8969-1885

Received: 18.08.2022, Accepted: 15.10.2022



©2023 The Author. Published by Galenos Publishing House on behalf of Turkish Pharmacists' Association.

This is an open access article under the Creative Commons Attribution-NonCommercial-NoDerivatives 4.0 (CC BY-NC-ND) International License.

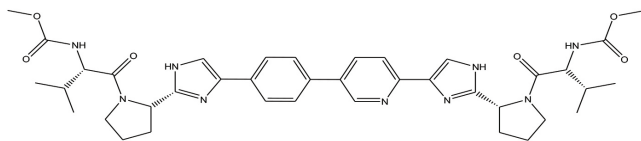


**Figure 1.** Structure of DCV  
DCV: Daclatasvir

thin-layer chromatography and liquid chromatography-tandem mass spectrometry (LC-MS/MS). Some bioanalytical methods such as ultra-performance liquid chromatography (UPLC)-MS/MS for DCV in human plasma and high performance liquid chromatography (HPLC) with ultraviolet (UV) detector were reported by Rezk et al.<sup>12</sup> and Nannetti et al.,<sup>13</sup> respectively. By using UHPLC-MS/MS and LC-MS, Ariado et al.<sup>14</sup> and Jiang et al.<sup>15</sup> demonstrated the measurement of several direct antiviral drugs in human blood plasma. All of these techniques are effective for detecting DCV in human blood plasma; however, they are not appropriate for routine assays to detect DCV in medication and tablet dosage forms. Several HPLC methods have been reported for determining DCV single and its combination with other drugs under different conditions according to a review of the literature.<sup>16-21</sup> As *per* regulatory guidelines, it is essential to ascertain the ability of assay method to quantify the drug component in presence of its degradation products. The mentioned above reported HPLC methods have not ascertained the ability of the assay method to quantify DCV in presence of its degradation products. Hassib et al.<sup>22</sup> demonstrated the reverse phase (RP)-HPLC method for determining DCV and the behavior of its degradation under diverse circumstances. This study used acetonitrile and potassium dihydrogen phosphate buffer as mobile phase, which is driven through column C<sub>18</sub> at a rate of 2 mL/min.<sup>22</sup> The flow rate in the above reported method is on higher side, which can adversely affect the quality of the chromatography not giving the analyst sufficient time to interact with the stationary phase. Moreover, ability of the method to quantify DCV in presence of its degradation product was not evaluated. The stability indicating HPLC-UV was developed by Zaman and Hassan<sup>23</sup> for characterizing forced degradation products and quantifying DCV. In the above method, the retention time ( $t_r$ ) of DCV is 16.4 min making it a time consuming method for assay of formulations containing DCV. The method can be preferred for quantitation of known impurities in DCV formulations. The preferred  $t_r$  in HPLC assay method is 3 to 6 min. Baker et al.<sup>24</sup> presented a stability-indicating HPLC-diode array detector method utilising a Waters C<sub>8</sub> column with isocratic elution of the mobile phase made up of a 75:25 v/v combination of acetonitrile and phosphate buffer with pH of 2.5.<sup>24</sup> While a novel QDa mass detector for DCV was developed by Jagadabi et al.<sup>25</sup> to determine the mass of possible contaminants, stability-indicating UPLC method was reported. However, the above method is primarily used for estimation of the process-related and known impurities in DCV. Considering limitations of the reported methods such as high flow rate, high  $t_r$ , and stability indicating property of assay method being not evaluated, it was thought worthwhile to develop and validate

stability indicating RP-HPLC method for DCV formulations, which is economical and less time consuming without affecting the quality of the method as *per* parameters given in International Council for Harmonisation (ICH) guidelines. In this research work, economical solvents and a simple procedure were used for the estimation of DCV by RP-HPLC. To evaluate the stability of DCV in drugs and their drug derivatives, force degradation research was conducted. This information helps to determine the shelf life of DCV under various settings. The quantitative examination of DCV following exposure to various stability-indicating experiments is described in the current piece of work. The approach was validated in accordance with International Council for Harmonisation (ICH) standards, demonstrating accuracy, precision, and reliability. Therefore, this method can be applied to the routine study of DCV stability under various conditions.

## MATERIALS AND METHODS

### Chemicals and reagents

Mylan Laboratories Ltd. (Hyderabad, India) kindly provided of DCV pure drug sample to us. All HPLC grade solvents were used throughout the analysis including water, methanol, and acetonitrile (Fisher Scientific, India). Analytical grade reagents such as hydrogen peroxide, hydrochloric acid, sodium hydroxide, and *o*-phosphoric acid were used throughout the analysis. DCV tablets "MyDeklaTM60" and "DACLACURE 60" were purchased from a local market drug store. They were manufactured by Mylan Laboratories Limited and Emcure Pharmaceutical Industry, respectively. Each tablet contained 60 mg of DCV.

### Instrumentation and chromatographic conditions

HPLC Agilent 1100 with variable detector (G1314A) and (G13104) pump was used for all the studies. The solutions were degassed using a DGU-20A3 prominence degasser. The data was gathered and processed using ChemStation software. The material employed was a stainless steel Hypersil C<sub>18</sub> that was 4.6 x 250 mm in size, 5  $\mu$ m particle size, filled with octadecyl silane stationary phase and had ligands bound to silica surface, and column temperature was set at 40 °C. For this research, a humidity chamber from Newtronic and a Rolex ultrasonicator were employed. An examination into photodegradation was conducted using a UV lamp (6 w, Vilber Lourmat, France) and photostability chamber. The light output was 200 Wh/m<sup>2</sup> and its intensity was 1.2 million lux h. A weighing balance (AX200, Shimadzu Corporation Japan) with minimum 0.1 mg and maximum 200 g capacity was employed throughout the analytical procedure. The isocratic mobile phase was used with acetonitrile and 0.05% *o*-phosphoric acid (50:50 v/v). Before being used in the study, the mobile phase was filtered through a membrane filter of size 0.45  $\mu$ m and using an ultrasonic sonicator for degassing the solvents for 10 min. The flow rate of the mobile phase was 0.7 mL/min and the injection had a 10  $\mu$ L volume. A variable wavelength detector was used to perform a wavelength scan and a wavelength of 315 nm was chosen for investigation.

### *Preparation of standard stock and tablet solution*

The standard stock solution was made by placing a quantity of 10 mg of DCV standard in a 10 mL volumetric flask with mobile phase, shaking well and adding mobile phase to achieve a concentration of 1000 µg/mL. The stock solution was diluted, mixed well, and used to test all DCV validation parameters with required concentrations. After 15 min of sonication, the mixture was filtered through a membrane filter paper of size 0.45 µm. Twenty DCV tablets (MyDekla™ 60 and DACLACURE 60) were weighed and the average weight was calculated. The tablet was triturated in a dry spotless mortar to create a fine powder. A quantity of tablet fine powder containing 10 mg of DCV was accurately taken, dissolved in minimum mobile phase, thoroughly mixed, and stirred for 5 min in 10 mL volumetric flask. To create a volume of 1000 µg/mL concentrated solution, up to 10 mL of mobile phase solvent was added. Sample solutions from the above solution were adequately diluted for future research examination. All the solutions were filtered using the membrane filter paper with a pore size of 0.45 µm.

### *Validation of proposed method*

#### *Linearity and range*

Different series of DCV solutions were made from standard stock solutions and diluted with diluent for linearity test. Concentration range of 10.00-50.00 µg/mL was identified and five concentrations (10, 20, 30, 40, and 50 µg/mL) were chosen. In order to evaluate linearity, peak area and peak height were subjected to least squares regression analysis to produce a calibration equation with slope, Y-intercepts, and correlation coefficient ( $r^2$ ).

#### *Accuracy*

In order to confirm the method accuracy for quantifying DCV, standard addition and recovery tests were carried out. Recovery studies employ a typical addition procedure to a synthetic mixture created in lab to assess the accuracy of the method in triplicate. Three different concentration levels of known amounts of DCV samples were put to a pure drug with a consistent weight of 10 µg/mL (80, 100, and 120% of label claim) in triplicates. To make up the volume of diluted samples, mobile phase was used. The recovery was calculated using the peak area.

#### *Precision*

For determination of DCV, repeatability (intraday) and intermediate precision (interday) of the procedure were used to establish its precision for each six samples. The intraday precision was conducted on the same day with the same sample at certain time. The same sample solution was used on one consecutive day to accomplish the interday precision. To determine the method accuracy, the results were obtained and the relative standard deviation (RSD) % was computed. For accuracy, RSD% of DCV peak areas was measured.

#### *Sensitivity*

Limit of detection (LOD) and limit of quantification (LOQ) estimates were used to determine the measurement of DCV

sensitivity. DCV was determined at signal-to-noise (S/N) ratios of 3:1 and 10:1 for LOD and LOQ, respectively.<sup>26</sup>

#### *Robustness*

Robustness analysis was used to examine the impact of small deliberate adjustments on the ideal chromatographic settings created for DCV. A 10% change in flow rate, a 2 nm shift in wavelength, and a 2% change in the composition of mobile phase were among the other modifications. Three samples of DCV (30 µg/mL) were evaluated using it in all the aforementioned circumstances. All system suitability traits and conditional changes were compared under all altered settings.

#### *Stability-indicating analytical method (CH Q1A)*

A crucial step in the process of developing drug medicine is stability testing. The purpose of stability testing is to demonstrate how product quantity fluctuates over time and in different environmental contexts. Recommendations can be made for shelf life period based on factors including temperature, humidity, and light. The assay of the active ingredient and the degradation products produced during stability tests are two key aspects of the drug product that are crucial in determining the shelf life duration. The conditions such as 0.1 N HCl, 0.1 N NaOH, 30% H<sub>2</sub>O<sub>2</sub>, humidity, hydrolysis, UV light, and temperature were used in the forced degradation investigation of DCV. 20 mL of 0.1 N HCl, 0.1 N NaOH, and water were used to treat 20 mg of DCV, which is the comparable amount. For four hours the solutions were refluxed at 60 °C. H<sub>2</sub>O<sub>2</sub> solution (30%) was employed for the oxidation investigation, which was refluxed at 60 °C for 6 h. After filtering the solution appropriate amount of dilution was added. For 10 days, a layer of dry solid DCV powder was placed in direct sunlight to perform photolytic testing. On the platform, a petridish held the medication. For 10 days, visible light at 1.2 million lux h and UV light at 200 Wh/m<sup>2</sup> were used in degradation experiment. All these conditions were applied continually until significant deterioration was attained. All degradation research samples were gathered and diluted to the proper concentration before analysis. This solution was put into HPLC instrument for testing. The standard untreated drug was compared to DCV assay of stressed samples. The conclusion drawn from the RP-HPLC analysis of all stressed samples is that the suggested analytical strategy can identify all degraded products, demonstrating the methods potential to indicate stability.

## **RESULTS**

### *Method development of daclatasvir*

The aim of this study was to develop and validate RP-HPLC method for the degradant separation using RP-HPLC data to clarify the structure. The chromatographic method was created to look into several important contaminants detected in DCVs. For method development, DCV was injected into HPLC simultaneously with all stress samples. To accomplish the effective separation, different ratios of various solvent combinations were explored. Using a C<sub>18</sub> column as the stationary phase and an acetonitrile: 0.05% OPA in water

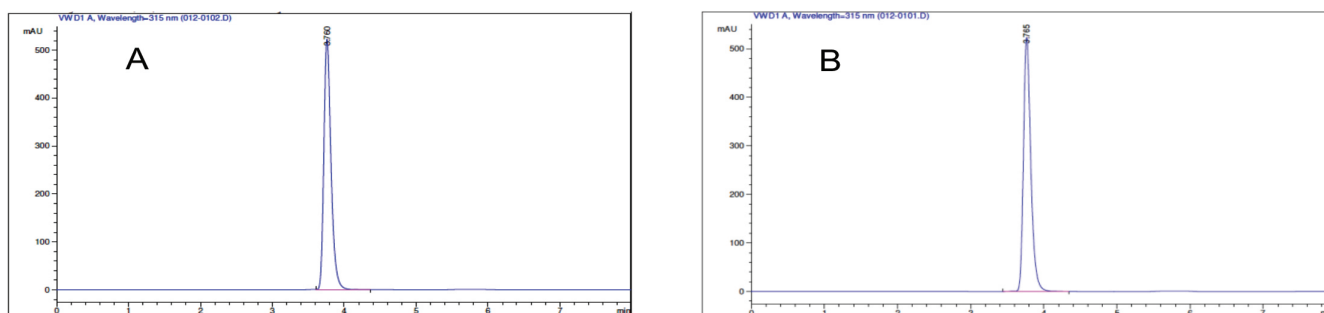


**Figure 2.** Chromatograms of DCV (A) and tablet (B) showing  $t_R$   $3.760 \pm 0.01$  min  
DCV: Daclatasvir,  $t_R$ : Retention time

(50:50  $v/v$ ) mobile phase with a flow rate of 0.7 mL/min, a wavelength of 315 nm, and a column temperature of 40 °C with a total run time of 10 min, the best separation of DCV from its related substance was observed. The measured DCV  $t_R$  was  $3.760 \pm 0.01$  min. The chromatogram of DCV is depicted in Figure 2.

#### Method validation

The HPLC instrument met the analysis criteria for the system suitability test for DCV chromatogram and is presented in Table 1.

#### Linearity and range

By injecting five different level concentrations of pure DCV ranging from 10 to 50  $\mu\text{g/mL}$ , the analytical method linearity was examined. Plotting peak area *versus* concentration yielded the slope, Y-intercepts, and correlation coefficient of each DCV concentration. Data generated from linearity studies displayed a correlation between peak area and concentration. DCV method was found to be linear (10 to 50  $\mu\text{g/mL}$ ) concentration ranges with regression coefficients of 0.9998. DCV linearity curve is depicted in Figure 3.

#### Accuracy

The correctness of an analytical procedure is determined by the agreement between true and experimental values. To ascertain the accuracy, three concentrations (18, 20, and 22  $\mu\text{g/mL}$ ) from various ranges of DCV standard curves were chosen. DCV recovery was examined in triplicate for concentrations of the drug sample at 80, 100, and 120%. Recovery experiments were used to examine the effects of excipients, which are frequently used in pharmaceutical formulations of drugs. A good level of quantitative skill was demonstrated by the recovery of DCV in the sample. Table 1 displays the accuracy results.

#### Precision

According to ICH regulations, the devised HPLC technology was evaluated for precision of the study. Intermediate precision (intraday precision) and percent RSD from six replicates of DCV samples were acquired. DCV samples were seen to have intraday precision on the same day. Three separate days were used to investigate DCV for inter-day precision for the repeatability study from the six replicates of DCV. The results are presented in Table 1.

**Table 1. A summary of system suitability test parameters for DCV**

Parameter	HPLC assay
Retention time	$3.760 \pm 0.01$
Number of theoretical plate (N)	8337
Tailing factor ( $A_s$ )	0.82
Range	10-50 $\mu\text{g/mL}$
Linearity (regression equation)	$y: 151.68x + 598.86$
Intercept (SD)	1.5595
Slope (SD)	19.09
Correlation coefficient	$r^2: 0.9998$
Accuracy at 80% level <sup>a</sup> (mean $\pm$ SD)	$100.78 \pm 0.6144$
Accuracy at 100% level <sup>a</sup> (mean $\pm$ SD)	$99.79 \pm 0.7622$
Accuracy at 120% level <sup>a</sup> (mean $\pm$ SD)	$97.95 \pm 0.1145$
Intermediate precision <sup>b</sup> (mean $\pm$ SD and RSD%)	$101.73 \pm 0.3281$ , and $0.3237$
Repeatability <sup>b</sup> (mean $\pm$ SD and RSD%)	$101.15 \pm 0.8914$ , and $0.8812$
LOD (limit of detection)	0.0416 $\mu\text{g/mL}$
LOQ (limit of quantification)	0.1261 $\mu\text{g/mL}$

<sup>a</sup>Replicates of three determinations, <sup>b</sup>Replicates of six determinations, SD: Standard deviation, RSD: Relative standard deviation, HPLC: High performance liquid chromatography, DCV: Daclatasvir, LOD: Limit of detection, LOQ: Limit of quantification

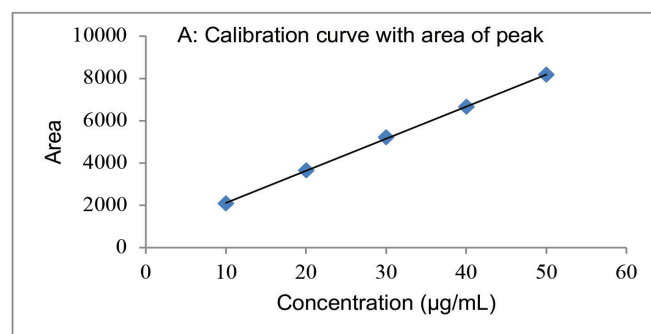


**Figure 3.** Calibration curve for DCV with area of peak (10-50  $\mu\text{g/mL}$ )  
DCV: Daclatasvir

### Quantitative aspects

S/N ratios of 3 and 10 were used to assess LOD and LOQ for DCV.<sup>26</sup> LOD of 0.0416 µg/mL and LOQ of 0.1261 µg/mL were obtained after DCV injection, indicating enhanced sensitivity for detection and quantification.

### Robustness

All the analyses were sufficiently resolved and order of elution was unaltered, when the chromatographic parameters such as flow rate, mobile phase composition, and wavelength were purposefully adjusted. Changes were made to the flow rate (0.2 mL/min), mobile phase composition (10%), and wavelength (2 nm).  $t_R$ , observed peak area, and RSD were reported in accordance with acceptable bounds. Table 2 presents the robustness results.

### Degradation behavior of the drug and characterization of degradants

DCV dramatically degrades in alkaline, acidic, and oxidative environments, but is found to be stable in neutral and photolytic situations. Table 3 includes the degradation study observation table for all conditions. According to data from mass spectra and HPLC chromatograms seen in various stress settings, some drug product impurities or derivatives were observed as D1,

D2, and D3 under various stress conditions including alkaline, acidic, and oxidative. All of the HPLC chromatograms, mass spectra, and ion fragmentation peaks are shown in Figure 4. To examine if any excipients were discovered, blank samples were firstly put through the same arduous testing as DCV samples. HPLC chromatograms and mass spectra of commercial tablets and blank samples were contrasted. In  $[M + H]^+$  ESI positive mode, the peak of DCV mass spectra was discovered to be at  $m/z$  739.3, which was further broken down into  $m/z$  370.1,  $m/z$  513.2, and  $m/z$  565.2. Considering that those are the  $m/z$  peaks most typical of pure DCV drug.

### Acidic condition

For the acidic condition, DCV was refluxed with 0.1 N HCl for 4 h (1 mg/mL). Then, this acidic solution (20 µg/mL) was added to the HPLC instrument while maintaining the same chromatographic conditions. The measured DCV  $t_R$  was 3.762 min. The other peaks named as D1, D2, and D3 were seen at  $t_R$  of 3.863, 4.121, and 4.783 min. The mass spectrometer  $[M + H]^+$  ESI mode employed the same sample. The fragmentation of additional peaks, which were not visible in pure DCV, was noticed as  $m/z$  339.1 and  $m/z$  561.2 in the mass spectrum shown in Figure 4. This shows that degradant is in acidic medium.

**Table 2. Evaluation data for robustness study of daclatasvir**

Robustness parameters	$t_R$ minute	Peak area*	Assay % ± SD	RSD%
Flow rate				
Flow rate (0.6 mL/min)	3.762	5237.72	100.63 ± 1.0443	1.0377
Flow rate (0.7 mL/min)	3.788	5257.81	101.05 ± 0.5272	0.5217
Flow rate (0.8 mL/min)	3.779	5263.78	101.13 ± 1.1720	1.1588
Mobile phase composition				
Acetonitrile: 0.05% <i>o</i> -phosphoric acid (49:51 v/v)	3.752	5207.84	100.05 ± 1.1663	1.1657
Acetonitrile: 0.05% <i>o</i> -phosphoric acid (50:50 v/v)	3.788	5238.12	100.63 ± 1.0078	1.0014
Acetonitrile: 0.05% <i>o</i> -phosphoric acid (51:49 v/v)	3.761	5220.25	100.29 ± 1.1329	1.1296
Wavelength				
Wavelength (314 nm)	3.721	5256.88	100.99 ± 0.5778	0.5721
Wavelength (315 nm)	3.742	5262.27	100.90 ± 0.7735	0.7804
Wavelength (316 nm)	3.761	5236.80	100.79 ± 0.8431	0.8498

\*Results of three replicates,  $t_R$ : Retention time, SD: Standard deviation, RSD: Relative standard deviation

**Table 3. Results of degradation products for DCV obtained under stress conditions**

Serial no stress condition	Name of degradation product	Retention time (min)	Major peak of fragmentation pattern ( $m/z$ )	Percentage of degradation
0.1N HCl	D1, D2, D3	3.863, 4.121, 4.783	339.1, 561.2	72%
0.1N NaOH	D1, D2	5.188, 5.469	294.1, 339.1, 505.2, 527.2	97%
H <sub>2</sub> O <sub>2</sub> (30%)	D3	4.038	301.1, 339.1	28%
H <sub>2</sub> O	-	-	370, 513, 565, 739	No degradation

DCV: Daclatasvir

### Alkaline condition

In the alkaline condition, DCV was refluxed with 0.1 N NaOH for 4 h at 60 °C (1 mg/mL). After that, this alkaline solution was added to the HPLC instrument, while still maintaining the same chromatographic conditions. The measured DCV  $t_R$  was the same as 3.648 min., while other chromatographic peaks were observed at  $t_R$  5.188 min and 5.469 min, another peak was named as D1 and D2, respectively. The other mass fragmented ions such as  $m/z$  294.1,  $m/z$  339.1,  $m/z$  505.2, and  $m/z$  527.2 in the mass spectrum  $[M + H]^+$ , which were not seen in pure DCV, are displayed in Figure 4. The same solution was used in the ESI mode of mass spectrometer.

### Oxidation condition

In the oxidation condition, DCV was refluxed with 3% hydrogen peroxide at 60 °C for 4 h (1 mg/mL). From this oxidized solution, a 20  $\mu\text{g/mL}$  solution was made and put into the HPLC device with the same chromatographic settings. The measured DCV  $t_R$  was 3.690 min, while one more additional peak named D1 at  $t_R$  4.038 min was observed. The mass spectrometer  $[M + H]^+$  ESI mode employed for the same sample. The mass spectrum shown in Figure 4 contains degradans fragments with  $m/z$  301.1 and 339.1, which are absent in pure DCV drug sample.

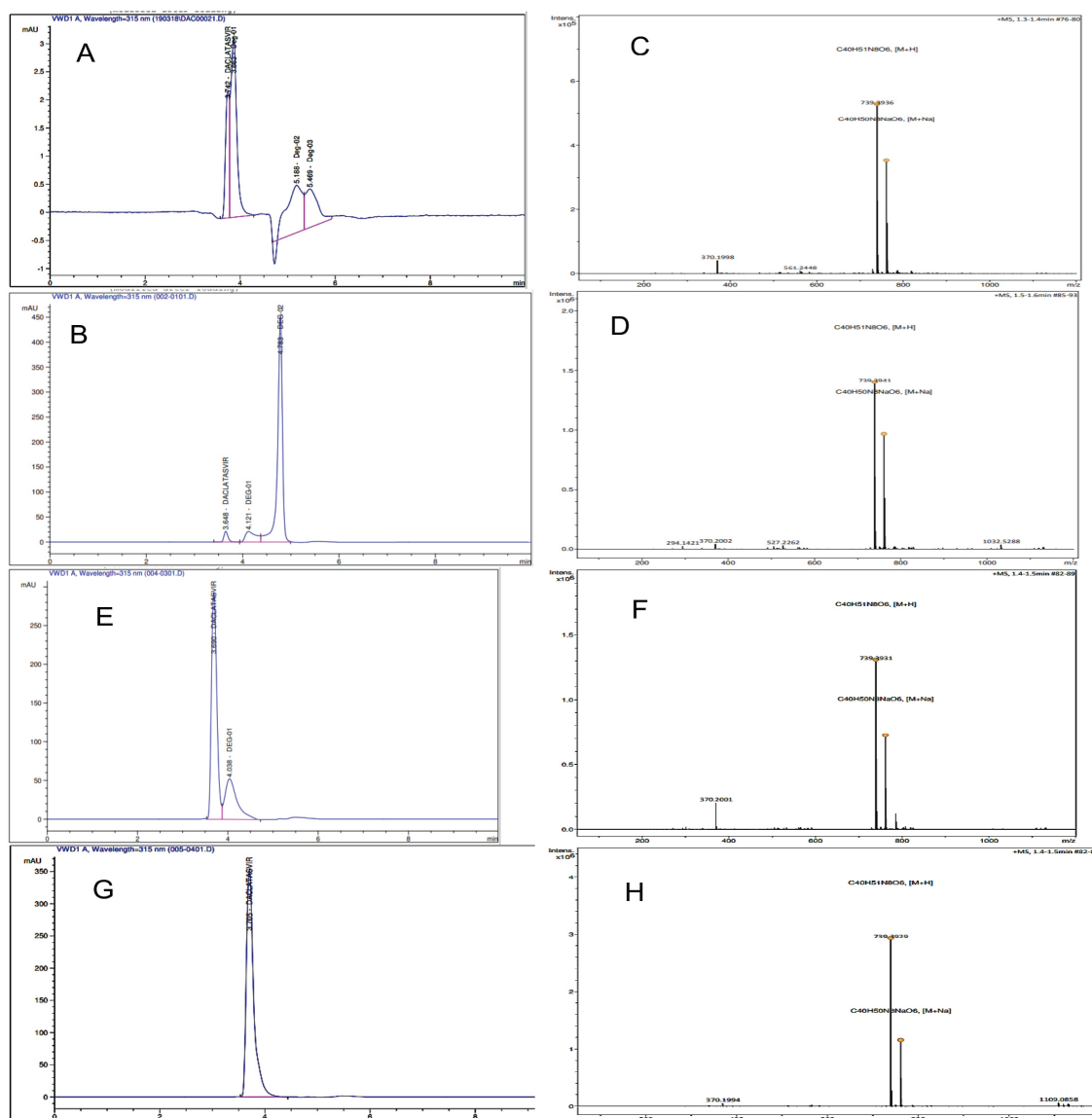


**Figure 4.** HPLC chromatograms and total ion MS/MS spectra scans relative to DCV stressed conditions. HPLC chromatogram of DCV exposed to 0.1N HCl, 60 °C for 4 h, degradant  $t_R$  at 3.863, 4.121, 4.783 min, and MS/MS spectra scans having  $m/z$  339.1, 561.2 fragment ion observed (A, B). HPLC chromatogram of DCV exposed to 0.1 N NaOH, 60 °C for 4 h, degradant  $t_R$  at 5.188, 5.469 min, and MS/MS spectra scans having  $m/z$  294.1, 339.1, 505.2, and 527.2 fragment ions observed (C, D). HPLC chromatogram of DCV exposed to 30% H<sub>2</sub>O<sub>2</sub>, 60 °C for 4 h, degradant  $t_R$  at 4.038 min and MS/MS spectra scans having  $m/z$  301.1, 339.1 fragment ions observed (E, F). HPLC chromatogram of DCV exposed to water, 60 °C for 8 h (G, H)

HPLC: High performance liquid chromatography, MS/MS: Tandem mass spectrometry, DCV: Daclatasvir,  $t_R$ : Retention time

### Neutral condition

In the neutral state, DCV was refluxed with water for 8 h at 60 °C (1 mg/mL). Under the same chromatographic conditions, 20 µg/mL solution made from this was fed into the HPLC instrument. The measured DCV  $t_R$  was 3.705 min. No other peaks were seen in the chromatogram. The mass spectrometer  $[M + H]^+$  ESI mode employed the same sample. In the mass spectrum shown in Figure 4, fragmented peaks are matched with pure DCV.

### Photochemical degradation

After 15 days of exposure to direct sunlight, DCV exhibited no symptoms of deterioration. UV chamber use was another stressor. For 15 days, DCV was exposed to 200 Wh/m<sup>2</sup> of UV radiation and 1.2 million lux/h of visible light. There was no change in DCV chromatogram. As a result, it was confirmed that there was no degradation. This suggests that the drug is durable to photochemical stress.

## DISCUSSION

In this work, a stability indicating a RP-HPLC assay method was developed and validated for the routine quality control of tablet formulations containing DCV. In most of the reported RP-HPLC methods for DCV, ability of the method to specifically quantitate DCV in the presence of its degradation products was not evaluated. Though some RP-HPLC methods have reported for estimation of DCV in the presence of process impurities and known impurities, the method is primarily for quantitation of impurities and is time consuming. The proposed HPLC method is primarily used for the estimation of DCV in tablet formulations in the presence of its degradation products. The chromatographic parameters selected such as mixture of acetonitrile and 0.05% *o*-phosphoric acid (50:50 v/v) as mobile phase in isocratic mode and Hypersil C<sub>18</sub> column with 0.7 mL/min flow rate was found to give acceptable peak shape as indicated by the system suitability parameters. The analyst DCV was eluted with acceptable  $t_R$  3.760 ± 0.01 min and, hence, the analysis is not time consuming. With linearity in the range of 10-50 µg/mL, the method, which was validated as per ICH guidelines, is well suited for DCV formulation. The percent recovery evaluated by standard addition method was found to be in range of 97.95% to 100.78% indicating that the method is accurate and can selectively quantify DCV in presence of the excipients present in the formulation. The standard deviation for intra- and inter-day precision was found in the range of ± 0.3281 and ± 0.8914 indicating the repeatability and reproducibility of the method for the quantification of DCV. DCV was treated under various conditions and degradation was observed. The data obtained in ruggedness and robustness studies expressed the lack of influence of operational and environmental variables on the test results obtained using the proposed method. To ascertain ability of the proposed method to selectively quantify DCV in the presence of its degradation products, forced degradation studies were performed under acidic, alkaline, oxidative, neutral, and photochemical conditions. The treated samples were analyzed by the proposed method. It was found that DCV degraded under acid, base, and oxidative stress

conditions, whereas it was found to be stable under neutral hydrolysis and photochemical stress condition. The method could separate the DCV peak from its degradation product peak and selectively quantify DCV, indicating the specificity of the method. The identity of degradation products was confirmed by high resolution ESI-MS/MS techniques.

## CONCLUSION

The current investigation illustrated the need to develop and validate a DCV stability-indicating RP-HPLC technique under varied stress levels in compliance with ICH requirements. RP-HPLC strategy was demonstrated to be a highly potent tool for separating and identifying degradation products of DCV medication in three different stress states discovered by high-resolution ESI-MS/MS techniques. As part of the validation process, the reported methodology linearity, accuracy, LOQ, LOD, precision, and ruggedness were all tested. Using this method, a commercial DCV tablet formulation was tested. The suggested method for regular analysis is relatively more straightforward and rapid because it avoids more tedious chemical procedures. It is also a simple, quick, and cost-effective method. The findings of DCV degradation study open up new directions for drug stability research and understanding, resulting in more tools for quality control and safer treatments.

### ACKNOWLEDGMENTS

The authors are grateful to Mylan Laboratories Ltd (Hyderabad, India) for providing the gift sample of DCV.

### Ethics

**Ethics Committee Approval:** Ethics committee approval is not required for the proposed research. Any kind of human being or animal matrices was not used in the current study.

**Informed Consent:** Not applicable.

**Peer-review:** Externally peer-reviewed.

### Authorship Contributions

Concept: H.M.N., Design: H.M.N., Data Collection or Processing: M.N.D., Analysis or Interpretation: H.M.N., M.N.D., S.J.P. Literature Search: H.M.N., S.J.P., Writing: H.M.N., S.J.P., M.N.D.

**Conflict of Interest:** No conflict of interest was declared by the authors.

**Financial Disclosure:** The authors declare that this study received no financial support.

## REFERENCES

1. Chukkapalli V, Berger KL, Kelly SM, Thomas M, Deiters A, Randall G. Daclatasvir inhibits hepatitis C virus NS5A motility and hyper-accumulation of phosphoinositides. *Virology*. 2015;476:168-179.
2. Gentile I, Borgia F, Coppola N, Buonomo AR, Castaldo G, Borgia G. Daclatasvir: the first of a new class of drugs targeted against hepatitis C virus NS5A. *Curr Med Chem*. 2014;21:1391-1404.
3. Bifano M, Hwang C, Oosterhuis B, Hartstra J, Grasela D, Tiessen R, Velinova-Donga M, Kandoussi H, Sevinsky H, Bertz R. Assessment of pharmacokinetic interactions of the HCV NS5A replication complex

- inhibitor daclatasvir with antiretroviral agents: ritonavir-boosted atazanavir, efavirenz and tenofovir. *Antivir Ther.* 2013;18:931-940.
- Lavanchy D. Evolving epidemiology of hepatitis C virus. *Clin Microbiol Infect.* 2011;17:107-115.
  - Herbst DA, Reddy KR. NS5A inhibitor, daclatasvir, for the treatment of chronic hepatitis C virus infection. *Expert Opin Investig Drugs.* 2013;22:1337-1346.
  - Australian Product Information- Daklinza (Daclatasvir). 2016. Available from: <https://www.tga.gov.au/sites/default/files/auspar-daclatasvir-dihydrochloride-151214-pi.pdf>
  - Keating GM. Daclatasvir: a review in chronic hepatitis C. *Drugs.* 2016;76:1381-1391.
  - Berger C, Romero-Brey I, Radujkovic D, Terreux R, Zayas M, Paul D, Harak C, Hoppe S, Gao M, Penin F, Lohmann V, Bartenschlager R. Daclatasvir-like inhibitors of NS5A block early biogenesis of hepatitis C virus-induced membranous replication factories, independent of RNA replication. *Gastroenterology.* 2014;147:1094-105.e25.
  - Indian Pharmacopoeia, vol II, 8<sup>th</sup> ed, The Indian Pharmacopoeia Commission, Ghaziabad, Government of India Ministry of Health and Family Welfare, January 2018; 1745-1747.
  - Nimje HM, Deodhar MN. Stability-Indicating HPTLC Method for determination of daclatasvir in pharmaceutical dosage form. *Indian Drugs.* 2021;58:56-62.
  - Nimje HM, Deodhar MN. Method development and force degradation study for daclatasvir using LC-MS/MS. *Advances in Science and Engineering Technology International Conferences.* 2020;1-6.
  - Rezk MR, Bendas ER, Basalious EB, Karim IA. Development and validation of sensitive and rapid UPLC-MS/MS method for quantitative determination of daclatasvir in human plasma: application to a bioequivalence study. *J Pharm Biomed Anal.* 2016;128:61-66.
  - Nannetti G, Messa L, Celegato M, Pagni S, Basso M, Parisi SG, Palù G, Loregian A. Development and validation of a simple and robust HPLC method with UV detection for quantification of the hepatitis C virus inhibitor daclatasvir in human plasma. *J Pharm Biomed Anal.* 2017;134:275-281.
  - Ariaudo A, Favata F, De Nicolò A, Simiele M, Paglietti L, Boglione L, Cardellino CS, Carcieri C, Di Perri G, D'Avolio A. A UHPLC-MS/MS method for the quantification of direct antiviral agents simeprevir, daclatasvir, ledipasvir, sofosbuvir/GS-331007, dasabuvir, ombitasvir and paritaprevir, together with ritonavir, in human plasma. *J Pharm Biomed Anal.* 2016;125:369-375.
  - Jiang H, Kandoussi H, Zeng J, Wang J, Demers R, Eley T, He B, Burrell R, Easter J, Kadiyala P, Pursley J, Cojocar L, Baker C, Ryan J, Aubrey AF, Arnold ME. Multiplexed LC-MS/MS method for the simultaneous quantitation of three novel hepatitis C antivirals, daclatasvir, asunaprevir, and beclabuvir in human plasma. *J Pharm Biomed Anal.* 2015;107:409-418.
  - Yamana AV, Bonnoth CS. Validated method development for estimation of sofosbuvir and daclatasvir in bulk and their dosage form by using RP-HPLC. *Res J Pharm Technol.* 2022;15:2447-2450.
  - Godela R, Sowjanya G. Concurrent determination of daclatasvir and sofosbuvir in pure binary mixture and their combined film coated tablets by a simple stability indicating RP-HPLC method. *Res J Pharm Technol.* 2021;14:5913-5918.
  - Fayed AS, Hegazy MA, Kamel EB, Eissa MS. HPLC-UV and TLC-densitometry methods for simultaneous determination of sofosbuvir and daclatasvir: application to Darvoni® tablet. *J Chromatogr Sci.* 2022;60:606-612.
  - Eldin AS, Azab SM, Shalaby A, El-Maamly M. The development of a new validated HPLC and spectrophotometric methods for the simultaneous determination of daclatasvir and sofosbuvir: antiviral drugs. *J Pharm Pharmacol Res.* 2017;1:28-42.
  - Saeed N, Afridi MS, Latif A, Fahham HH, Aslam I, Mazhar M, Afridi MS. Development and validation of HPLC method for quantification of daclatasvir in pure and solid dosage form. *Egypt J Chem.* 2022;65:81-91.
  - Hussain Shah SS, Nasiri MI, Sarwar H, Ali A, S Naqvi SB, Anwer S, Kashif M. RP-HPLC method development and validation for quantification of daclatasvir dihydrochloride and its application to pharmaceutical dosage form. *Pak J Pharm Sci.* 2021;34:951-956.
  - Hassib ST, Taha EA, Elkady EF, Barakat GH. Reversed-phase liquid chromatographic method for determination of daclatasvir dihydrochloride and study of its degradation behavior. *Chromatographia.* 2017;80:1101-1107.
  - Zaman B, Hassan W. Development of stability indicating HPLC-UV method for determination of daclatasvir and characterization of forced degradation products. *Chromatographia.* 2018;81:785-797.
  - Baker MM, El-Kafrawy DS, Mahrous MS, Belal TS. Validated stability-indicating HPLC-DAD method for determination of the recently approved hepatitis C antiviral agent daclatasvir. *Ann Pharm Fr.* 2017;75:176-184.
  - Jagadabi V, Nagendra Kumar PV, Mahesh K, Pamidi S, Ramaprasad LA, Nagaraju D. A stability-indicating UPLC method for the determination of potential impurities and its mass by a new QDa mass detector in daclatasvir drug used to treat hepatitis C infection. *J Chromatogr Sci.* 2019;57:44-53.
  - International Conference on Harmonization (ICH) Guidelines Q2 (R1). *Validation of Analytical Procedures: Text and Methodology.* 2005.





# LC-MS/MS Method Development and Validation for Determination of Favipiravir Pure and Tablet Dosage Forms

✉ Nandeesh ITIGIMATH<sup>1</sup>, ✉ Hadagali ASHOKA<sup>2</sup>, ✉ Basappa C. YALLUR<sup>1</sup>, ✉ Manjunatha Devagondanahalli HADAGALI<sup>3\*</sup>

<sup>1</sup>Ramaiah Institute of Technology, Department of Chemistry, Visvesvaraya Technological University, Bangalore, Belagavi, India

<sup>2</sup>BMS College of Engineering, Department of Biotechnology, Bengaluru, India

<sup>3</sup>Davangere University, Department of Studies in Chemistry, Davangere, India

## ABSTRACT

**Objectives:** Analytical method development and validation for determination of favipiravir (FVPR) in pure and tablet dosage forms by liquid chromatography with tandem mass spectrometry/mass spectrometry (LC-MS/MS) technique.

**Materials and Methods:** A simple LC-MS/MS method was developed for determination of a new antiviral drug, FVPR in pharmaceutical formulations. The stationary phase employed was a Shim pack GISS, C<sub>18</sub> (100 mm × 2.1 mm, 1.9 μm) column and mobile phase used in pump A was 10.0 mM ammonium acetate and in pump B methanol was used. The gradient program was used with fixed mobile phase flow rate at 0.4 mL min<sup>-1</sup>. Total run time was 5.0 min. The proposed method was validated according to International Conference on Harmonization (ICH) guidelines. The established method found better outcomes.

**Results:** The linearity graph was found in the range of 50-200 μg/mL and the correlation coefficient value (R<sup>2</sup>) obtained was found to be 1.0. The limit of detection (LOD) and limit of quantification (LOQ) were 4.044 μg/mL and 12.253 μg/mL, respectively. Tremendous recovery outcomes were observed and found to be 101%, 99.0%, and 99.5% for FVPR at 150% upper, 100% middle, and 50% lower concentrations, respectively.

**Conclusion:** All outcomes obtained comply with ICH guidelines. The developed method was simple, unique, accurate, robust, precise, and reproducible for determination of FVPR in tablet formulation. The method is novel and could be adopted in formulation industry.

**Key words:** Favipiravir, LC-MS/MS, method development, method validation, quantification

## INTRODUCTION

Favipiravir (FVPR) is an antiviral drug used for the treatment of all three types of influenza A, B, and C.<sup>1</sup> The International Union of Pure and Applied Chemistry (IUPAC) name of FVPR is 6-fluoro-3-hydroxy-2-pyrazine carboxamide with molecular formula C<sub>5</sub>H<sub>4</sub>FN<sub>3</sub>O<sub>2</sub> (Figure 1). This is a pyrazine carboxamide derivative. The melting point is about 187 °C to 193 °C. It is sparingly soluble in water, but completely soluble in organic solvents such as ethanol, dimethyl sulfoxide, and dimethylformamide. FVPR is a prodrug that goes through intracellular ribosylation and phosphorylation into adynamic form of FVPR ribofuranosyl-5'-triphosphate, inhibits viral RdRp (RNA-dependent RNA polymerase) and, can bind, transcript,

replicate the viral genome, and thereby inhibit the viral RNA polymerase.<sup>2-4</sup> Despite being vital against influenza, it was also revealed that FVPR exhibits antiviral activity against alpha-, filo-, bunya-, arena-, flavi-, and noroviruses and currently coronavirus disease-2019 (COVID-19).<sup>5,6</sup>

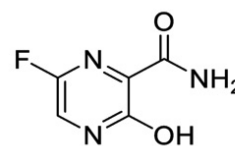


**Figure 1.** Structure of FVPR  
FVPR: Favipiravir

\*Correspondence: manjunathdh@davangereuniversity.ac.in, Phone: +91 9886646232, ORCID-ID: orcid.org/0000-0002-0634-6198

Received: 11.07.2022, Accepted: 15.10.2022



©2023 The Author. Published by Galenos Publishing House on behalf of Turkish Pharmacists' Association.

This is an open access article under the Creative Commons Attribution-NonCommercial-NoDerivatives 4.0 (CC BY-NC-ND) International License.

Literature survey revealed that few analytical methods are reported for determination of FVPR. A chromatographic separation method using high performance liquid chromatography (HPLC) with a runtime of 60 min was reported.<sup>7,8</sup> A liquid chromatography with tandem mass spectrometry/mass spectrometry (LC-MS/MS) method reported for the bioanalysis of antiviral drug FVPR in human plasma.<sup>9</sup> Quantification of FVPR in pharmaceutical formulations by HPLC-ultraviolet (UV) method, in which the total run time showed 15 min and limit of detection (LOD) and limit of quantification (LOQ) concentrations were in mg/mL.<sup>10</sup> HPLC and spectrofluorimetric methods were developed by Mikhail et. al.<sup>11</sup> for determination of FVPR. In the HPLC method, FVPR peak was eluted at 4.0 min and total run time was 10.0 minutes.<sup>11</sup> A pharmacokinetics method was developed by Nguyen et al.<sup>12</sup> for estimation of FVPR in Ebola-infected patients. The spectrofluorimetric method has been developed by Megahed et al.<sup>13</sup> for determination of FVPR and quantified in human

plasma. An LC-MS/MS method was reported for determination of multiple antiviral drugs.<sup>14</sup> Another LC-MS/MS method was reported for quantification of FVPR in human plasma.<sup>15,16</sup> A RP-HPLC method was reported for determination of FVPR in spiked human plasma.<sup>17</sup> LOQ of reported method was 0.72 µg/mL, where the linearity range was 0.2 µg/mL to 3.2 µg/mL. In the proposed method, the results were obtained in µg/mL. Another LC-MS method has been developed for the assay of FVPR in human plasma, LOQ of the method was found to be at 80 µg/mL, where the linear range reported was between 80 µg/mL to 30000 µg/mL.<sup>18</sup> The sensitivity of this method is quite more than the proposed method. An LC/LC-MS method<sup>19</sup> was reported in the literature for the determination of FVPR. This method is quite different from the proposed method. In this method, the route of degradation mechanism and degradation impurities are studied. LOD and LOQ of the method were 0.09 µg/mL and 0.027 µg/mL, respectively. The results of the reported methods are tabulated in Table 1.

**Table 1. Comparison of the statistical data of the reported methods and proposed methods**

Ref. no.	Analytical method	Results	Remarks
7	HPLC	LOD - 0.2 µg/mL LOQ - NA	Analyzed related substances of FVPR
8	HPLC	LOD - 0.2 µg/mL LOQ - NA	Analyzed related substances of FVPR
9	LC-MS/MS	LOD - NA LOQ - 100 µg/mL	FVPR determined in human plasma
10	HPLC-UV	LOD - 1.20 µg/mL LOQ - 3.60 µg/mL	Different mobile phase used, mixture of 50 mM potassium dihydrogen phosphate (pH 2.3) and acetonitrile (90:10, v/v)
11	HPLC and spectrofluorimetric	LOD - 0.985 LOQ - 2.986	FVPR determined in human plasma samples Mobile phase used as 0.02 M Brij-35, 0.15 M sodium dodecyl sulfate, and 0.02 M disodium hydrogen phosphate, pH 5.0
12	Pharmacokinetics	LOD - NA LOQ - NA	Other than HPLC-UV method developed
13	Spectrofluorimetric	LOD- 9.44 µg/mL LOQ- 28.60 µg/mL	Other than HPLC-UV method developed
14	LC-MS/MS	LOD - 25990 µg/mL LOQ - NA	FVPR determined in human serum
15	LC-MS/MS	LOD- NA LOQ- 60 µg/mL	FVPR identified in human plasma
16	LC-MS/MS	LOD - NA LOQ - 0.062 µg/mL	FVPR estimated in human serum
17	LC-MS/MS	LOD - NA LOQ - 0.72 µg/mL	FVPR spiked in human plasma
18	LC-MS/MS	LOD - NA LOQ - 80 µg/mL	FVPR determined in human plasma
19	LC-MS/MS	LOD - 0.09 µg/mL LOQ - 0.027 µg/mL	Determine impurity of FVPR and degradation route mechanism

NA: Not available, HPLC: High-performance liquid chromatography, LOD: Limit of detection, LOQ: Limit of quantification, FVPR: Favipiravir, LC-MS/MS: Liquid chromatography with tandem mass spectrometry, UV: Ultraviolet

Keeping the drawbacks of the reported LC-MS methods in mind, we developed and validated the LC/MS-MS method for determination of FVPR in pure and tablet dosage forms. In the proposed LC-MS/MS method, total run time was 5.0 min and the FVPR peak was eluted at 1.9 min. LOD and LOQ concentrations were found in  $\mu\text{g}/\text{mL}^{-1}$  concentrations. Hence, the proposed method is more sensitive than other reported methods. These results clearly indicate that the established method is simpler, accurate, reproducible, and robust than the reported methods.

## MATERIALS AND METHODS

### Instruments

Shimadzu prominence HPLC and LCMS-8045 instruments were used for the proposed method development and validation for determination of FVPR. HPLC instrument consisted of a deuterium lamp as the source of light, a UV detector, a quaternary pump, and an auto-injector. MS/MS system used was Shimadzu LCMS-8045, which achieves both high sensitivity and ultra-high-speed detection, outfitted by a heated electrospray ionization (ESI) probe. LCMS-8045 has maximum sensitivity in its category, which is designed to maximize sensitivity and minimize contamination by high-temperature heating block, heated ESI probe, drying gas, and heated desolvation line. The Lab Solutions software was used for the analysis and interpretation of data. All these factors provide robust instrumentation for the determination of FVPR.

### Chemicals and reagents

More than 98% purity of FVPR pure drug was provided by Karnataka Antibiotics and Pharmaceuticals Ltd. (Bengaluru, India) as a gift sample. FVPR tablets (label claim, 200 mg, commercial name-Avigan-200 mg, manufacturer-Dr. Reddy's Lab Ltd., India) were commercially purchased from local medical shops. HPLC-grade methanol and ammonium acetate were procured from Merck Ltd. (India). HPLC-grade ultrapurified water by Millipore purifier instrument was employed in the study. The stationary phase used was Shim-pack GISS, column (C<sub>18</sub>, 2.1 x 100 mm, and 1.9  $\mu\text{m}$ ) was obtained from Shimadzu Ltd. (Japan).

### Mobile phase preparation, standard stock solution and dilutions

The mobile phase consisted of 0.1 M ammonium acetate buffer of pH 6.5 in pump A and methanol in pump B. The standard stock solution of FVPR was prepared by dissolving accurately weighed 100 mg of FVPR into a 100 mL standard volumetric flask and made up to the mark with mobile phase. The prepared standard stock solution was of the concentration of 1000  $\mu\text{g}/\text{mL}$ . From

the above stock solution 1.0 mL was pipetted out into another 1000 mL standard volumetric flask and made up to the mark with the mobile phase. The concentration of resulting working standard solution was 10  $\mu\text{g}/\text{mL}$ . Similarly, working standard solutions of different concentrations of FVPR were prepared from least to maximum dilutions to examine the parameters of interest such as linearity, accuracy, recovery, LOD, and LOQ of the proposed method. For the assay analysis, the test sample weights were taken according to the standard equivalent and the following formula was used for the determination of test sample weights:

$$\text{Sample weight} = \frac{\text{Standard weight} \times \text{Average weight of 20 tablets}}{\text{Label claim of 1 tablet}}$$

### Chromatographic conditions

In method development, chromatographic conditions play an important role. The mobile phase consists of 10 mM ammonium acetate buffer of pH 6.5 in pump A and methanol in pump B, followed by a gradient program, as in Table 2. The stationary phase used was a Shim-pack GISS column. The flow rate of mobile phase was fixed at 0.4 mL/min. Column oven temperature was kept at 40 °C and wavelength of detection was fixed at 323 nm throughout the method development and validation. Sample injection volume was fixed at 10  $\mu\text{L}$ . With these chromatographic conditions, FVPR sharp peak was eluted at 1.9 min. Total run time was fixed at 5.0 min.

### Mass spectroscopy conditions

MS/MS system used was Shimadzu LC-MS-8045 consisting of heated ESI probe high-temperature gas supplements the nebulizer gas which improves the the desolvation efficiency. This facilitates the ionization of various compounds. High-voltage power supply for polarity switching, which assists fork ultrafast scan speed (30,000 u/s) and maintains a polarity switching time of 5 ms. High-speed acquisition benefits the laboratory by reducing run times for increased throughput and shortening the method development time. The system is designed to be robust. The heated desolvation line, high-temperature heating block, heated ESI probe, drying gas, and center optics all proceed to minimize contamination and maximize sensitivity. Lab Solutions software was used to analyze the complete method development and validation for the determination of FVPR and offers the latest features designed to streamline workflows and allow analysis to be started without long hours of method establishment.

**Table 2. Mobile phase gradient program**

Time in minutes	Pump A (10 mM ammonium acetate of pH 6.5)	Pump B (methanol)
0.01	90	10
2.00	40	60
3.10	90	10
5.00	90	10

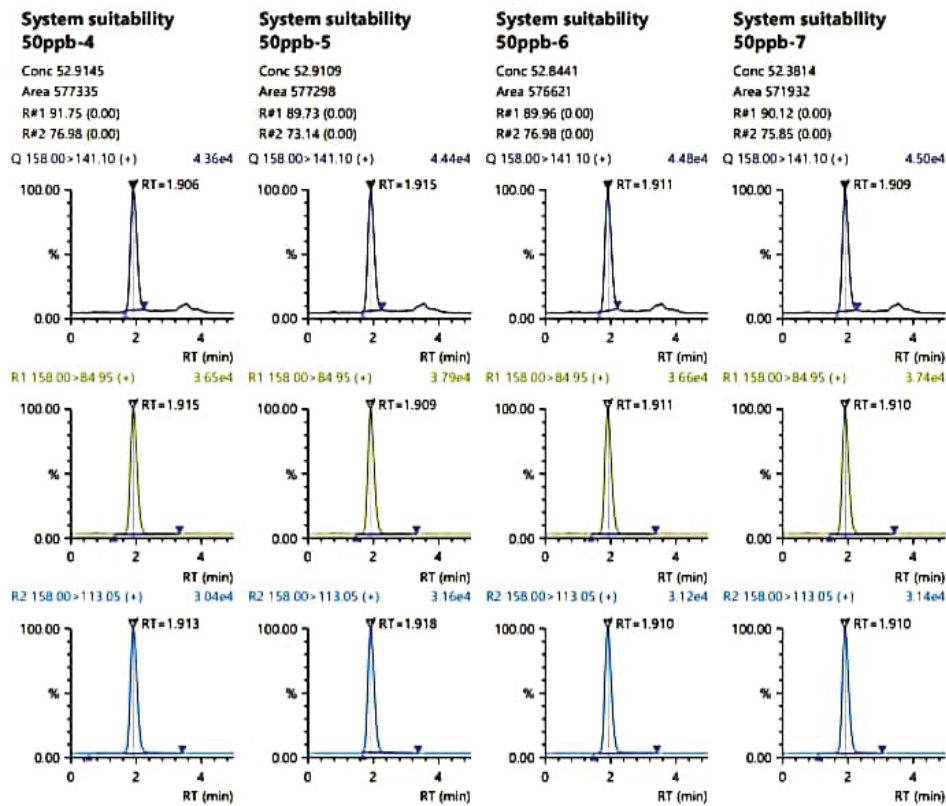


**Figure 2.** LC chromatograms of FVPR

LC: Liquid chromatography, FVPR: Favipiravir

The mass spectrometer with ESI probe operated in positive polarity, the data acquisition and processing were performed using Lab Solutions software. The distinguishing working conditions were as follows: nebulization gas flow was fixed at 3 L min, heating gas flow was kept constant at 10 L min, interference temperature was fixed at 150 °C, heat block temperature was kept constant at 300 °C, and drying gas flow was fixed at 10 L min. These conditions were maintained for mass spectrometer throughout the method development and validation process.

## RESULTS

### Method development

Mobile and stationary phases play an important role in the proposed method development and validation for determination of FVPR. The mobile phase was balanced by analyzing different trials with various mixtures of solution A (pump A) and solution B (pump B) followed by gradient time programs. FVPR sharp peak was eluted after various trials in mobile phase ratios. The expected peak was not eluted suitably after analyzing different ratios of pump A and B mobile phases. Hence, pump A mobile phase was replaced by 10 mM ammonium acetate of pH 6.5 and methanol in pump B. The wavelength of detection was fixed at 323 nm. Gradient time program was fixed as shown in Table 2. Under these conditions, FVPR sharp peak was eluted with a good baseline

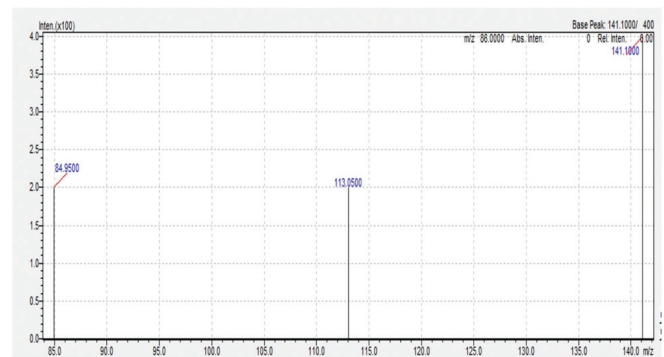


**Figure 3.** Mass spectrum of FVPR

FVPR: Favipiravir

in chromatograms as in Figure 2. In the mass spectrum, three peaks were observed  $m/z$ : 84.95,  $m/z$ : 113.05, and  $m/z$ : 141.1 (Figure 3). Hence, for the whole method development and validation, pump A was used for 10 mM ammonium acetate of pH 6.5 and pump B for methanol followed by the gradient time program as mentioned in Table 1. With these various trials, good peaks were observed in both chromatogram as well as mass spectrum and approximate fragment structures (ionized ion fragments) found and revealed in Figure 4. All the parameters of the proposed method were in compliance with the International Conference on Harmonization (ICH) guidelines.<sup>20</sup>

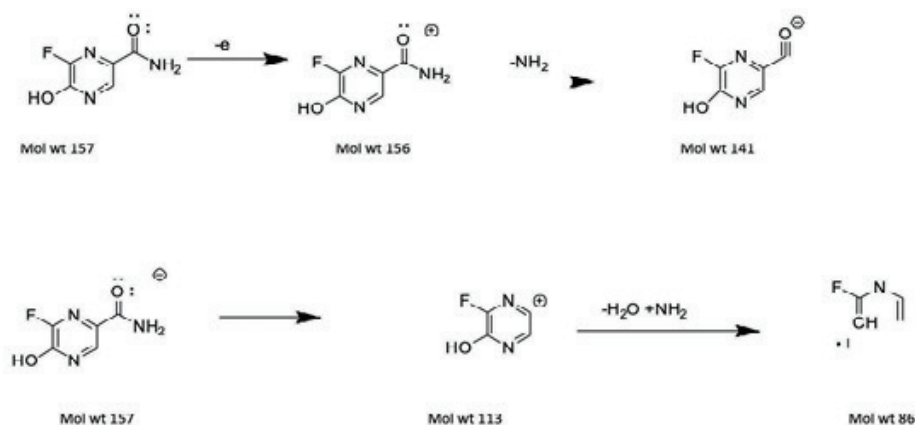


**Figure 4.** Fragmentation pattern of FVPR

FVPR: Favipiravir

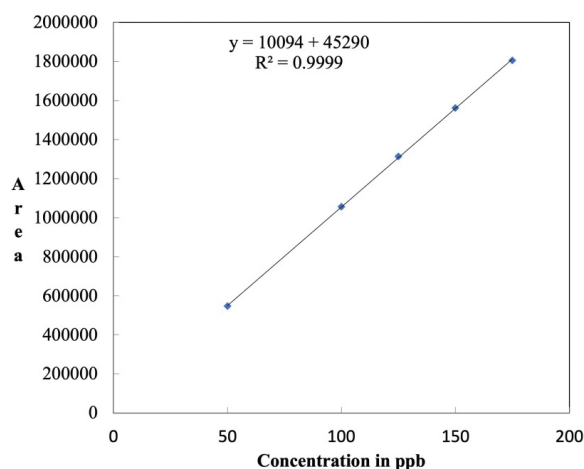


**Figure 5.** Linearity graph of FVPR

FVPR: Favipiravir

### Method validation

#### Linearity

In the proposed LC-MS/MS method, five concentrations between 50 and 200  $\mu\text{g}/\text{mL}$  standard solutions of FVPR were injected and examined. The regression significance was found suitable ( $R^2: 1.0$ ).  $Y = bX + C$  equation was used for determination of  $R^2$  values. The linearity graph of FVPR was designed by different areas against different concentrations of FVPR solutions. The resultant graph revealed a straight line for the FVPR as shown in Figure 5. The outcomes indicated that the method could be analyzed at various concentrations. Hence the developed an LC-MS/MS method is supposed to be validated. The results are presented in Table 3.

#### Precision

In the proposed method, precision data were found to be excellent and in accordance with ICH guidelines. The outcomes were found to be precise and well within the range. On the same day and on different days, six separately spiked standard

**Table 3.** Precision, LOD, LOQ, and linearity outcomes

Parameters	Results	Limit
<b>Precision</b>		
Intraday	0.09 RSD%	NMT - 2.0%
Interday	0.05 RSD%	NMT - 2.0%
LOD	4.044 $\mu\text{g}/\text{mL}$	-
LOQ	12.253 $\mu\text{g}/\text{mL}$	-
<b>Linearity</b>		
Range	50-200 $\mu\text{g}/\text{mL}$	-
Slope (b)	10122	-
Intercept (c)	42721	-
The correlation coefficient ( $R^2$ )	1.000	$R^2$ - above 0.995
Standard error of intercept	5063.3606	-
Standard deviation of intercept	12402.650	-

LOD: Limit of detection, LOQ: Limit of quantification, RSD: Relative standard deviation, NMT: Not more than

solutions and test solution were analyzed repetitively for the precision parameter. The intra- and inter-day performances were examined and outcomes revealed that there were not many deviations in the obtained results. The percentage of relative standard deviation of the test solution of six individual assay outcomes was found to be less than 2.0%. Therefore, it can be concluded that the developed LC-MS/MS method is precise. The results are revealed in Table 3.

#### The LOD and LOQ

Several methods for determining detection and quantification limits are described in ICH guideline.<sup>20</sup> These include visual assessment, signal-to-noise ( $S/N$ ) ratio calculations, response standard deviation calculations, and calibration curve slope calculations.

**Table 4. Recovery and assay results**

Parameter	Brand and label claim/tablet	Amount found mg/tablet	Concentrations in %	Assay, %	Recovery, %	RSD%	Limit
Assay (spiking FVPR)	Avigan 200 mg	201.0	100	100.5	-	0.02	98.0-102.0%
			50	-	100.1	0.51	
Recovery	-	-	100	-	101.5	0.72	
			150	-	101.2	0.64	

RSD: Relative standard deviation, FVPR: Favipiravir

**Table 5. Robustness data of FVPR**

Parameters	Actual	Low	High
Flow variation	0.4 mL/min	0.3 mL/min	0.5 mL/min
Column temperature (°C)	40	38	42
RSD%	0.9	1.1	1.3

RSD: Relative standard deviation, FVPR: Favipiravir

LOD and LOQ in the current study were determined using the third approach and were based on the  $3.3 \times (\sigma/m)$  and  $10 \times (\sigma/m)$  criteria, respectively.  $\sigma$  stands for the standard deviation of y-intercept of the regression line and  $m$  for the slope of the calibration curve. LOD and LOQ of the proposed method were found to be 4.044  $\mu\text{g/mL}$  and 12.253  $\mu\text{g/mL}$ , respectively. These results indicated that the method was very sensitive for the determination of FVPR. The results are tabulated in Table 3.

#### Recovery

In the recovery parameter, data was accomplished by three different concentration solutions of FVPR; lower, middle, upper, and blank was spiked at 50%, 100%, and 150% against the standard solution. The results obtained fulfilled the ICH guidelines. Hence, the established method was excellent. The standard formula was used to calculate outcomes. The data of the recovery parameter was found satisfactory as shown in Table 4. The limit of recovery range accepted is 98-102%. The obtained outcomes were well within the range for all three different concentrations. Therefore, the recovery parameter indicated that the proposed method can be used in industry.

#### Specificity

Standard procedures were used for the assay of FVPR. The clear and separated peak was found in liquid chromatography and in the case of mass spectrometer there were three peaks eluted at  $m/z$  84.95,  $m/z$  113.05, and  $m/z$  141.1, respectively. When injected these solutions separately, the consistent retention time and  $m/z$  obtained for both the standard (working standard) as well as test solution (formulation) were found to be between 98.0% and 102.0%. Thus, assay data were complying with the ICH guidelines. It was also observed that there was no probable excipient peak interference for the determination of FVPR. The following excipients were used for the specificity parameter: microcrystalline cellulose, starch, magnesium stearate, lactose monohydrate, micropowder silica gel, and magnesium sulfate.

These excipients did not interfere during the assay of FVPR using the LC-MS/MS method. Therefore, the proposed method revealed specificity for FVPR assay. Results of the assay were found to be satisfactory and are displayed in Table 4.

#### Robustness studies

The robustness parameter contains deliberate changes in the developed method. The known concentration of the standard solution of FVPR was injected at different conditions, *i.e.*, column oven temperature was changed from 40 °C to 35 °C and 45 °C and flow rate variation in the mobile phase ranging from 0.3 mL/min to 0.5 mL/min. The results are exhibited in Table 5. The acquired outcomes were satisfactory and comply with the ICH guidelines. There were no many deviations in the overall results. Hence, the established method can be used under varying conditions. Thus, the established LC-MS/MS method is robust.

#### Solution stability

Solution stability of FVPR was studied up to 48 h by keeping the solutions at 8 °C. To study this parameter, the standard (50  $\mu\text{g/mL}$ ) as well as the test solutions from 0 h to 48 h were injected. The obtained assay results were found to be 101.5%, 101.1%, 99.8%, and 99.0% for the 0, 12, 24, and 48 h, respectively. On observing these data, it can be concluded that there was no much deviation in the area and the calculated assay values up to 0 h to 48.0 h. Since the FVPR solution stability results were found stable up to 48 h, the developed LC-MS/MS is stable for determination of FVPR.

## DISCUSSION

The critical literature survey (Table 1) exposed that there were not many analytical methods on LC-MS/MS for estimating FVPR in bulk and formulations. Most of LC-MS/MS methods report the analysis of FVPR in biomatrix including plasma and body fluids. Further, some LC methods used different stationary and mobile phases for determination of FVPR in bulk and formulation forms. The reported analytical methods for the determination of FVPR were less sensitive and took more time for the analysis. Hence, it was planned to develop a highly sensitive, simple, reproducible, rugged, and robust analytical method for the determination of FVPR in pure and pharmaceutical formulations. In the proposed method, LOD and LOQ values were found to be 4.044  $\mu\text{g/mL}$  and 12.253  $\mu\text{g/mL}$ , respectively, while linearity range was found between

50 µg/mL to 200 µg/mL for five concentrations ( $R^2$ : 1.0). The results of solution stability studies were found to fit well within the limit. Recovery and assay data were found to be acceptable and better than literature methods. The developed method was highly sensitive, simple, accurate, rugged, reproducible, and robust. The proposed method is novel and exclusive, which can be employed in industries for the routine analysis of FVPR. The proposed method overcomes most of the limitations of the reported methods. The proposed method is cost-effective. Total run time of the method was much less. Hence, the method is reliable for the rapid analysis of FVPR and can reproduce accurate and precise results for the formulation samples as well.

## CONCLUSION

Majority of the formulations of an antiviral drug has analytical methods for their determination, such as LC-MS/MS, HPLC, UPLC, and UV-spectroscopic methods. FVPR is an antiviral drug used to prevent COVID-19 and other influenza. We developed an analytical method and validated it by LC-MS/MS instrument. The established method was highly sensitive, reproducible, and rugged. Above all, all parameters outcomes were complying with the ICH guidelines. Thus, the proposed LC-MS/MS method exposed the determination of FVPR in bulk and formulations.

### Ethics

**Ethics Committee Approval:** There is no requirement for ethical approval.

**Informed Consent:** Not applicable.

**Peer-review:** Externally peer-reviewed.

### Authorship Contributions

Concept: M.D.H., N.I., Design: N.I., H.A., Data Collection or Processing: H.A., N.I., Analysis or Interpretation: H.A., N.I., Literature Search: N.I., B.C.Y., Writing: M.D.H., N.I.

**Conflict of Interest:** No conflict of interest was declared by the authors.

**Financial Disclosure:** The authors declared that this study received no financial support.

## REFERENCES

1. Furuta Y, Gowen BB, Takahashi K, Shiraki K, Smee DF, Barnard DL. Favipiravir (T-705), a novel viral RNA polymerase inhibitor. *Antiviral Res.* 2013;100:446-454.
2. Furuta Y, Komeno T, Nakamura T. Favipiravir (T-705), a broad spectrum inhibitor of viral RNA polymerase. *Proc Jpn Acad Ser B Phys Biol Sci.* 2017;93:449-463.
3. Sissoko D, Laouenan C, Folkesson E, M'Lebing AB, Beavogui AH, Baize S, Camara AM, Maes P, Shepherd S, Danel C, Carazo S, Conde MN, Gala JL, Colin G, Savini H, Bore JA, Le Marcis F, Koundouno FR, Petitjean F, Lamah MC, Diederich S, Tounkara A, Poelart G, Berbain E, Dindart JM, Duraffour S, Lefevre A, Leno T, Peyrouset O, Irengue L, Bangoura N, Palich R, Hinzmann J, Kraus A, Barry TS, Berette S, Bongono A, Camara MS, Chanfreau Munoz V, Doumbouya L, Souley Harouna, Kighoma PM, Koundouno FR, René Lolamou, Loua CM, Massala V, Moumouni K, Provost C, Samake N, Sekou C, Soumah A, Arnould I, Komano MS, Gustin L, Berutto C, Camara D, Camara FS, Colpaert J, Delamou L, Jansson L, Kourouma E, Loua M, Malme K, Manfrin E, Maomou A, Milinouno A, Ombelet S, Sidiboun AY, Verreckt I, Yombouno P, Bocquin A, Carbonnelle C, Carmoi T, Frange P, Mely S, Nguyen VK, Pannetier D, Taburet AM, Treluyer JM, Kolie J, Moh R, Gonzalez MC, Kuisma E, Liedigk B, Ngabo D, Rudolf M, Thom R, Kerber R, Gabriel M, Di Caro A, Wölfel R, Badir J, Bentahir M, Deccache Y, Dumont C, Durant JF, El Bakkouri K, Gasasira Uwamahoro M, Smits B, Toufik N, Van Cauwenberghe S, Ezzedine K, D'Ortenzio E, Pizarro L, Etienne A, Guedj J, Fizet A, Barte de Sainte Fare E, Murgue B, Tran-Minh T, Rapp C, Piguët P, Poncin M, Draguez B, Allaford Duverger T, Barbe S, Baret G, Defourny I, Carroll M, Raoul H, Augier A, Eholie SP, Yazdanpanah Y, Levy-Marchal C, Antierrens A, Van Herp M, Günther S, de Lamballerie X, Keita S, Mentre F, Anglaret X, Malvy D; JIKI Study Group. Experimental treatment with favipiravir for ebola virus disease (the JIKI trial): a historically controlled, single-arm proof-of-concept trial in guinea. *PLoS Med.* 2016;13:e1001967. Erratum in: *PLoS Med.* 2016;13:e1002009. D'Ortenzio, Eric [corrected to D'Ortenzio, Eric]. Erratum in: *PLoS Med.* 2016;13:e1002066.
4. Dong L, Hu S, Gao J. Discovering drugs to treat coronavirus disease 2019 (COVID-19). *Drug Discov Ther.* 2020;14:58-60.
5. De Clercq E. New nucleoside analogues for the treatment of hemorrhagic fever virus infections. *Chem Asian J.* 2019;14:3962-3968.
6. Delang L, Abdelnabi R, Neyts J. Favipiravir as a potential countermeasure against neglected and emerging RNA viruses. *Antiviral Res.* 2018;153:85-94.
7. Feng G. A kind of Favipiravir has the HPLC assay method of related substance. 2016. China patent CN104914185B, 21 Sept 2016. <https://patents.google.com/patent/CN104914185B/en>
8. Feng G. HPLC method for measuring related substances in favipiravir; China patent. 2015. CN104914185A. <https://patents.google.com/patent/CN104914185A/en>
9. Morsy MI, Nouman EG, Abdallah YM, Zainelabdeen MA, Darwish MM, Hassan AY, Gouda AS, Rezk MR, Abdel-Megied AM, Marzouk HM. A novel LC-MS/MS method for determination of the potential antiviral candidate favipiravir for the emergency treatment of SARS-CoV-2 virus in human plasma: application to a bioequivalence study in Egyptian human volunteers. *J Pharm Biomed Anal.* 2021;199:114057.
10. Bulduk, I. HPLC-UV method for quantification of favipiravir in pharmaceutical formulations. *Acta Chromatogr.* 2021;33:209-215.
11. Mikhail IE, Elmanshi H, Belal F, Ehab Ibrahim A. Green micellar solvent-free HPLC and spectrofluorimetric determination of favipiravir as one of COVID-19 antiviral regimens. *Microchem J.* 2021;165:106189.
12. Nguyen TH, Guedj J, Anglaret X, Laouenan C, Madelain V, Taburet AM, Baize S, Sissoko D, Pastorino B, Rodallec A, Piorkowski G, Carazo S, Conde MN, Gala JL, Bore JA, Carbonnelle C, Jacquot F, Raoul H, Malvy D, de Lamballerie X, Mentre F; JIKI study group. Favipiravir pharmacokinetics in Ebola-infected patients of the JIKI trial reveals concentrations lower than targeted. *PLoS Negl Trop Dis.* 2017;11:e0005389.
13. Megahed SM, Habib AA, Hammad SF, Kamal AH. Experimental design approach for development of spectrofluorimetric method for determination of favipiravir; a potential therapeutic agent against COVID-19 virus: application to spiked human plasma. *Spectrochim Acta A Mol Biomol Spectrosc.* 2021;249:119241.
14. Habler K, Brügel M, Teupser D, Liebchen U, Scharf C, Schönermarck U, Vogeser M, Paal M. Simultaneous quantification of seven repurposed

- COVID-19 drugs remdesivir (plus metabolite GS-441524), chloroquine, hydroxychloroquine, lopinavir, ritonavir, favipiravir and azithromycin by a two-dimensional isotope dilution LC-MS/MS method in human serum. *J Pharm Biomed Anal.* 2021;196:113935.
15. Rezk MR, Badr KA, Abdel-Naby NS, Ayyad MM. A novel, rapid and simple UPLC-MS/MS method for quantification of favipiravir in human plasma: application to a bioequivalence study. *Biomed Chromatogr.* 2021;35:e5098.
  16. Eryavuz Onmaz D, Abusoglu S, Onmaz M, Yerlikaya FH, Unlu A. Development and validation of a sensitive, fast and simple LC-MS/MS method for the quantitation of favipiravir in human serum. *J Chromatogr B Analyt Technol Biomed Life Sci.* 2021;1176:122768.
  17. Duse PV, Baheti KG. Bioanalytical method development and validation for the determination of favipiravir in spiked human plasma by using RP-HPLC. *J Pharm Res Int.* 2021;33:275-281.
  18. Saraner N, Guney B, Sevici G, Saglam O. Determination of favipiravir in human plasma by using liquid chromatography-tandem mass spectrometry: application to pharmacokinetic studies. *Int J Analyt Bioanalyt Methods.* 2021;3:016.
  19. Vemuri DK, Gundla R, Konduru N, Mallavarapu R, Katari NK. Favipiravir (SARS-CoV-2) degradation impurities: identification and route of degradation mechanism in the finished solid dosage form using LC/LC-MS method. *Biomed Chromatogr.* 2022;36:e5363.
  20. International Council of Harmonization. Q2B validation of analytical procedures: methodology and availability. Federal Register. 1997;62:27463-27467.





# Development and Validation of a Spectrofluorimetric Method for the Quantification of Capecitabine in Bulk and Tablets

Swathi NARAPARAJU<sup>1\*</sup>, Ambati MUKTI<sup>2</sup>, Durga Panikumar ANUMOLU<sup>2</sup>, Soujanya CHAGANTI<sup>1</sup>

<sup>1</sup>Gokaraju Rangaraju College of Pharmacy, Department of Pharmaceutical Chemistry, Hyderabad, India

<sup>2</sup>Gokaraju Rangaraju College of Pharmacy, Department of Pharmaceutical Analysis, Hyderabad, India

## ABSTRACT

**Objectives:** A new, simple, and affordable spectrofluorimetric method was established for quantification of capecitabine in bulk and in marketed formulations.

**Materials and Methods:** Native fluorescence of capecitabine in 0.1% (w/v) cetrimide was measured at 386 nm after excitation at 313 nm.

**Results:** A linear relationship between fluorescence intensity and capecitabine concentration was noticed in 0.2-1.0 µg/mL range. The method was supported by checking several validation parameters as stated using International Conference on Harmonization (ICH) guidelines. The limit of detection (LOD) and quantification (LOQ) values (0.032 and 0.096 µg/mL, respectively) and results of validation parameters demonstrated that the method procedure were sensitive, accurate, precise, and reproducible (% relative standard deviation <2.0). The percentage assay in commercial formulation was found to be 99.2, which agrees with ICH guidelines.

**Conclusion:** Due to the above findings, developed method can be successfully adopted for routine analysis of capecitabine in pharmaceutical dosage forms.

**Key words:** Capecitabine, spectrofluorimetry, linearity, accuracy

## INTRODUCTION

Capecitabine is chemically known as pentyln-[1-[(2R,3R,4S,5R)-3,4-dihydroxy-5-methyloxolan-2-yl]-5-fluoro-2-oxypyrimidin-4-yl] carbamate (Figure 1). Being an antineoplastic drug, it is used for treating breast and colorectal cancers.<sup>1,2</sup> Extensive literature review of capecitabine disclosed several analytical methods for its quantification either alone or in combination with other drugs. Visible spectroscopic methods in methanol,<sup>3</sup> ultraviolet (UV) spectrophotometric methods in various solvents, such as methanol, ethanol, water, 0.1 N NaOH, 0.1 N HCl, water:acetonitrile (50:50),<sup>4-12</sup> electrochemical analysis,<sup>13</sup> atomic absorption spectroscopic method,<sup>14</sup> high performance liquid chromatography (HPLC) methods in combinations of

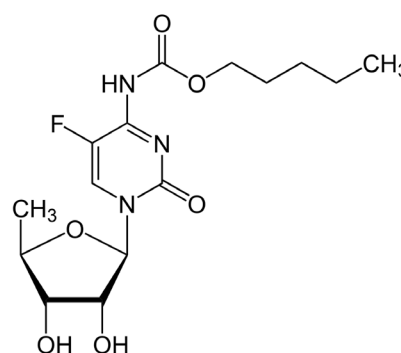


Figure 1. Chemical structure for capecitabine

\*Correspondence: swa.pharma@gmail.com, Phone: +91 909849059163, ORCID-ID: orcid.org/0000-0003-1442-6435

Received: 01.08.2022, Accepted: 23.10.2022



©2023 The Author. Published by Galenos Publishing House on behalf of Turkish Pharmacists' Association.

This is an open access article under the Creative Commons Attribution-NonCommercial-NoDerivatives 4.0 (CC BY-NC-ND) International License.

stationary and mobile phases,<sup>15-27</sup> high-performance thin-layer chromatographic (HPTLC) method,<sup>11,28</sup> ultra-high performance liquid chromatography (UPLC) method,<sup>29,30</sup> bioanalytical methods using HPLC,<sup>31-35</sup> HPTLC,<sup>36</sup> LC-MS/MS,<sup>37</sup> and UHPLC-MS/MS method<sup>38</sup> were reported in literature.

Although numerous instrumental techniques are available till date, no spectrofluorimetric method has been reported so far for capecitabine using cetrimide as solvent to the best of our knowledge. Chromatographic methods (HPLC, HPTLC, UPLC, etc.) require costly instrumentation, skilled technicians, and expensive solvents. Spectrofluorimetry attained exceptional status in drug analysis because of its appreciable specificity and sensitivity. Unlike spectrophotometry, the analysis can be achieved at both excitation and emission wavelengths in spectrofluorimetry.<sup>39</sup> Keeping these facts in view, a simple extraction free and sensitive spectrofluorimetric method was attempted for capecitabine using cetrimide as solvent. The method was validated as stated in International Conference on Harmonization (ICH) guidelines<sup>40</sup> and the same with success used for the quantification of capecitabine in marketed dosage form.

## MATERIALS AND METHODS

### Chemicals

Capecitabine (active pharmaceutical ingredient) was procured from Gland Pharma (Hyderabad, India). The marketed formulation containing capecitabine (Xeloda tablets, Sunrise Remedies Pvt. Ltd., Gujarat, India) was acquired from nearby drug store.

### Instrumentation

Various instruments including digital balance (Shimadzu, AUX 220D, Japan), pH Meter (Elico L120, Hyderabad, India), ultra sonicator (Sonica Ultrasonic Cleaner, Italy), melting point apparatus (DBK, Mumbai, India), UV-visible spectrophotometer (1800, Shimadzu, Japan), fourier transform infrared-spectrophotometer (IR affinity 1, DRS 8000, Shimadzu, Japan), and spectrofluorometer (Shimadzu, RF 5301 PC, Japan) were used in the present investigation. The standard statistical functions in MS-EXCEL were used to compute statistical parameters such as arithmetic mean, standard deviation (SD), and percent relative standard deviation (RSD%).

### Chemicals and reagents

#### Cetrimide (0.1% w/v)

Cetrimide was accurately weighed (0.1 g) and dissolved in adequate distilled water (in a volumetric flask) and diluted to 100 mL.

#### Capecitabine stock solution

A stock containing 1000 µg/mL of capecitabine was produced by transferring 10 mg of analyte to 10 mL of 0.1% (w/v) cetrimide in a volumetric flask and the contents were mixed well. These aliquots were transferred into 10 mL volumetric flasks and were suitably diluted with 0.1% (w/v) cetrimide to obtain final concentration of 10 and 100 µg/mL of capecitabine.

### Analytical method development

The spectrofluorimetric method development for capecitabine was attempted by dissolving the analyte in various solvents. Cetrimide 0.1% (w/v) was found to be suitable through optimization studies. The stock solution containing 10 µg/mL of capecitabine in cetrimide 0.1% (w/v) was used to identify the excitation and emission wavelengths. The excitation wavelength was fixed and solutions were scanned to get emission spectra. Capecitabine showed fluorescence at emission wavelength 386 nm following excitation at 313 nm, when 0.1% (w/v) cetrimide was used as a blank.

### Analytical method validation

The emerged method was validated as stated in the ICH specifications to prove applicability of the analytical method in quality control of capecitabine.

### Linearity

A set of 10 mL volumetric flasks holding aliquots of capecitabine in 0.2-1.0 µg/mL range in 0.1% (w/v) cetrimide was prepared. Intensities of above solutions were recorded for fluorescence at  $\lambda_{em}$  386 nm using an appropriate blank. The features of the calibration curve such as slope, intercept along with correlation coefficient were computed.

### Accuracy (recovery studies)

Degree of closeness of the results was determined by computing recoveries of capecitabine using the standard addition method. Standard solutions of capecitabine at 80, 100, and 120% levels were spiked to a fixed concentration of capecitabine from the tablet powder (equivalent to 0.5 µg/mL) contained in volumetric flasks. The volume in each flask was made up to mark with 0.1% (w/v) cetrimide. Fluorescence intensities of the emerged solutions were resolved at the emission wavelength of 386 nm. The recovery was verified by analyzing analyte in triplicate preparations at each concentration level.

### Precision

The repeatability/intra-day precision of the present method was set by assessing the corresponding response three times in a single day for three distinct concentrations of capecitabine (0.2, 0.6, and 1.0 µg/mL). The intermediate/inter-day precision was deliberated by estimating selected concentrations (0.2, 0.6, and 1.0 µg/mL) response in triplicate on three different days over a week period. The results of both studies were expressed as percentage relative standard deviation (% RSD).

### Sensitivity and robustness

Sensitivity of the analytical method was represented by determining the lowest detectable amount (LOD) and the lowest quantifiable amount (LOQ) using samples containing very low concentrations of capecitabine as per ICH guidelines. LOD and LOQ were calculated using the formulae  $3.3 \times (SD/slope)$  and  $10 \times (SD/slope)$ , respectively. Fluorescence intensity of the analyte solutions was also recorded by making small changes in emission wavelength to establish robustness in the analytical method.

### Assay of capecitabine in pharmaceutical dosage form

Twenty tablets of marketed formulation (Xeloda®) containing 500 mg of capecitabine were taken, precisely weighed and powdered. A quantity of powder analogous to 10 mg of capecitabine was transferred into a 10 mL volumetric flask and the volume was made up to mark with 0.1% (w/v) cetrimide (1000 µg/mL). The resulting solution was screened *via* Whatman filter paper (no: 41). An aliquot of the clear filtrate was suitably diluted to obtain 0.5 µg/mL of capecitabine in 0.1% (w/v) cetrimide and the same was used for testing. The amount of capecitabine was determined by substituting responses into equations of the straight line representing the calibration curves with a correction for dilution.

## RESULTS AND DISCUSSION

### Analytical method optimization

Capecitabine structure contains 5-fluoro-pyridimidin-2-one moiety in conjugation with amide group. The fluorescence potential of capecitabine may be attributed to the abovementioned chromophoric groups. This fluorometric method was optimized by studying type and concentration of the solvents. Stock solutions of capecitabine in solvents such as water, methanol, chloroform, dimethylsulfoxide, acetate buffer (pH 5.0), potassium dihydrogen orthophosphate (pH 3.0), tween 80 (0.25% v/v), sodium lauryl sulphate (0.1 N), urea (0.1 M), cetrimide, sodium hydroxide (0.1 N), and hydrochloric acid (0.1 N) were prepared separately from respective standard solutions (1000 µg/mL). Fluorescence intensity of capecitabine in cetrimide was found to be maximum among all. Hence, cetrimide was chosen as a suitable solvent for further analysis. Capecitabine in cetrimide exhibited maximum fluorescence at emission wavelength 386 nm, following excitation at 313 nm (Figure 2). Therefore, the same wavelengths were used in further method optimization. The effect of concentration of cetrimide on fluorescence intensity of the analyte was studied by testing different concentrations of cetrimide (0.1, 0.25, 0.5, 0.75, and 0.1% w/v). Sample solutions of capecitabine (10 µg/mL) prepared using the above cetrimide solutions were scanned and the results are provided in Table 1. Cetrimide, 0.1% (w/v) was found to be optimum as maximum fluorescence potential was noticed with the same. Capecitabine sample solutions prepared by dissolving in 0.1% (w/v) cetrimide were found to be stable up to 48 h at room temperature.

### Analytical method validation

#### Linearity

The optimized method was further justified as *per* ICH guidelines. The relationship between capecitabine concentration and corresponding fluorescence intensity was found linear over 0.2-1.0 µg/mL concentration range with an  $r^2$  of 0.9991. The regression equation obtained was  $y = 9.8571x + 0.1514$ . The method established a good correlation between concentration and fluorescence intensity of capecitabine over the studied concentration range. The results of linearity studies are given in Table 2 and Figure 3.

### Accuracy (recovery studies)

Three distinct levels (80, 100, and 120%) of standards (in triplicate) were spiked to commercial tablet powder to determine the accuracy of the proposed method. The mean percentage

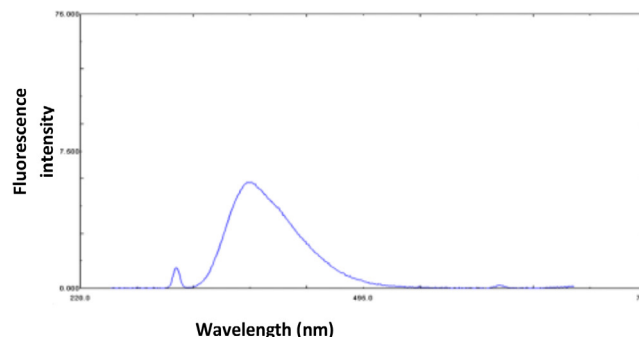


Figure 2. Excitation and emission spectra of capecitabine in 0.1% w/v cetrimide

Table 1. Effect of concentrations of cetrimide on capecitabine at  $\lambda_{em}$  386 nm

Serial no	Concentration (% w/v)	Fluorescence intensity at 386 nm
1	0.1	106.627
2	0.25	74.588
3	0.5	44.781
4	0.75	56.643
5	1.0	35.618

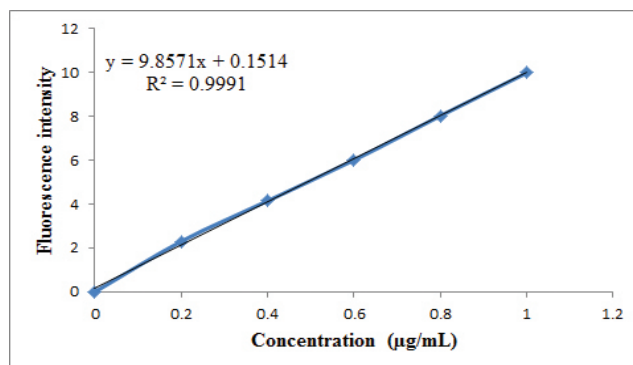


Figure 3. Calibration curve of capecitabine (0.2-1.0 µg/mL) in 0.1% (w/v) cetrimide

Table 2. Calibration curve data of capecitabine at  $\lambda_{em}$  386 nm

Serial no	Concentration (µg/mL)	Fluorescence intensity at 386 nm (AM $\pm$ SD) (n=3)
1	0.2	2.30 $\pm$ 0.095
2	0.4	4.15 $\pm$ 0.253
3	0.6	6.01 $\pm$ 0.303
4	0.8	8.03 $\pm$ 0.297
5	1.0	9.99 $\pm$ 0.143

AM: Arithmetic mean, SD: Standard deviation

**Table 3. Data for accuracy studies of capecitabine**

Analyte	Recovery level (%)	Conc. of sample ( $\mu\text{g/mL}$ )	Conc. of standard spiked ( $\mu\text{g/mL}$ )	Total amount ( $\mu\text{g/mL}$ )	Amount recovery (AM $\pm$ SD) ( $\mu\text{g/mL}$ ) (n=3)	%Recovery	%RSD <sup>a</sup>
Capecitabine	80	0.5	0.4	0.9	0.866 $\pm$ 0.0035	96.22	0.40
	100	0.5	0.5	1.0	1.08 $\pm$ 0.006	108.00	0.56
	120	0.5	0.6	1.1	1.16 $\pm$ 0.020	105.45	1.72

<sup>a</sup>Acceptance criteria: % RSD should not be more than 2.0, AM: Arithmetic mean, SD: Standard deviation, RSD: Relative standard deviation

**Table 4. Data for precision of analytical method**

Concentration ( $\mu\text{g/mL}$ )	Intra-day precision		Inter-day precision	
	Concentration estimated ( $\mu\text{g/mL}$ ) (AM $\pm$ SD)	% RSD <sup>a</sup>	Concentration estimated ( $\mu\text{g/mL}$ ) (AM $\pm$ SD)	%RSD <sup>a</sup>
0.2	0.23 $\pm$ 0.0018	0.78	0.224 $\pm$ 0.0026	1.16
0.6	0.727 $\pm$ 0.0047	0.65	0.658 $\pm$ 0.0053	0.81
1.0	0.946 $\pm$ 0.0034	0.36	0.927 $\pm$ 0.0071	0.77

<sup>a</sup>Acceptance criteria: %RSD should not be more than 2.0, AM: Arithmetic mean, SD: Standard deviation, RSD: Relative standard deviation

**Table 5. Assay of capecitabine in the marketed formulation**

Formulation	Label claim (mg)	Amount found (mg) (AM $\pm$ SD) (n=3)	% Assay	% RSD*
Xeloda <sup>®</sup>	500	496 $\pm$ 2.83	99.2	0.55

\*Acceptance criteria: %RSD should not be more than 2.0, AM: Arithmetic mean, SD: Standard deviation, RSD: Relative standard deviation

recoveries and percentage RSD of the same were calculated and reported in Table 3. Percentage recoveries were found to be 96.22, 108.00, and 105.45, respectively, for the three levels. The results were found to be satisfactory, which was indicated by %RSD <2.0.

#### Precision

Triplicate samples of three dissimilar concentrations containing 0.2, 0.6, and 1.0  $\mu\text{g/mL}$  of capecitabine were used for ascertaining the intra- and inter-day variability. Results of these studies are provided in Table 4. %RSD values were found to be <2.0, indicating the satisfactory exactness of the method.

#### Sensitivity and robustness

Sensitivity of analytical method was evidenced with LOD and LOQ values, which were found to be 0.032 and 0.096  $\mu\text{g/mL}$ , respectively. Furthermore, robustness of the proposed method was established by evaluating the influence of small variations in the emission wavelength at 386  $\pm$  2 nm. The results indicated that these changes did not greatly affect the fluorescence intensity.

#### Analysis of capecitabine in marketed formulation

The contemplated method was applied with success in commercial tablets. The amount of capecitabine in the formulation was found to be 496  $\pm$  2.83 mg and assay% was 99.2 (Table 5), which is in the acceptance range of 98.0-101.0% for capecitabine as per ICH guidelines. Percentage RSD less than 2.0 indicated the reliability of this method. The details of optimized conditions for the spectrofluorimetric method of capecitabine are given in Table 6.

**Table 6. System suitability parameters**

Parameters	Capecitabine
Excitation wavelength (nm)	313
Emission wavelength (nm)	386
Linearity range ( $\mu\text{g/mL}$ )	0.2-1.0
Slope (m)	9.8571
Intercept (c)	0.1514
Regression equation	Y= 9.8571x + 0.1514
Correlation coefficient ( $r^2$ )	0.9991
Accuracy (%RSD)	Less than 2.0
Precision (%RSD)	Less than 2.0
LOD ( $\mu\text{g/mL}$ )	0.032
LOQ ( $\mu\text{g/mL}$ )	0.096
Assay (%)	99.2

LOD: Lowest detectable amount, LOQ: Lowest quantifiable amount

## CONCLUSION

This spectrofluorimetric method developed for quantification of capecitabine in 0.1% (w/v) cetrimide was found to be simple, sensitive, and rapid. High scope of the method was evidenced through analysis of validation parameters. This method is more suitable, while working with low levels of capecitabine as the linearity range established over 0.2-1.0  $\mu\text{g/mL}$  concentrations

confirms the same. Adoptability of the method in quality control analysis of capecitabine was ascertained in the marketed tablets. Non-interference of the formulation excipients in the actual determination of capecitabine was noticed. Assay values (%) and %RSD values obtained during accuracy and precision studies were within the ICH stated limits. With the said features, the contemplated spectrofluorimetric method can be employed for routine quality control analysis of capecitabine in tablet dosage forms.

#### ACKNOWLEDGEMENTS

The authors are grateful to Prof. Giriraj T Kulkarni, Principal, Prof. CVS Subrahmanyam, Ex-Principal, Gokaraju Rangaraju College of Pharmacy and the Gokaraju Rangaraju Educational Society for providing necessary laboratory facilities.

#### Ethics

**Ethics Committee Approval:** Not applicable.

**Informed Consent:** Not applicable.

**Peer-review:** Externally peer-reviewed.

#### Authorship Contributions

Concept: S.N., A.M., D.P.A., S.C., Design: S.N., A.M., D.P.A., S.C., Data Collection or Processing: S.N., A.M., D.P.A., S.C., Analysis or Interpretation: S.N., A.M., D.P.A., S.C., Literature Search: S.N., A.M., D.P.A., S.C., Writing: S.N., A.M., D.P.A., S.C.

**Conflict of Interest:** No conflict of interest was declared by the authors.

**Financial Disclosure:** The authors declared that this study received no financial support.

#### REFERENCES

- Mader RM, Schrolnberger C, Rizovski B, Brunner M, Wenzel C, Locker G, Eichler HG, Mueller M, Steger GG. Penetration of capecitabine and its metabolites into malignant and healthy tissues of patients with advanced breast cancer. *Br J Cancer*. 2003;88:782-787.
- Kelly C, Cassidy J. Capecitabine in the treatment of colorectal cancer. *Expert Rev Anticancer Ther*. 2007;7:803-810.
- Harini U, Pawar AKM. Validated UV and visible spectrophotometric method for the estimation of capecitabine – a cancer drug. *Der Pharm Lett*. 2016;8:11-16.
- Kar AK, Kar B, Mahanti B, Kumar C. Method validation of capecitabine in API and pharmaceutical form by UV spectrophotometric method. *Asian J Pharm Clin Res*. 2020;13:191-194.
- Mishra MR, Agrawal P, Das SN. Newly developed highly sensitive method for the determination of capecitabine by using UV-spectroscopy. *Int J Pharm Sci Drug Res*. 2019;11:91-97.
- Vijaya Sri K, Prajawala K, Deepthi S, Niharika K. Method development and validation of UV and RP-HPLC method for the estimation of capecitabine in bulk and pharmaceutical dosage forms. *Asian J Res Chem*. 2018;11:731-738.
- Pallavi K, Srinivasa Babu P, Kishore Babu G. Development and validation of UV spectrophotometric method and RP-HPLC method for estimation of capecitabine in bulk and tablet dosage forms. *Int J Appl Pharm*. 2016;8:24-29.
- Mondal S, Narendra R, Ghosh D, Ganapaty S. Development and validation of RP-HPLC and UV spectrophotometric methods for the quantification of capecitabine. *Int J Pharm Pharm Sci*. 2016;8:279-287.
- Ramesh G, Subba Rao M. Development and validation of a simple and specific UV spectrophotometric method for capecitabine assay in active pharmaceutical ingredients (API) and in its dosage forms. *Int J Pharm Pharm Res*. 2015;2:152-160.
- Naveen Kumar M, Ravi Sankar P, Viswanath A, Srinivasa Babu P. Validated UV spectrophotometric method for quantitative analysis of capecitabine in pharmaceutical dosage form. *J Chem Pharm Sci*. 2013;6:231-233.
- Kandimalla R, Nagavalli D. Validated estimation of capecitabine by UV-spectroscopic, RP-HPLC and HPTLC method. *Int Res J Pharm*. 2012;3:163-166.
- Sreenivasa Rao T, Sukanya K, Chandanam Sreedhar, Akkamma HG, Sai Kumar SM. Development and validation of new analytical methods for the estimation of capecitabine in pharmaceutical dosage form. *Res J Pharm Bio Chem Sci*. 2012;3:713-721.
- Zhang Q, Xiaojun S, Fu Y, Liu P, Li X, Lui B, Zhang L, Li D. Electrochemical determination of the anticancer drug capecitabine based on a graphene-gold nanocomposite-modified galssy carbon electrode. *Int J Electrochem Sci*. 2017;12:10773-10782.
- Moeinpour F, Eshaghi Z. Indirect determination of anticancer drug capecitabine using hollow fiber supported multiwalled carbon nanotube coated on polyurethane foam. *Iranian J Anal Chem*. 2018;5:9-16.
- Vijaya Jyothi M, Bhargav E, Keerthana B, Varalakshmi Devi K. RP-HPLC method development and validation for the simultaneous estimation of irinotecan hydrochloride and capecitabine in active pharmaceutical ingredients (APIs). *Int J Res Pharm Sci*. 2018;9:63-67.
- Bhaskar Rao G, Sulochana K, Saicharan Kumar T, Dhanalakshmi U, Sami Mohamed Nasarbushara, Vinodkumar M, Parthiban P. A new method development and validation for the simultaneous estimation of capecitabine and gemcitabine by using RP-HPLC in a bulk and pharmaceutical dosage forms. *Int J Pharm Pharm Anal*. 2018;23-29.
- Patel DR. Method development, degradation pathway and kinetic of capecitabine. *Int J Pharm Chem Anal*. 2018;5:133-140.
- Bhatia MS, Raut JN, Barve AC, Patil PS, Jadhav SD. HPLC assay method development and validation for quantification of capecitabine in tablets and forced degradation samples. *Marmara Pharm J*. 2017;21:660-668.
- Chettupalli AK, Vivek K, Narender B, Vasudha Bakashi. Development and validation of capecitabine tablet (pharmaceutical dosage form) by using RP-HPLC method. *Indo J Pharm Sci*. 2017;4:550-557.
- Chaitanya G, Venkata Ramana G, Pawar AKM. RP-HPLC method development and validation of capecitabine in bulk drug and formulation. *Int J Pharm Anal Res*. 2016;5:190-198.
- Alagar Raja M, Anusha S, David Banji, Rao KNV, Selva Kuamar D. Analytical method development and validation of anticancer drugs (imatinib and capecitabine) by RP-HPLC method. *Asian J Res Chem Pharm Sci*. 2015;3:51-65.
- Rohit AP, Rajendra CD, Pravin DL, Pournima SS. Analytical method development and validation of capecitabine from tablet dosage form by using RP-HPLC. *Asian J Pharm Res Dev*. 2015;3:1-8.
- Devanaboyina N, Kishore YS, Pushpalatha P, Mamatha N, Venkatesh P. Development and validation of new RP HPLC method for analysis of capecitabine in pharmaceutical dosage form. *Int J Sci Inven Today*. 2013;2:21-30.

24. Sreevatsav ASK, Harishbabu AK. RP-HPLC method development and validation of capecitabine extended-release tablet dosage form. *Int J Pharm Sci Res.* 2013;4:4477-4487.
25. Pani Kumar AD, Venkata Raju Y, Sunitha G, Rama Krishna K, Ceema M, Venkateshwara Rao A. Development of validated stability indicating RP-HPLC method for the estimation of capecitabine in pure and pharmaceutical formulations. *Int J Res Pharm Biomed Sci.* 2011;2:175-181.
26. Rajesh V, Anupama B, Jagathi V, Sai Praveen P. Simultaneous estimation of gemcitabine hydrochloride and capecitabine hydrochloride in combined tablet dosage form by RP-HPLC method. *E-J Chem.* 2011;8:1212-1217.
27. Prakash KV, Rao JV, Raju NA. Validated, reversed phase high performance liquid chromatography method for the estimation of capecitabine in pharmaceutical formulations. *Orient J Chem.* 2008;24:335-338.
28. Patel PB, Patel PU. Development and validation of high performance thin layer chromatographic method for simultaneous estimation of temozolomide and capecitabine in synthetic mixture. *World J Pharm Res.* 2016;5:1308-1316.
29. Deepali G, Nema RK, Singhvi IJ. Isolation, characterization and quantification of potential hydrolytic degradant (5'-deoxy-5-fluorocytidine) of an anti-cancer agent capecitabine. *Int J Innov Pharm Sci Res.* 2014;2:2332-2343.
30. Hanumantha Rayudu K, Sreeramulu J, Maheswara Reddy M. Determination of stability indicating assay method for capecitabine in pharmaceutical drug substances a comparative study by UPLC and HPLC. *J Pharm Res.* 2012;5:5515-5519.
31. Salomi P, Purushothaman M, Satyanarayana SV. Bioanalytical method development and validation of capecitabine in plasma by RP-HPLC. *J Global Trends Pharm Sci.* 2017;8:4106-4111.
32. Hassanlou S, Rajabi M, Shahrasbi AA, Afshar M. Development and validation of an ecofriendly HPLC-UV method for determination of capecitabine in human plasma: Application to pharmacokinetic studies. *S Afr J Chem.* 2016;69:174-179.
33. Piórkowska E, Kaza M, Fitatiuk J, Szlaska I, Pawiński T, Rudzki PJ. Rapid and simplified HPLC-UV method with on-line wavelengths switching for determination of capecitabine in human plasma. *Pharmazie.* 2014;69:500-505.
34. Farkouh A, Ettlinger D, Schueller J, Georgopoulos A, Scheithauer W, Czejka M. A rapid and simple HPLC assay for quantification of capecitabine for drug monitoring purposes. *Anticancer Res.* 2010;30:5207-5211.
35. Jayaseelan S, Bajivali SK, Ramesh U, Sekar V, Perumal P. Bioanalytical method development and validation of capecitabine by RP-HPLC method. *ChemTech.* 2010;2:2086-2090.
36. Thorat SG, Chikhale RV, Tajne MR. A rapid and simple HPTLC assay for therapeutic drug monitoring of capecitabine in colorectal cancer patients. *Biomed Chromatogr.* 2018;32.
37. Singhal P, Shah PA, Shah JV, Sharma P, Shrivastav PS. Determination of capecitabine - an anticancer drug in dried blood spot by LC-ESI-MS/MS. *Int J Pharm Pharm Sci.* 2015;7:238-245.
38. Wang Z, Li X, Yang Y, Zhang F, Li M, Chen W, Gao S, Chen W. A sensitive and efficient method for determination of capecitabine and its five metabolites in human plasma based on one-step liquid-liquid extraction. *J Anal Methods Chem.* 2019;2019:9371790.
39. Naraparaju S, Anumolu PKD, Gurrula S, Galennagari R. Quantification of tamsulosin hydrochloride and solifenacin succinate by discriminative derivative synchronous emission spectroscopy. *Turk J Pharm Sci.* 2018;15:149-155.
40. Q2 (R1), International Conference on Harmonisation, Guideline on Validation of Analytical Procedure: Text and Methodology; 2005. Available from: [https://www.ema.europa.eu/en/documents/scientific-guideline/ich-q-2-r1-validation-analytical-procedures-text-methodology-step-5\\_en.pdf](https://www.ema.europa.eu/en/documents/scientific-guideline/ich-q-2-r1-validation-analytical-procedures-text-methodology-step-5_en.pdf)



# Role of Chitosan-Loaded Solanine Glycoalkaloid from *Solanum scabrum* Mill. Leaf Extract as Anti-Inflammatory and *In Vitro* Anticancer Agents

Cletus Anes UKWUBILE<sup>1\*</sup>, Emmanuel Oise IKPEFAN<sup>2</sup>, Ademola Clement FAMUREWA<sup>3</sup>

<sup>1</sup>University of Maiduguri, Faculty of Pharmacy, Department of Pharmacognosy, Maiduguri, Nigeria

<sup>2</sup>Delta State University, Faculty of Pharmacy, Department of Pharmacognosy and Traditional Medicine, Abraka, Nigeria

<sup>3</sup>Alex Ekwueme Federal University, Faculty of Basic Medical Sciences, College of Medicine, Department of Medical Biochemistry, Abakaliki, Nigeria

## ABSTRACT

**Objectives:** *Solanum scabrum* Mill. commonly “African nightshade” or “huckleberry” is a plant, whose leaves are used by tribes in Nigeria and Cameroon for making the popular “Kombi” and “Njama Njama” soups, respectively. This study aimed to evaluate the anti-inflammatory and anticancer activities of the leaf crude methanol extract from *S. scabrum*.

**Materials and Methods:** Fractions of the plant were tested for anti-inflammatory potential and *in vitro* anticancer activity on MCF-7 and HMVII cell lines by carrageenan-induced oedema in mice, and cytotoxicity assays such as 3-(4,5-dimethylthiazol-2-yl)-2,5-diphenyl-2H-tetrazolium bromide, transwell migration and invasion assays, and apoptosis study by flow cytometry, respectively.

**Results:** Bioguided isolation yielded a white crystalline compound 3-nitro dibenzofuran (C<sub>12</sub>H<sub>7</sub>NO<sub>3</sub>, *m/z*: 213.19 g/mol, *m.p.*: 181.49 °C). <sup>1</sup>H-NMR showed seven signals at δ (ppm) 2.8-4.3 consisting of two doublets and five singlets, while <sup>13</sup>C-NMR revealed twelve carbons, which are majorly methyl carbons at δ (ppm) between 120 and 195. All tested samples demonstrated dose-dependent anti-inflammatory activity in carrageenan-induced mice. The isolated compound, *i.e.* solanine, and chitosan-loaded drugs showed significant inhibitory activity on the cell lines with inhibitory concentration 50 (IC<sub>50</sub>) values of 8.52, 0.82, and 22.1 µg/mL, respectively on MCF-7 cell line and 4.54, 0.08, and 12.1 µg/mL, respectively, on HMVII cell line, while doxorubicin (adriamycin) positive control, had IC<sub>50</sub> values of 0.02 and 0.06 µg/mL, respectively, on MCF-7 and HMVII cancer cells. Selectivity index of solanine was the lowest in the study, hence, it lacks the ability to differentiate between cancerous and normal cell Vero E6 cell lines. Chitosan-loaded drugs quicken early apoptosis and sustained late apoptosis in cells with much improved selective indices.

**Conclusion:** The results obtained from this study further affirmed the use of chitosan nanoparticles as carriers for anticancer drugs.

**Key words:** *Solanum scabrum*, anti-inflammatory, anticancer, chitosan, solanine, glycoalkaloid

## INTRODUCTION

Humans have relied on natural products such as medicinal plants for their day-to-day needs such as medicines, food, and shelter since time immemorial. Plants have played crucial roles in mitigating the deleterious effects of various diseases from different regions of the world.<sup>1,2</sup> As one moves from one geographical location to the other, plant's morphological parts such as leaves, stembarks, roots, flowers, seeds,

and buds are used ethnobotanically in various forms such as anti-inflammatory, antimalarial, anticancer, antioxidant, anticonvulsant, antihelminthic, antidiabetic, antihypertensive, antiviral, and antiulcer agents. Some preparations are used as decoctions, infusions, tinctures, ointments or powders. Regardless of their mode of preparation, the main goal is to confirm a possible ethnopharmacological effect on the targeted disease. Recently, use of plants and compounds from plants as

\*Correspondence: doccletus@yahoo.com, Phone: +90 08035985667, ORCID-ID: orcid.org/0000-0001-7183-4510

Received: 16.06.2022, Accepted: 12.11.2022



©2023 The Author. Published by Galenos Publishing House on behalf of Turkish Pharmacists' Association.

This is an open access article under the Creative Commons Attribution-NonCommercial-NoDerivatives 4.0 (CC BY-NC-ND) International License.

anti-inflammatory and anticancer agents has gained popularity, especially in countries with low access to conventional anti-inflammatory and anticancer drugs due to a lack of income and availability of quality drugs. In addition, the side effects of most anti-inflammatory and anticancer drugs have paved the way for the lack of trust in these conventional drugs in African countries such as Nigeria, Cameroon, Ghana, South Africa, Egypt, Kenya, Congo DR, Gambia, Sudan, and others.<sup>3-6</sup> The ability of medicinal plants to illicit remarkable ethnopharmacological effects on organs, tissues, and cells is solely dependent on the secondary metabolites present in the plant. For instance, alkaloids, flavonoids, saponins, tannins, and terpenoids play various roles in the disease conditions of humans.<sup>7-9</sup>

Inflammatory disease is a type of illness that is usually characterized by swelling of a part of the body, organ or tissues. It usually occurs as a result of immunological response to bacterial invasion, ruptured cells or tissues, poisonous substances in the body and immune breakdown, which could be either acute or chronic.<sup>10</sup> Treatment of inflammation is commonly carried out using non-steroidal anti-inflammatory drugs and some of these drugs have been reported to cause various degrees of side effects in the body pharmacologically, notably some proton pump inhibitors like diclofenac sodium.<sup>11</sup> Like inflammation, cancer has been one of the greatest nightmares in human health challenges before the coronavirus disease-2019 pandemic (COVID-19) in 2019.

Cancer accounts for about 40% of deaths worldwide. The major causes of cancer are not fully understood, but it is caused by mutations in oncogenes. Cancers are named according to the organ or part of the body they are found and all have semblances in how they illicit pathological effects in humans.<sup>12,13</sup> To date, treatment of cancers with conventional drugs has yielded little or no results due to the negative side effects of most anticancer drugs. Current research is focused on the use of natural anticancer agents from plants that have shown potent ethnopharmacological effects on cancer cells. These phytoconstituents have been used ethnomedically to successfully treat cancers such as those of the breast, cervix, colon, scrotum, and ovary.<sup>3</sup>

Currently, in order to overcome the challenges experienced by most anticancer drugs in targeting cancer cells successfully, chemotherapeutic drugs are loaded either actively or passively in carriers such as chitosan to deliver their contents onto cancer cells, thereby inducing apoptosis in the cell.<sup>14,15</sup> Chitosan nanoparticles (CSNP) are particles of size 1-1000 nm that are made by the exoskeletons of crustaceans (crabs and prawns). They are used as carriers for anticancer, antifungal, and antimicrobial drugs.<sup>16,17</sup> Chitosan is a drug and protein carrier because of its numerous advantages such as biodegradability, target specificity, accessibility, little or no toxicity, easy method of preparation, ability to pass over, and evade the body's defence unnoticed.

Among the plants used to treat inflammation and cancers in Mambila (Taraba State, Nigeria) is *Solanum scabrum* Mill. (commonly called African nightshade or garden huckleberry) (Solanaceae). It is locally called "kombi" in the Hausa and

"fulfulde" languages. The leaf is used to make "kombi" and "njama" soups in Gembu (Mambila, Taraba state) and Cameroon, respectively. It grows well in countries of West Africa (Nigeria and Ghana), Central Africa Republic, and East Africa (Cameroon) at very low temperatures.<sup>3</sup> The leaf of *S. scabrum* is an important delicacy in Nigeria and Cameroon because it is believed to possess antioxidant, anticancer, analgesic, anti-inflammatory, antispasmodic, and vasodilatory activities, while these claims are still being verified. Phytochemical screening of the leaves and roots showed that *S. scabrum* contains flavonoids, alkaloids, saponins, and tannins as well as steroidal saponins such as solanine, a glycoalkaloid derivative. It also contains numerous nutrients like proteins, iron, ascorbic acid, and vitamins.<sup>18</sup> Despite the health and nutritional benefits derived from *S. scabrum*, there is a major concern regarding the presence of solanine glycoalkaloid in the leaf and root extracts of many nightshade families, even though it has not been confirmed in *S. scabrum*.<sup>19,20</sup> Solanine is found in almost all the nightshade family (Solanaceae) and has been termed an alkaloid poison, which is used as fungicide and pesticide.<sup>21</sup> In traditional medicine, the leaves and roots are also used as sedative and anticonvulsant agents and for treating asthma, acute cough, and cold.<sup>22</sup>

In the present study, we evaluated the anti-inflammatory potential and *in vitro* anticancer activity of *S. scabrum* on breast and vaginal melanoma cell lines. We isolated solanine as a glycoalkaloid from the leaf crude methanol extract and checked its purity using thin-layer chromatography (TLC) and high-performance liquid chromatography (HPLC). The effects of crude extracts, fractions, solanine, and chitosan loaded with these samples on the cell lines were also evaluated *in vitro*. The study further investigated the pH, at which chitosan-loaded drugs release more drugs *in vitro* release study. Therefore, this study was designed to evaluate the therapeutic effects of solanine glycoalkaloid in cancer treatment and chitosan-loaded drugs against cancer cell lines.

## MATERIALS AND METHODS

### Materials and reagents

Acetic acid, NH<sub>4</sub>OH solution, sulphuric acid, HPLC grade, Dulbecco's minimum essential medium (DMEM), and 3-(4,5-dimethylthiazol-2-yl)-2,5-diphenyl-2H-tetrazolium bromide (MTT) reagent were purchased from Sigma-Aldrich (St. Louis Mo, USA). MCF-7 human breast cancer cell, HMVII woman vaginal melanoma cancer cell, and Vero E6 cell line from an African green monkey were obtained from the ATCC (USA), dimethyl sulfoxide (DMSO), glutaraldehyde (GA), propidium iodide (PI), 0.5% tween 20 solution, and 0.1% RNase were obtained from Benrocks' Medicals Nigeria (Sigma Aldrich). Apo alert caspase-3-colorimetric assay kit was purchased from Clontech (USA), while chitosan 100 G (purity: 99+ % deacetylated) was purchased from Chemsaver (USA). Doxorubicin USP and diclofenac BP were supplied by Jude Pharmacy Ltd. (Nigeria). The remaining reagents and solvents were of analytical grade.



### Collection plant material

Fresh leaves of *S. scabrum* (kombi) were collected in the early morning hours (5-6 a.m.) (temperature: 4-8 °C) from a farm land in Gembu, Sarduana Local Government Area, Taraba State, Nigeria (a border town between Nigeria and Cameroon). Identification of the plant was done by a taxonomist, Dr. Jones Ponè of the Forest Guide, Ogurugu, Nigeria, with voucher number OFG/SOL/0024. The leaves were air-dried under shade for two weeks and pulverized into fine powder using an electronic blender, weighed, and stored in a clean container for further use.

### Preparation of extract

Powdered leaves of *S. scabrum* weighing 1500 g were extracted with 2.5 L of methanol using a cold maceration technique for 72 h. It was carefully filtered three times using whatman no. 9 filter papers into a clean beaker. The filtrate obtained was evaporated to dryness using a Buchi R-300 rotary evaporator (Thomas Scientific, USA) at 45 °C to produce a final yield of 50% (w/w). The dark green colored extract was then stored in a clean sample bottle and kept in a refrigerator at -4 °C for onward use.

### Isolation of solanine

Exactly 80 g of powdered leaves were subjected to cold maceration with 250 mL 5% acetic acid solution (v/v) in a 500 mL capacity beaker for 24 h. The extract was filtered using whatman no. 1 filter paper to remove any cellular debris present. The content was warmed to 70 °C and allowed to cool. pH was adjusted to 10 by adding 10 mL solution of concentration NH<sub>4</sub>OH dropwise and centrifuged at 1200 rpm for 5 min. The supernatant was discarded while the precipitate was washed with NH<sub>4</sub>OH (1%), recentrifuged, and concentrated *in vacuo* to obtain crude solanine. Presence of solanine was qualitatively confirmed by an instant production of red to violet coloration with formaldehyde and sulfuric acid solutions.<sup>23</sup> The crude solanine isolated was purified by boiling for 5 min in 50 mL methanol solution, filtered, and concentrated to obtain brownish solanine crystals (weight: 8.4 g). A TLC plate was used to check the purity of solanine using acetic acid:ethanol (1:3) as the solvent system by obtaining a single spot on the TLC plate.<sup>24</sup>

### Purity check of isolated solanine using HPLC analyses

HPLC analyses were performed on an Agilent 1290 Infinity Series HPLC system (Agilent Technologies, UK) with a G4212A diode array detector, G1316C thermostatted column compartment (TCC). Column temperature was 25 °C, a G4220A binary pump with 5 mL/min flow rates and a G4226A infinity autosampler. Solvent A mobile phase was made up of acetonitrile solution, while B was water mixed with phosphoric acid solution (0.2%). Elution was performed using a gradient elution at a flow rate of 1 mL/min. The wavelength was 270 nm, while the sample injection was 5 µL. Total runtime for the analyses was 45 min.

### Bioguided partitioning of extract

The methanol extract weighing 250 g was dissolved in a 500 mL capacity separating funnel (Thomas Scientific, USA) containing mixture of distilled water and methanol (7:3) and partitioned

three times each with 500 mL of *n*-hexane (HF), ethyl acetate (EF), and *n*-butanol (BF) for bioguided anti-inflammatory and anticancer activities. Each fraction was concentrated *in vacuo* to produce respective yields of 8 g, 48.6 g, and 22.4 g fractions, and tested for their anti-inflammatory and anticancer activities *in vitro*. The fractions with most active bioactivities were each subjected to silica gel (60 x 120 mesh; 100 g) column chromatography using gradient elution fractions with the following solvent systems: HF:EF (7:3); HF:EtOAc:MeOH (5:3:2), and BF; HF:EtOAc:BF (6:3:1). 50 sub-fractions of 30 mL were collected from each fraction. Subfractions with similar profiles (R<sub>f</sub> values) each on the TLC plates were pooled together and further subjected silica gel column to obtain additional subfractions. Subfractions with the best activity was subjected to Sephadex® G5050-10G (Merck, Germany) and eluted with EtOAc:MeOH (2:8). Characterization of bioactive compounds was performed using NMR and gas chromatography-mass spectrometry (GC-MS).

### Preparation and characterization of CSNPs loaded extract

Extracts weighing 1 g each were dissolved in 400 mL acetic acid solution (1%, v/v) in a beaker and mixed with 4 g of chitosan (100% purity; 90+ % deacetylated, Chemsaver, USA), which was previously dissolved in 10 mL deionized water, and made up to 100 mL, then stirred properly for 10 min. Then, 500 µL GA (a cross-linker) was added in dropwise under constant magnetic stirring using a 10 mL sterilized syringe at 3000 rpm for 30 min on a Young-Ji HMZ 20DN magnetic stirrer (made in China). Chitosan-loaded drugs were prepared in batch codes of CE1 to CE4 for chitosan-loaded with crude leaf extract. CS1 to CS4 for chitosan-loaded with solanine and CDR1 to CDR4 for chitosan-loaded with doxorubicin as the reference anticancer drug. Batch codes CE1, CS1, and CDR1 were not crosslinked with GA for the sake of comparison. The prepared chitosan formulations were each spray-dried using a nano spraying drying apparatus (Shanghai, China) with 0.5 mm nozzle diameter, inlet and outlet temperatures of 130 °C and 65 °C, respectively, atomization air pressure of 38 mbar, liquid flow rate of 2.5 mL/min, and drying airflow of 1.5 m<sup>3</sup>/min. Characterization of drug loaded microspheres was carried out in terms of yield, morphology, particle size, % drug entrapment or encapsulation efficiency, and *in vitro* drug release.<sup>25-27</sup>

### Percentage yield of CSNPs

The developed CSNPs were dried using nanospray dryer (Shanghai, China). The dried microspheres were collected and weighed, while percentage yield was calculated using the formula below:

% Yield = (Final weight of dried CSNPs / initial weight of starting materials) 100.<sup>25</sup>

### Morphology of CSNPs

The surface morphology of CSNPs using a phenom desktop scanning electron microscope (SEM) with fully integrated energy dispersive spectroscopy and scanning electron detector (Thermo Fisher Scientific, Nigeria). Diethyl pyrocarbonate dissolved CSNPs were observed at 3000x magnification for the morphology and the extent of encapsulation.<sup>25-27</sup>

### Particle size of CSNPs

CSNPs were diluted in 0.1 M KCl and placed in an electrophoresis cell of field potential 15.4 v/cm connected to a Zetasizer apparatus (Malvern Zetasizer 3000 HS, UK) to determine the sizes and charges of the microspheres. Three readings were taken and means taken.<sup>27</sup>

### Percentage entrapment or encapsulation efficiency of CSNPs

The developed CSNPs were re-dispersed in deionized water and centrifuged at 3000 rpm for 30 min at 25 °C to separate the microspheres from the supernatant. Thereafter, CSNPs were diluted with phosphate buffer saline (PBS) (pH: 7.4) and the solution concentration was then measured using Shimadzu Ultraviolet (UV)-1900 UV-Visible (vis) Spectrophotometer (Shimadzu Europa GmbH, Duisburg, Germany) at 266 nm. The percentage entrapment was then calculated using the formula below:<sup>27</sup>

Entrapment/encapsulation efficiency% = (experimental drug contents/total drug contents) 100

The prepared nanoencapsulated formulations were used in *in vitro* anticancer study.

### Drug release study of CSNPs

The *in vitro* drug release study was carried out using dialysis tubes method. In this procedure, the CSNPs prepared were dissolved in 5 mL PBS of pH 7.4. Then, 500 mL-volume beakers were filled with 150 mL PBS for each formulation code. The dialysis tubes were then filled with 10 mL of formulated chitosan/drugs and both ends of the dialysis bags were tied using clean ropes. It was then placed in the beakers and subjected to stirring under a magnetic stirrer at 1500 rpm at 37 °C. In every one hour, 5 mL of the contents from the beaker was drawn and replaced with a fresh 5 mL of PBS and continued for 6 h. The amount of drug release in the study was then determined by measuring the contents using UV-vis spectrophotometer at 570 nm.<sup>26,27</sup>

### Experimental animals

Thirty Swiss albino mice of opposite sexes weighing between 15 and 25 g were purchased from the animal house of the Department of Pharmacology, University of Jos, Nigeria. The animals were housed in a metal cage (90 cm x 45 cm) with access to clean water and feed and were maintained at normal temperature. They were allowed to acclimatize for two weeks in the laboratory before the *in vivo* experiment. Ethical approval for the use of these animals was given by Research Ethical Committee of the University of Jos, Nigeria (UJ/FPS/ F17-00379, date: 31.07.2018).

### *In vivo* anti-inflammatory: carrageenan-induced anti-inflammatory mouse model

The mice were grouped into five groups of six animals. Mice in group 1 served as the negative control which received 2 mL normal saline, group 2 was the positive control which received 100 mg/kg diclofenac BP, while groups 3, 4, 5, and 6 were the treatment groups which received 200, 400, 800, and 1.200 mg/kg *b.w.* doses of *S. scabrum* extracts (*i.p.*). The doses were

calculated on 30% lethal dose obtained from previous toxicity studies.<sup>27</sup> Paw edema was induced in the mice by sub-plantar injection of carrageenan (0.1 mL of 1% carrageenan solution in 0.9% normal saline). The volume of paw edema was measured at 0, 1, 2, and 3 h using a Harvard apparatus plethysmometer (Massachusetts, USA). Average paw edema volumes at various intervals were measured.<sup>28</sup> This procedure was repeated using chitosan loaded with: crude EF (CE3); EF was loaded into chitosan because it was the most bioactive fraction, solanine (CS2) and pure solanine (S). Percent inhibition of paw edema volume was thereafter calculated from the formula below:

$$\text{Inhibition\%} = (\text{Pc} - \text{Pt}/\text{Pc}) \times 100$$

where, Pc= paw edema volume of control group, Pt= paw edema volume of treated groups.

### *In vitro* anti-inflammatory study: inhibition of protein denaturation

The *in vitro* anti-inflammatory study was performed using protein denaturation model with slight adjustment.<sup>29,30</sup> Briefly, different concentrations of extracts according to the doses used in encapsulation (*i.e.*, HF, EF, BF, chitosan loaded with EF extract (CE3), chitosan loaded with solanine (CS2), and solanine (S); 500, 1000, 1500, and 2000 µg/mL, were mixed with 5% bovine serum albumin (BSA, 1 mL) incubated at 27 °C for 15 min. The control was made up of distilled water and BSA. Denaturation of proteins was achieved by placing the mixture in a water bath at 65 °C for 15 min and allowed to cool. Sample absorbance was measured at 615 nm in triplicates. Percentage inhibition of inflammation was calculated from the formula below:

$$\text{Inhibition\%} = (\text{absorbance of control} - \text{absorbance of sample}/\text{absorbance of control}) \times 100$$

### *In vitro* anticancer studies

#### Culturing cell lines

Antiproliferative potentials of each extract were determined using human breast cancer (MCF-7) and woman vagina melanoma (HMVII) cell lines. HMVII cell line was maintained in DMEM supplemented with 10% (*v/v*) fetal bovine serum (FBS), penicillin/streptomycin (1%), and 2 mM L-glutamine, while the MCF-7 cell line (ATCC, USA) was grown in serum free (with glutamine) Roswell Park Memorial Institute medium (RPMI-1640, Biocompare) with similar treatment condition. Each cell line was seeded at  $1 \times 10^5$  cells/mL regularly in a humidified atmospheric condition of 5% carbon dioxide maintained at  $37 \pm 2$  °C.<sup>30</sup>

#### Cytotoxicity study

Evaluation of crude extracts, solanine, and chitosan-loaded extracts/drug cytotoxicity was performed by MTT assay. Briefly, cancer cell lines were seeded at a cell density of 8.000 cells/well in 96 well plates and incubated for 24 h before transfection. After 24 h of transfection, the medium was removed and 20 µL of MTT (5 mg/mL) was added to each well and incubated for 4 h. The medium was then removed and the cells were rinsed

with PBS (pH: 7.4). The formazan crystals formed in living cells were dissolved in 100  $\mu$ L DMSO *per* well. Relative cell viability (%) was then calculated for each experiment based on absorbance at 550 nm using a microplate reader. The viability of non-treated control cells was arbitrarily defined as 100%.<sup>31,32</sup>

#### *Transwell migration assay (modified Boyden chamber assay)*

*In vitro* cell invasion and migration ability were performed by transwell assay. In this procedure, 8.0  $\mu$ m pore size transwell filters were placed in 24 well plates coated with 50 g matrigel (Corning Inc., USA). Then, 0.2 mL of cells ( $1 \times 10^8$  cells/L) in serum free medium was added to the top chambers of the transwells, while 0.2 mL of RPMI-1640 medium containing FBS (10%) was added to the bottom chambers. The cells were then incubated in the transwells at 37 °C with 5% CO<sub>2</sub> for 24 h. The non-migratory cells on the upper surface of the filter were wiped with cotton swab, while the migrated cells on the lower surface of the filter were fixed with 98.1% (*v/v*) methanol (Sigma Aldrich, USA) for 30 min, and then stained with Giemsa stain for 15 min. Four fields were counted on each filter under a microscope (Olympus, England) using 400x magnification. The mean values of readings were calculated.<sup>33</sup>

#### *Apoptosis assay by flow cytometry*

Programmed cell death (apoptosis) was evaluated using a BD FACSLyric™ flow cytometer (BD Biosciences, USA). Briefly, cancer cell lines (MCF-7 and HMVII) were each seeded at a density of 100,000 cells/well in 24 well plates (Costar, USA). The cells were then incubated at 37 °C in a 5% CO<sub>2</sub> incubator for 24 h. After this, the cell lines were each treated with various concentrations (2.5, 5, and 10  $\mu$ g/mL) of solanine as well as chitosan-loaded extracts (CE3, CS2, and CDr2), and were then washed in 0.1 M PBS (serum free), trypsinized, and later fixed in 90% ethanol (*v/v*) (JoeChem Ltd, Nigeria). Finally, the cells were stained with a prepared solution containing a mixture of 20  $\mu$ g/mL PI (Sigma Aldrich, USA), 0.5% tween 80, and 0.1% (10 mg/mL) RNase A (Biocompare, USA) and incubated at 37 °C for 30 min. The apoptotic cells were sorted out at 405 nm scan and analyzed.<sup>34-36</sup> The untreated cells served as the control. The experiment was conducted in triplicate. The percentages of apoptotic cells were determined according to the following formula:

$$\text{Apoptotic cells\%} = (\text{Lna} + \text{Dna}/\text{Lnc} + \text{Lna} + \text{Dnc} + \text{Dna}) \times 100$$

where Lnc = live cells with normal nuclei, Lna = live cells with apoptotic nuclei, Dnc = dead cells with normal nuclei, and Dna = dead cells with apoptotic nuclei.

#### *In vitro caspase-3-like activity assay*

Cell lines were seeded at  $1 \times 10^5$ /cell on coverslips and treated with equal concentrations (100  $\mu$ g/mL) of plant extracts (E, S, CE3, CS2, and CDr4). It was then incubated overnight for 24 h. To detect caspase-3-like protease activities, Apo Alert caspase-3 colorimetric assay kit (Clontech, Palo Alto, USA) was used. After treatment, cells were rinsed in PBS solution and fixed in *para*-formaldehyde (4%) for 10 min at 45 °C. Pre-chilled methanol (-20 °C) was then used to permeabilize the

cells for 30 min. Total DNA was then stained with 4,6-diamidino-2-phenylindole for 15 min. The apoptotic strand breaks and total DNA were visualized using transmission epifluorescence microscopy.<sup>37-40</sup>

#### *Evaluation of cellular morphology*

Chitosan-loaded extracts (formulations) and extracts were trypsinized, fixed in 5% GA, and dehydrated to remove water before observing them with the Phenom SEM (ThermoFisher, USA). Cells not treated were used as control.

#### *Statistical analysis*

The data are presented as mean  $\pm$  standard deviation (SD) of three different experiments. Significance differences between treated and control groups were compared using analysis of variance (One-Way ANOVA). The values of  $p < 0.05$  were taken as statistically significant using GraphPad prism version 9.1.

## RESULTS

#### *Isolation of solanine glycoalkaloid*

Only brief properties of this compound were mentioned here since it has been previously isolated from some plant families.<sup>41</sup> A brownish solid crystal of solanine weighing 8.0 g was obtained with the following data: EI-MS *m/z* ( $M^+$ ) 867 g/mol; molecular formula: C<sub>45</sub>H<sub>73</sub>NO<sub>15</sub>; <sup>1</sup>H-NMR (CDCl<sub>3</sub>, 3,500 MHz): 73 protons with olefin groups at chemical shift 5.3 ppm, O-H groups at 0.5-5.0 ppm all peaks were in the aliphatic regions; <sup>13</sup>C-NMR showed 45 carbons mainly methyl carbons, melting point; 272.5 °C and HPLC analyses showed a retention time of 19 min with sharp peak area.

#### *Bioguided fractionation of Solanum scabrum extract*

Bioguided fractionation was carried out following solvents in increasing order of their polarities using HF, EF, and BF. Fractionations of the extract yielded the following fractions: HF, EF, and BF. Each of the fractions was bioguided by anti-inflammatory and anticancer activities to determine the most active fraction. Results were expressed as a percentage inhibition of paw edema volume in mice and cell viability of MCF-7 cell line, respectively (Table 1). The most active fractions (BF; 52.41  $\pm$  41% inhibition in inflammation model and EF; inhibitory concentration 50 (IC<sub>50</sub>): 14.28  $\pm$  0.12  $\mu$ g/L) were further fractionated into four subfractions (BF.1, BF.2, BF.3, and BF.4) (EF.1, EF.2, EF.3, and EF.4) for their anti-inflammatory and anticancer activities, respectively. *n*-Butanol (BF.4) and ethyl acetate subfractions (EF.2) were the most active for anti-inflammatory and anticancer activities, respectively, and were further purified in silica gel column chromatography. Purification of isolated bioactive compounds was confirmed by the presence of single spots on the TLC plate.

#### *Identification of isolated compound from leaf*

The isolated most bioactive anti-inflammatory and anticancer compound from *S. scabrum* leaf was structurally elucidated and identified based on the data obtained from <sup>1</sup>H, <sup>13</sup>C, HSQC, and HMBC-NMR (500 MHz, Bruker) as well as MS (Agilent technologies). <sup>1</sup>H-NMR showed seven signals, while <sup>13</sup>C-NMR

displayed twelve carbons, which are mainly methyl carbons. These data were compared with those reported in literature (NIST, 2014). The anti-inflammatory compound was identified as 3-nitrodibenzofuran (dBF3N) with the following properties: color; white crystal,  $m/z$ ; 213, and  $m.p.$ ; 181.49 °C (Figure 1).

#### Preparation and characterization of chitosan loaded extracts

From the results, nano-formulated extracts yielded 12.14 to 18.25 g (CE1-CE4), 10.05 to 16.22 g (CS1- CS4), and 8.12 to 14.06 g (CDr1-CDr4). Developed microspheres with larger sizes (in  $\mu\text{m}$ ;  $1 \mu\text{m} = 1000 \text{ nm}$ ) possessed higher percentage EE than those with smaller sizes as seen from the table below. The data

**Table 1. Bioguided fractionation of extracts for their anti-inflammation and anticancer effects**

Extract	Anti-inflammation (%)	MCF-7 IC <sub>50</sub> ( $\mu\text{g/mL}$ )
HF	12.01 $\pm$ 0.20	88.24 $\pm$ 4.12
EF	42.11 $\pm$ 1.20	14.28 $\pm$ 0.12
BF	52.41 $\pm$ 2.11	92.24 $\pm$ 4.02
Aspirin (reference for anti-inflammation assay)	76.32 $\pm$ 2.04	NA
Doxorubicin (reference for anticancer assay)	NA	0.80 $\pm$ 0.01

Results are mean  $\pm$  SD (at  $p < 0.05$ ; one-way ANOVA), NA: Not applicable, HF: *n*-hexane fraction, EF: Ethyl acetate, BF: *n*-butanol, SD: Standard deviation, IC<sub>50</sub>: Inhibitory concentration 50

from the characterization of formulated CSNPs are presented in Tables 2 and 3; Figure 2 below:

#### Anti-inflammatory activity test of extracts

The results of anti-inflammatory effects of the extracts by carrageenan-induced paw edema and protein denaturation assays are shown in Figure 3. From the results, the highest paw edema reduction of  $2.68 \pm 0.01 \text{ mm}$  was obtained in the treated group, which received 1200 mg/kg EF as well as mice that received 0.5  $\mu\text{g/mL}$  CE3 and solanine (S) with  $1.44 \pm 0.01 \text{ mm}$ , and  $2.52 \pm .02 \text{ mm}$  after 3 h of carrageenan induction. Mice treated with HF at 200, 400, 800, and 1200 mg/kg *b.w.* *S. scabrum* extract and CSNPs loaded solanine (CS2) does not show significant decrease in paw volume from 1 to 3 h compared to the standard drug (Figure 3a). Similar results were obtained in Figure 3b where chitosan loaded solanine and HF recorded the lowest percentage inhibition of protein denaturation when compared with those of other treatment groups ( $p < 0.05$ ; One-Way ANOVA).

#### Anticancer activities of extracts

##### Cytotoxicity study of extracts

Chitosan-loaded doxorubicin (CDr4) showed the highest IC<sub>50</sub> value of  $0.02 \pm 0.01$  and  $0.01 \pm 0.01 \mu\text{g/mL}$  against MCF-7 and HMVII cells, respectively. These values were followed by those obtained when the cells were exposed to solanine alone (S) with IC<sub>50</sub> value of  $8.13 \pm 0.01$  and  $12.01 \pm 1.10 \mu\text{g/mL}$ , respectively. However, the selective index (SI) of exposing the

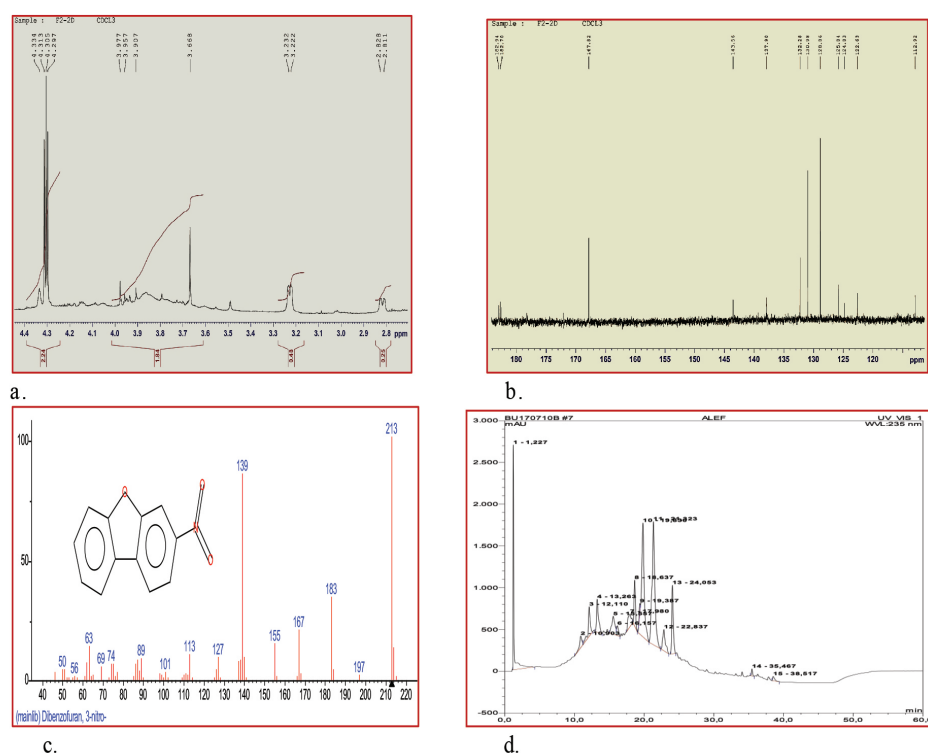


**Figure 1.** NMR and MS spectra and HPLC chromatogram of the isolated compound from *Solanum scabrum* leaf; a; <sup>1</sup>H-NMR with seven protons between 2.81-4.33  $\delta$  (ppm), b; <sup>13</sup>C-NMR with twelve carbon atoms, c; MS with  $m/z$  213 and molecular peak ion 139 at 62.89% peak area for 3-nitrodibenzofuran, d; HPLC chromatogram showed 19.11 min with isocratic elution.  $\text{CDCl}_3$  was used as a solvent for NMR analysis. MS: Mass spectrometry, HPLC: High-performance liquid chromatography

**Table 2. Preparation and characterization of chitosan NPs loaded with *Solanum scabrum* extract, solanine, and doxorubicin by spray drying technique**

Batch code	GA ( $\mu\text{g/mL}$ )	Yield (%)	Size ( $\mu\text{m}$ )	% EE	Zeta* (mV)
CE1	500	12.14	0.05 $\pm$ 0.01	32.01 $\pm$ 1.2	20.22 $\pm$ 0.2
CE2	1000	12.22	0.06 $\pm$ 0.01	63.04 $\pm$ 2.1	25.14 $\pm$ 1.2
CE3	1500	18.25	0.01 $\pm$ 0.01	98.51 $\pm$ 1.3	25.66 $\pm$ 1.2
CE4	2000	18.10	0.02 $\pm$ 0.02	96.42 $\pm$ 1.2	24.15 $\pm$ 0.6
CS1	500	10.05	0.05 $\pm$ 0.01	44.24 $\pm$ 0.4	22.00 $\pm$ 0.1
CS2	1000	16.11	0.02 $\pm$ 0.01	92.12 $\pm$ 2.1	24.14 $\pm$ 0.2
CS3	1500	10.14	0.01 $\pm$ 0.02	93.22 $\pm$ 2.1	25.13 $\pm$ 0.1
CS4	2000	16.22	0.01 $\pm$ 0.10	66.12 $\pm$ 2.2	25.15 $\pm$ 0.2
CDr1	500	8.12	0.06 $\pm$ 0.01	46.08 $\pm$ 1.2	20.14 $\pm$ 0.1
CDr2	1000	8.99	0.08 $\pm$ 0.02	79.14 $\pm$ 2.1	24.00 $\pm$ 0.1
CDr3	1500	12.54	0.09 $\pm$ 0.03	92.16 $\pm$ 2.2	25.04 $\pm$ 0.1
CDr4	2000	14.06	0.02 $\pm$ 0.01	98.01 $\pm$ 2.2	24.99 $\pm$ 0.2

Results are mean  $\pm$  SD, chitosan concentration is 1.0% (w/v); drug loading is 2% (w/v). Drug released in 6 hours increases with the concentration of glutaraldehyde in all batch codes. The particle size was expressed in  $\mu\text{m}$  i.e., 1  $\mu\text{m}$ : 1000 nm. The particle sizes range from 0.01 to 0.09  $\mu\text{m}$  (i.e., 10 to 90 nm), GA: Glutaraldehyde, EE: Entrapment efficiency, \*: Zeta potential, SD: Standard deviation, NPs: Nanoparticles, CE: Chitosan NPs loaded with *Solanum scabrum* extract, CS: Chitosan NPs loaded with solanine, CDr: Chitosan NPs loaded with doxorubicin

**Table 3. *In vitro* drug release study of formulated chitosan NPs**

Batch code	Drug release in 6 h (%)
CE1	22.01 $\pm$ 1.12
CE2	15.01 $\pm$ 0.10
CE3	44.11 $\pm$ 1.42*
CE4	18.22 $\pm$ 1.20
CS1	28.04 $\pm$ 2.12
CS2	64.18 $\pm$ 2.40*
CS3	25.10 $\pm$ 1.14
CS4	18.24 $\pm$ 1.24
CDr1	33.08 $\pm$ 2.54
CDr2	38.44 $\pm$ 0.22
CDr3	40.11 $\pm$ 1.50
CDr4	52.10 $\pm$ 2.01*

\*Best optimized conditions were selected for anti-inflammatory and anticancer studies. Results are mean  $\pm$  SD (n: 3). SD: Standard deviation, NPs: Nanoparticles, CE: Chitosan NPs loaded with *Solanum scabrum* extract, CS: Chitosan NPs loaded with solanine, CDr: Chitosan NPs loaded with doxorubicin

MCF-7 breast cancer cell to solanine alone was not all that encouraging as compared with that of CDr4 after 72 h and with same concentrations (12.5, 25, 40, and 50  $\mu\text{g/mL}$ ) *in vitro*. From the results also, chitosan-loaded EF (CE3) established improved values in  $\text{IC}_{50}$  and SI than other treatment groups (Table 4).

#### *Invasion and migration assay*

Transwell assay helps us to know how cancer cells migrate and invade other tissues and respond to chemoattractants and move toward them. From the results in Figure 4 below, exposure of the cancer cells to chitosan-loaded solanine (CS2) does not remarkably prevent the migration and invasion of the human vaginal melanoma cells HMVII. However, the exposure of cell lines (HMVII and MCF-7) to solanine alone significantly prevented the migration and invasion of MCF-7 breast cancer cell lines. These results were comparable with that of the doxorubicin anticancer drug ( $p < 0.05$ ; one-way ANOVA).

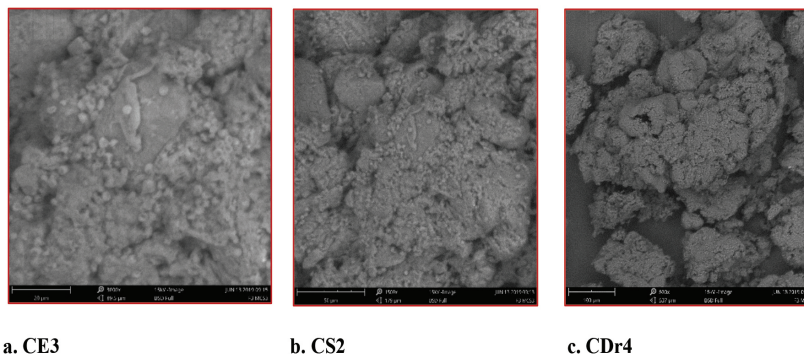


**Figure 2.** SEM morphology of chitosan loaded with crude *Solanum scabrum* extract (CE3), solanine (CS2), and doxorubicin (CDr4). Glutaraldehyde was used as cross-linking agent 3000x. SEM: Scanning electron microscope

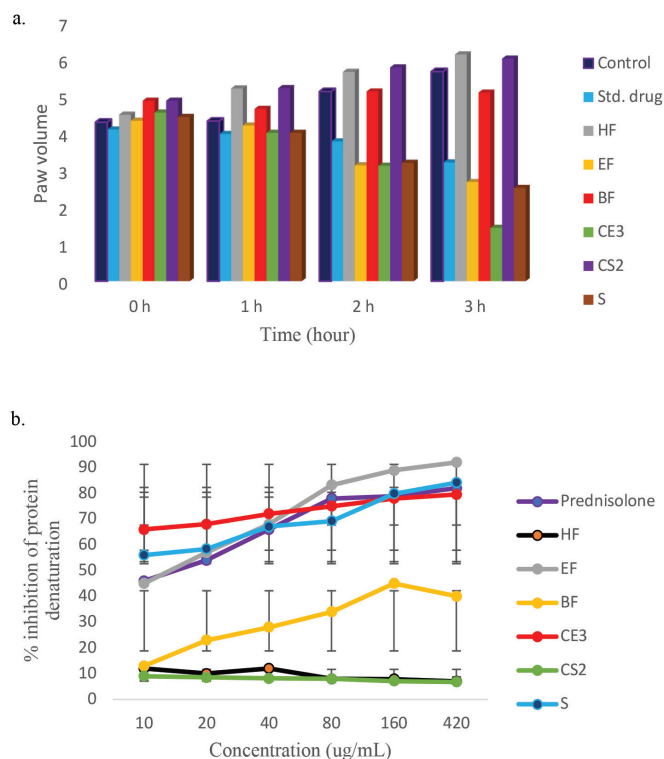


**Figure 3.** Anti-inflammatory activity of *Solanum scabrum* extracts and chitosan NPs loaded extracts; a; (carrageenan-induced paw oedema), b; (effects on protein denaturation). Results are means ± SD. The values of  $p < 0.05$  were statistically significant. HF: Hexane fraction, EF: Ethyl acetate fraction, BF: Butanol fraction, CE3: Chitosan-loaded crude extract batch code 3, CS2: Chitosan-loaded solanine batch code 2, S: Solanine, SD: Standard deviation, NPs: Nanoparticles

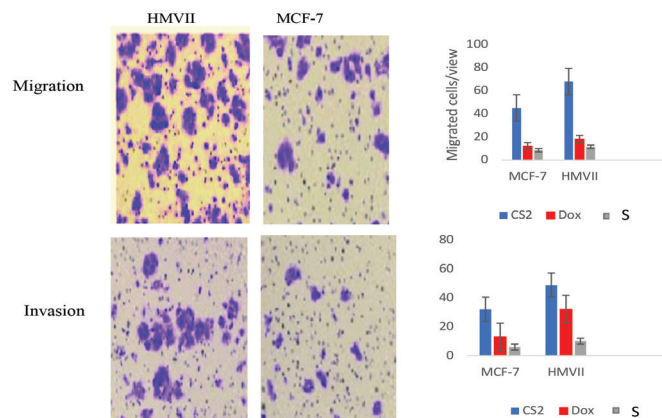


**Figure 4.** Transwell migration and invasion assay of solanine (S) and chitosan-loaded solanine batch code 2 (CS2) as viewed using a hemocytometer. Results are mean ± SD for three replicate readings. Cellular migration and invasion were much more pronounced with CS2 treatment when compared to cells exposed to solanine alone. S: Solanine, CS2: Chitosan-loaded solanine batch code 2, SD: Standard deviation, Dox: Doxorubicin

*Apoptosis study*

From the results obtained in the figures below, exposure of the cancer cells to CS2 does not result in early apoptosis of the cells, however, cellular integrity was lost as seen from the flow cytometry images. Early apoptosis was induced on exposure of cells to solanine glycoalkaloid after 72 h with shrinking nuclei after staining with PI. Percentage apoptosis in cells was high with increased concentration of solanine (S) in the early and late stages of apoptosis as well as increased caspase-3-activity in MCF-7 breast cancer cell line (Figure 5 a-c). This result was comparable to that of doxorubicin as reference drug.

**Table 4.** Inhibition of MCF-7 and HMVII cancer cells growth by crude fractions and chitosan NPs-loaded extracts after 72 h incubation by MTT assay

Extracts	IC <sub>50</sub> (µg/mL)		CC <sub>50</sub> (µg/mL)	
	MCF-7	HMVII	VeroE6 (normal cell)	Selectivity index (MCF-7)
HF	234.17 ± 6.12	128.44 ± 4.20	132.11 ± 1.24	0.56
EF	10.10 ± 0.01	18.32 ± 1.21	96.34 ± 2.11	9.54
BF	22.10 ± 0.01	88.21 ± 2.52	112.24 ± 1.42	5.08
S	8.13 ± 0.01	12.01 ± 1.10	206.94 ± 2.21	25.45
E	21.01 ± 0.21	24.00 ± 1.22	88.94 ± 0.18	4.23
CE3	10.04 ± 0.01	12.44 ± 1.14	128.14 ± 4.12	12.76
CS2	96.22 ± 4.12	102.10 ± 6.12	220.45 ± 4.22	2.29
Dox	0.8 ± 0.01	0.24 ± 0.01	22.02 ± 1.01	27.53
CDr4	0.02 ± 0.01	0.01 ± 0.01	56.36 ± 0.14	>100

Results are mean ± SD (n: 3). MCF-7, HMVII, and VeroE6 cells (1 x 10<sup>6</sup>/cells) were treated with each of the extract alone, CE3, CS2, and CDR4 loaded chitosan NPs as well as doxorubicin alone for 72 h. Cancer cells were pre-treated 30 min separately for each sample prior to chitosan-loaded drugs treatment. Each experiment was performed in triplicate. The concentration of doxorubicin was 0.5 mg/mL in all the experiments involving doxorubicin. The selectivity index of these treatments against the MCF-7 was determined from the normal cell VeroE6. HF: Hexane fraction, EF: Ethyl acetate fraction, BF: Butanol fraction, S: Solanine, E: *Solanum scabrum* leaf methanol extract, CE3: Chitosan-loaded extract batch code 3, CS2: Chitosan-loaded solanine batch code 2, Dox: Doxorubicin, CDR4: Chitosan-loaded doxorubicin batch code 4, SD: Standard deviation, NPs: Nanoparticles, MTT: 3-(4,5-dimethylthiazol-2-yl)-2,5-diphenyl-2H-tetrazolium bromide

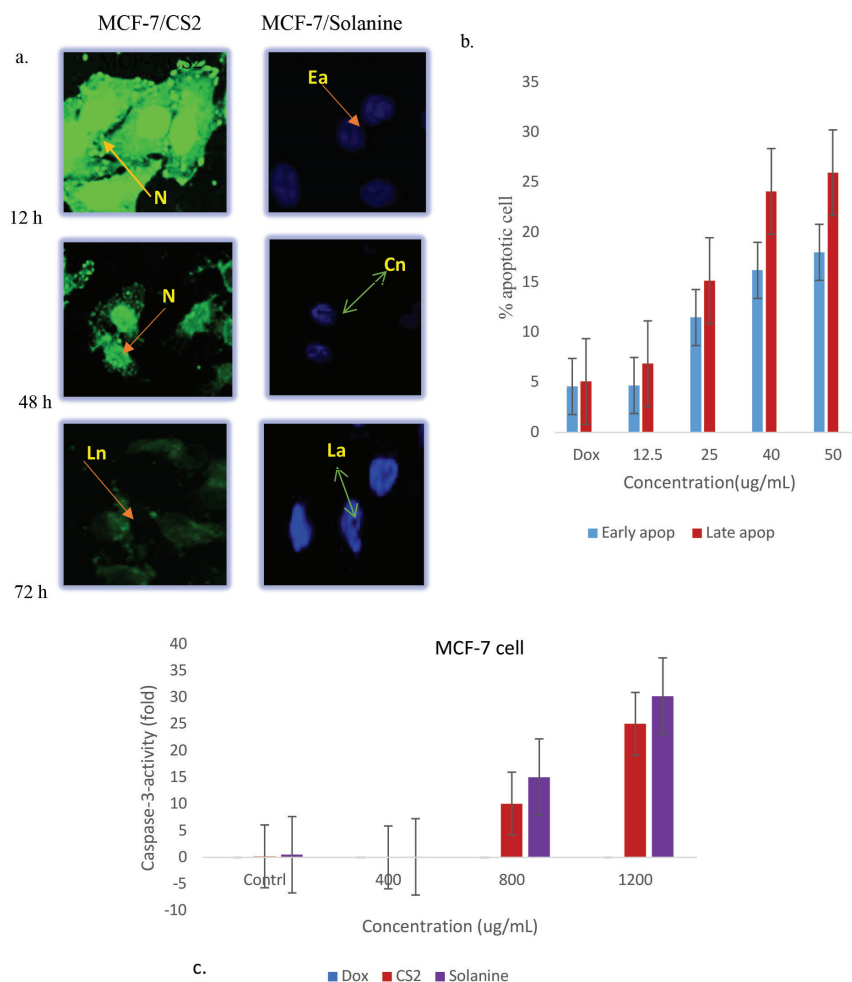


**Figure 5.** Fluorescence images of MCF-7 cancer cells after treatment with CS2 and solanine (S) with various concentrations (12.5, 25, 40, and 50  $\mu\text{g}/\text{mL}$ ) at 12, 48 and 72 hours. Apoptotic cellular death and necrosis were detected by staining with propidium iodide and analysed with flow cytometry. Results are mean  $\pm$  SD for three consecutive readings.  $p < 0.05$  was taken as a significance different. Ea: Early apoptosis, La: Late apoptosis, Cn: Clear nuclear, N: Necrosis of cells, Ln: Late necrosis, S: Solanine, SD: Standard deviation

Similarly, chitosan-loaded extract (CE3) and solanine (CS2), do not induce higher percentage of cellular apoptosis in human vaginal melanoma cell HMVII when compared to that in breast cancer cell MCF-7. The result further showed that solanine induced the highest percentage of cellular apoptosis in all the cell lines followed by chitosan loaded doxorubicin (CDr4) after 72 h (Table 5). These values obtained were statistically significantly different from the control ( $p < 0.05$ ; one-way ANOVA).

## DISCUSSION

In traditional medicine, plant parts such as leaves are reduced into fine powders using mechanical means to improve their contact with solvents and promote the penetration of extracting solvents into the tissues. Extraction, which normally follows pulverization, is usually carried out by a cold maceration technique, where the powdered leaves are soaked in an appropriate volume of methanol to obtain the active phytoconstituents from the leaves. In this study, the use of

this extraction method also helps to prevent the loss of active metabolites due to heat. This is because active constituents (secondary metabolites) in plants are readily destroyed on exposure to heat,<sup>5</sup> hence, the main reason why the leaves of *S. scabrum* we collected were air-dried under shade. Moreover, drying of medicinal plant parts helps to reduce the moisture content thereby preventing microbial and enzymatic action, hence, extending the shelf life of the part.<sup>41</sup>

Nanotechnology as an aspect of medical sciences involves the engineering of functional systems at the molecular scale. Nanomedicine is an emerging aspect of nanotechnology where NPs are employed to prevent, diagnose, and treat diseases. Because of their biocompatibility, specificity, non-toxicity, and biodegradability, NPs have been used to deliver various drugs to a specific sites in the body.<sup>42</sup> In our current study, CSNP was used to deliver various extracts and doxorubicines to cancer cells. Chitosan is naturally obtained by chitin deacetylation. It is a positively charged nanocarrier. Because of its ability to adhere to cells and readily absorbed in the body, it is the most

**Table 5. Percentage apoptosis induced by exposure of MCF-7 and HMVII cancer cell lines to CE3, CS2, CDr4, solanine, and doxorubicin**

Cancer cells	Sample	Concentration ( $\mu\text{g/mL}$ )			
		12.5	25	40	50
MCF-7	CE3	25.12 $\pm$ 0.01*	28.02 $\pm$ 1.01	28.98 $\pm$ 1.20	30.41 $\pm$ 2.01*
	CS2	5.10 $\pm$ 0.01*	5.88 $\pm$ 0.01*	6.15 $\pm$ 0.01	4.02 $\pm$ 0.01*
	CDr4	76.87 $\pm$ 2.11	78.82 $\pm$ 2.56	88.14 $\pm$ 4.22	88.14 $\pm$ 2.88*
	Solanine	68.24 $\pm$ 2.41*	72.12 $\pm$ 4.01	78.99 $\pm$ 3.24*	84.44 $\pm$ 4.10*
	Dox	44.22 $\pm$ 2.08	58.38 $\pm$ 2.11	58.88 $\pm$ 2.21	62.10 $\pm$ 2.24
HMVII	CE3	5.12 $\pm$ 0.01*	25.04 $\pm$ 2.11*	28.10 $\pm$ 1.01	36.02 $\pm$ 2.01*
	CS2	5.44 $\pm$ 0.01*	5.88 $\pm$ 0.01	6.21 $\pm$ 0.01*	5.02 $\pm$ 0.01*
	CDr4	28.10 $\pm$ 2.01	35.82 $\pm$ 2.01*	38.40 $\pm$ 2.01	45.15 $\pm$ 2.03
	Solanine	36.22 $\pm$ 1.01*	48.26 $\pm$ 2.01	56.44 $\pm$ 2.44	56.88 $\pm$ 2.10*
	Dox	15.18 $\pm$ 1.11*	28.02 $\pm$ 1.02	28.42 $\pm$ 1.01	36.56 $\pm$ 1.11*

Results are mean  $\pm$  SD, \*Significance different at  $p < 0.05$  (one-way ANOVA) for  $n = 3$ . CE3: Chitosan-loaded crude extract batch code 3 from ethyl acetate fraction, CS2: Chitosan-loaded solanine batch code 2, CDr4: Chitosan-loaded doxorubicin batch code 4, Dox: Doxorubicin

favorable nanocarrier for targeted drug delivery. It also has the characteristics of always being attracted to negatively charged cells and this is the feature that makes CSNPs a candidate of choice for the treatment of solid tumors.<sup>43,44</sup> Apart from the aforementioned, CSNPs have also shown the capacity to increase the permeability of cell membranes in both *in vitro* and *in vivo* studies, stabilizing agent owing to its ability to form film, ability to be modified chemically and its low cost.<sup>45-47</sup> From the results obtained in this study, drugs loaded into CSNPs exhibited more biological activities than when the drugs were used directly on the organs or tissues.

In this study, *S. scabrum* extracts were evaluated for their anti-inflammatory and anticancer effects on human vaginal melanoma (HMVII) and breast cancer cell lines (MCF-7) *in vitro*. In our study, bioguided fractionation of *S. scabrum* extracts indicated that BF and EF exhibited high anti-inflammatory activity *in vitro*. No anti-inflammatory and anticancer activities were observed in the HF. EF was the most sensitive and biologically active of all the fractions in the MCF-7 cell line at the concentration investigated (Table 1). Further subsection of EF to chromatography isolation gave rise to 3-nitrobenzofuran (dBF3N) as characterized by GC-MS and NMR spectroscopy, which is the bioactive compound from the fraction, and it is one of the active compounds responsible for the observed biological activities of the fraction in this study. Similarly, in a previous study, solanine alkaloids were isolated from *S. scabrum*, where a broad range of glycoalkaloids of solasodine were reported in *S. scabrum* berries by using HPLC-UV/VIS-MS or MS/MS methods.<sup>48</sup> This study was the first time that it is being isolated from the leaf extract.

In this present study, cross-linking of CSNPs with GA slightly affected the yield, size (expressed in  $\mu\text{m}$ ), zeta potential, and percentage entrapment from 500 to 2000  $\mu\text{g/mL}$  (Table 2, Figure 2), as was also reported that the use of GA as a cross-

linking agent resulted in increase in size of NPs with narrow polydispersity index and highest zeta potential.<sup>49</sup> The presence of some aggregates in the morphology of the prepared CSNPs as displayed by the SEM (Figure 2) do not mean that it was not uniform with the drugs but they represent medium sized CSNPs which ranges from 0.01 to 0.09  $\mu\text{m}$  (*i.e.*, 10 to 90 nm). This is because NPs range for 1-100 nm in size.<sup>49</sup> From the present study, as the conditions of prepared CSNPs were optimized, the particle size, encapsulation efficiency, and yield increased linearly with the concentration of GA (Table 2). Size and amount of drug entrapped or encapsulated by NPs are very crucial in drug delivery as these will affect the amount of drug release.<sup>26,27</sup> In this current study, the small and medium sizes of formulated CSNPs greatly assisted in effective delivery of these encapsulated drugs. This is because the smaller the size of a NP, the more it is unnoticed by the body's defence mechanisms until it reaches the targeted site to deliver its contents in controlled release.<sup>27</sup>

Similarly, concentration of the cross-linking agent GA plays crucial roles in optimization conditions of nanosized materials as seen in the study (Table 3). Anti-inflammatory agents are substances that are capable of reducing inflammations such as redness of eyes, swellings, and pains in the body. The mechanism of these agents is by blocking some pain receptors in the body, which can cause inflammation. In this current study, CSNP-loaded solanine resulted in a percentage increase in paw volume, whereas the animals treated with solanine alone showed a significant reduction in paw volume within 3 h (Figure 3a, b). Apart from chitosan loaded with solanine, other chitosan-loaded drugs showed similar reduction in paw volume, which is a sign of anti-inflammation, thereby reducing swelling. Similarly, mice exposed to solanine glycoalkaloid produced the best denaturation of proteins than CS2, HF, and BF. The implication of this may be that chitosan must have



exhibited activity reducing effects on solanine glycoalkaloid. The reasons for such reduction were not fully understood in the current study, however, it can be linked to the presence of nitrogen atom in the compound since chitosan also possessed some nitrogen atoms.<sup>50</sup> Solanine-treated carrageenan-induced inflammation, EF and CE3 exhibited the highest percentage protein denaturation (Figure 3b). These results were compared with that of the control drug prednisolone ( $p < 0.05$ ; one-way ANOVA). The result further showed that CSNP drug delivery act synergistically with other drugs and extracts except solanine. The presence of aglycone moiety in solanine must have been responsible for the observed characteristics since solanine like other steroidal glycoalkaloids were reported to possess anti-inflammatory, anticarcinogenic, and antimicrobial activities.<sup>50</sup> It has been reported that most anti-inflammatory agents exert their pharmacological potentials by inhibiting the enzyme cyclooxygenase, which produces the hormone prostaglandins, from inducing cytokines, which are usually released during inflammation.<sup>51</sup> Chitosan-loaded drugs and extracts must have exerted their action similarly but the release pattern was sustained release.

An ideal anticancer agent must be able to inhibit the growth of cancer cells, prevent metastasis, and induce cellular apoptosis.<sup>52</sup> In this study, nanoencapsulated drug and extracts showed some levels of cytotoxicity against cancer cells (Table 4). For instance, chitosan-loaded doxorubicin (CDr4) has the highest cytotoxic effects on breast cancer cell MCF-7 and human vaginal melanoma cell HMVII with  $IC_{50}$  values of  $0.02 \pm 0.01 \mu\text{g/mL}$  and  $0.01 \pm 0.01 \mu\text{g/mL}$ , respectively and with a SI of greater than 100 against MCF-7 cell line. Likewise, cancer cells exposed to CE3 treatment had  $IC_{50}$  values of  $10.04 \pm 0.01 \mu\text{g/mL}$  and  $12.44 \pm 1.12 \mu\text{g/mL}$  against MCF-7 and HMVII cell lines, respectively. In all treatments, there were greater synergistic effects among these drugs and CSNPs. However, exposure of cancer cells to solanine steroidal glycoalkaloid showed the highest cytotoxic effects on MCF-7 and HMVII cancer cell lines with  $IC_{50}$  values of  $8.13 \pm 0.01 \mu\text{g/mL}$  (SI; 25.45) and  $12.01 \pm 0.01 \mu\text{g/mL}$ , respectively. For effective cancer therapy, drug agents must be able to initiate cellular apoptosis in cancer cells, resulting in the death of cancer cells.<sup>35,40</sup> The present study revealed that chitosan loaded with solanine does not result in elevated percentage apoptosis induction in all cancer cell lines unlike other treatments where there was significant rise in percentage apoptosis induction (Table 5). From the study, cancer cells treated with chitosan-loaded doxorubicin anticancer drug showed the highest percentage of apoptosis induction. It was followed by cancer cells treated with solanine unloaded into CSNPs. The significant reduction in apoptotic effect of CS2 was not fully understood in this current study but may be due to the presence of similar nitrogen atoms in solanine and CSNPs that work in anti-synergism with each other. However, this mechanism needs to be further studied for a conclusive report. Also, in the transwell migration assay, migration and invasion were greatly reduced in MCF-7 cancer cells exposed to solanine alone than chitosan-loaded solanine glycoalkaloid (CS2) at various concentrations (Figure 4). Our

study further revealed that MCF-7 breast cancer cells exposed to solanine alone induced both early and late apoptosis with minimal clear nuclei in concentration dependent fashion as seen from the fluorescence images after 72 h (Figure 5). Chitosan loaded solanine glycoalkaloid (CS2) does not induce significant apoptosis. Moreover, exposure of MCF-7 breast cancer cells to solanine alone results in an increase in caspase-3 activity from 400 to 1200  $\mu\text{g/mL}$  concentrations.

It was suggested from previous studies that the toxicity mechanism of solanine was due to chemical interactions within mitochondrial complexes. This is because exposure of cancer cells to solanine alone opens  $K^+$  channel of mitochondria thereby setting up membrane potential difference, which will in turn force  $Ca^{2+}$  to be transported down the concentration gradient into the mitochondria complexes. This elevated calcium ion concentration created cellular damage and apoptosis of cells.<sup>53</sup> This claim was consistent with the role of solanine in the current study. It has been reported that caspase-3 is important for proper development of the brain as well as necessary for other apoptotic processes in cancer cells.<sup>54,55</sup> Caspase-3 is implicated in apoptosis and is very crucial for the condensation of chromatin as well as fragmentation of DNA in many cells, especially cancer cells. This elevated level of caspase-3 activity witnessed in this study from MCF-7 breast cancer cells exposed to solanine alone was responsible for the observed high percentage of apoptosis obtained from this study (Table 4). Furthermore, this study affirmed that solanine isolated from *S. scabrum* leaf extract exerted cytotoxic effects on MCF-7 and HMVII cancer cells by inducing early- and late-stage apoptosis as well as necrosis.

## CONCLUSION

Our studies showed that CSNPs loaded with *S. scabrum* extracts possessed anti-inflammatory in carrageenan-induced paw edema and anticancer activity against MCF-7 breast cancer and HMVII human vaginal melanoma cell lines. However, the study also revealed that the encapsulation of solanine into CSNPs produced lower activities than when solanine was used alone. It disclosed that the use of solanine alone reduced percentage paw volume, decreased migration and invasion, increased apoptosis, and elevated caspase-3 activity. Finally, due to the reported toxicity of solanine, the concentration was reduced in this study. It is suggested therefore that the lack of synergistic effects between solanine and CSNPs should be further investigated.

## ACKNOWLEDGEMENTS

The authors are grateful to Santa Maria Medical Research/Clinic, Mr. Mejida of Central Research Laboratory, University of Lagos, Nigeria, and Dr. Asiri of King Abdul-Azizi University, Jeddah, Saudi Arabia for NMR analysis.

## Ethics

**Ethics Committee Approval:** The approval was issued by the University of Jos Research and Ethical Committee with the approval number of UJ/FPS/F17-00379, date: 31.07.2018.

**Informed Consent:** Not applicable.

**Peer review:** Externally peer-reviewed.

#### Authorship Contributions

Concept: C.A.U., Design: C.A.U., E.O.I., Data Collection or Processing: C.A.U., E.O.I., A.C.F., Analysis or Interpretation: C.A.U., E.O.I., Literature Search: C.A.U., E.O.I., A.C.F., Writing: C.A.U., E.O.I.

**Conflict of Interest:** No conflict of interest was declared by the authors.

**Financial Disclosure:** The authors declared that this study received no financial support.

## REFERENCES

- Kuete V, Efferth T. Cameroonian medicinal plants: pharmacology and derived natural products. *Front Pharmacol.* 2010;1:123.
- van Andel T, van Onselen S, Myren B, Towns A, Quiroz D. "The medicine from behind": the frequent use of enemas in western African traditional medicine. *J Ethnopharmacol.* 2015;174:637-643.
- Iwu MM. *The Medicinal plants of West Tropical Africa*, 2<sup>nd</sup> ed. Taylor and Francis, 2014.
- Ntie-Kang F, Lifongo LL, Mbaze LM, Ekwelle N, Owono Owono LC, Megnassan E, Judson PN, Sippl W, Efange SM. Cameroonian medicinal plants: a bioactivity *versus* ethnobotanical survey and chemotaxonomic classification. *BMC Complement Altern Med.* 2013;13:147.
- Sofowora A. *Traditional Medicine in Africa*, 2<sup>nd</sup> ed. Spectrum Book, Ibadan, 2006; p. 25.
- Adodo A. *Medicinal Plants of Southeast Nigeria*. Uhum Monastery Pub, 2007.
- Tsobou R, Mapongmetsem PM, Van Damme P. Medicinal plants used for treating reproductive health care problems in Cameroon, Central Africa. *Econ Bot.* 2016;70:145-159.
- Boadu AA, Asase A. Documentation of herbal medicines used for the treatment and management of human diseases by some communities in Southern Ghana. *Evid Based Complement Alternat Med.* 2017;2017:3043061.
- Tabuti JR, Kukunda CB, Kaweesi D, Kasilo OM. Herbal medicine use in the districts of Nakapiripirit, Pallisa, Kanungu, and Mukono in Uganda. *J Ethnobiol Ethnomed.* 2012;8:35.
- Nguyen T, Chen X, Chai J, Li R, Han X, Chen X, Liu S, Chen M, Xu X. Antipyretic, anti-inflammatory and analgesic activities of *Periplaneta americana* extract and underlying mechanisms. *Biomed Pharmacother.* 2020;123:109753.
- Belachew TF, Asrade S, Geta M, Fentahun E. *In vivo* evaluation of wound healing and anti-inflammatory activity of 80% methanol crude flower extract of *Hagenia abyssinica* (Bruce) J.F. Gmel in mice. *Evid Based Complement Alternat Med.* 2020;2020:9645792.
- WHO. *The traditional relevance of plants in ethnomedicine*, 2018; vol XXII.
- NCI. *Cancer biology and metastasis of cancer cells*. 2018.
- Li Y, Pan A, Wang DD, Liu X, Dhana K, Franco OH, Kaptoge S, Di Angelantonio E, Stampfer M, Willett WC, Hu FB. Impact of healthy lifestyle factors on life expectancies in the US population. *Circulation.* 2018;138:345-355. Erratum in: *Circulation.* 2018;138:e75.
- Chen W, Zheng R, Baade PD, Zhang S, Zeng H, Bray F, Jemal A, Yu XQ, He J. Cancer statistics in China, 2015. *CA Cancer J Clin.* 2016;66:115-132.
- Rajitha P, Gopinath D, Biswas R, Sabitha M, Jayakumar R. Chitosan nanoparticles in drug therapy of infectious and inflammatory diseases. *Expert Opin Drug Deliv.* 2016;13:1177-1194.
- Ukwubile CA, Ahmed A, Katsayal UA, Ya'u J, Netthey H. *In vitro* anticancer activity of *Melastomastrum capitatum* Fern. loaded chitosan nanoparticles on selected cancer cells. *Drug Discovery.* 2019;13:46-54.
- Abubakar AR, Haque M. Preparation of medicinal plants: basic extraction and fractionation procedures for experimental purposes. *J Pharm Bioallied Sci.* 2020;12:1-10.
- Yuan B, Byrnes D, Giurleo D, Villani T, Simon JE, Wu Q. Rapid screening of toxic glycoalkaloids and micronutrients in edible nightshades (*Solanum* spp.). *J Food Drug Anal.* 2018;26:751-760.
- Manoko MLK, van den Berg RG, Feron RMC, van der Weerden GM, Mariani C. Genetic diversity of the African hexaploid species *Solanum scabrum* Mill. and *Solanum nigrum* L. (Solanaceae). *Genet Resour Crop Evol.* 2008;55:409-418.
- Jayakumar K, Murugan K. *Solanum* alkaloids and their pharmaceutical roles: a review. *J Anal Pharm Res.* 2016;3:00075.
- Neugart S, Baldermann S, Ngwene B, Wesonga J, Schreiner M. Indigenous leafy vegetables of Eastern Africa - a source of extraordinary secondary plant metabolites. *Food Res Int.* 2017;100:411-422.
- Ashutosh K. *Pharmacognosy and Pharmacobiotechnology*, 2<sup>nd</sup> ed, New-Delhi, India, 2007; p. 505.
- Harborne JB. *Phytochemical methods a guide to modern techniques of plant Analysis*, 3<sup>rd</sup> edition, Chapman & Hall London Weinheirn. New York, Tokyo, Melbourne Madras, 1998; p. 214.
- Hejazi R, Amiji M. Chitosan-based gastrointestinal delivery systems. *J Control Release.* 2003;89:151-165.
- Desai KG, Park HJ. Preparation of cross-linked chitosan microspheres by spray drying: effect of cross-linking agent on the properties of spray dried microspheres. *J Microencapsul.* 2005;22:377-395.
- Anes UC, Netthey H, Jen JV. Antimicrobial activity and characterization of *Annona muricata* Linn (Annonaceae) leaf-loaded chitosan nanoparticle against cancer associated microbes. *Int J Res Stud Microbiol Biotechnol.* 2016;2:15-21.
- Kumar N, Devineni SR, Gajjala PR, Dubey SK, Kumar P. Synthesis, isolation, identification and characterization of new process related impurity in isoproterenol hydrochloride by HPLC, LC/ESI-MS and NMR. *J Pharm Anal.* 2017;7:394-400.
- Padmanabhan P, Jangle SN. Evaluation of *in-vitro* anti-inflammatory activity of herbal preparation, a combination of four medicinal plants. *Int J Basic Med Sci.* 2012;2:109-116.
- Elias G, Rao MN. Inhibition of albumin denaturation and antiinflammatory activity of dehydrozingerone and its analogs. *Indian J Exp Biol.* 1988;26:540-542.
- Mosmann T. Rapid colorimetric assay for cellular growth and survival: application to proliferation and cytotoxicity assays. *J Immunol Methods.* 1983;65:55-63.
- Zainuddin NASN, Sul'ain MD. Phytochemical analysis, toxicity and cytotoxicity evaluation of *Dendrophthoe pentandra* leaves extracts. *Int J Appl Biol Pharm Tech.* 2015;6:108-116.

33. Senger DR, Perruzzi CA, Streit M, Kotliansky VE, de Fougerolles AR, Detmar M. The  $\alpha(1)\beta(1)$  and  $\alpha(2)\beta(1)$  integrins provide critical support for vascular endothelial growth factor signaling, endothelial cell migration, and tumor angiogenesis. *Am J Pathol.* 2002;160:195-204.
34. Joensuu H. Systemic chemotherapy for cancer: from weapon to treatment. *Lancet Oncol.* 2008;9:304.
35. Brady HJM. *Apoptosis Methods and Protocols*, Humana Press, Totowa, NJ, USA, 2004.
36. Syed Abdul Rahman SN, Abdul Wahab N, Abd Malek SN. *In vitro* morphological assessment of apoptosis induced by antiproliferative constituents from the rhizomes of *Curcuma zedoaria*. *Evid Based Complement Alternat Med.* 2013;2013:257108.
37. Gupta DD, Mishra S, Verma SS, Shekher A, Rai V, Awasthee N, Das TJ, Paul D, Das SK, Tag H, Gupta SC, Hui PK. Evaluation of antioxidant, anti-inflammatory and anticancer activities of diosgenin enriched *Paris polyphylla* rhizome extract of Indian Himalayan landraces. *J Ethnopharmacol.* 2021;270:113842.
38. Solowey E, Lichtenstein M, Sallon S, Paavilainen H, Solowey E, Lorberboum-Galski H. Evaluating medicinal plants for anticancer activity. *Sci World J.* 2014;2014:721402.
39. Neidle S. DNA minor-groove recognition by small molecules. *Nat Prod Rep.* 2001;18:291-309.
40. Zhao YR, Li HM, Zhu M, Li J, Ma T, Huo Q, Hong YS, Wu CZ. Non-benzoquinone geldanamycin analog, WK-88-1, induces apoptosis in human breast cancer cell lines. *J Microbiol Biotechnol.* 2018;28:542-550.
41. Milner SE, Brunton NP, Jones PW, O'Brien NM, Collins SG, Maguire AR. Bioactivities of glycoalkaloids and their aglycones from *Solanum* species. *J Agric Food Chem.* 2011;59:3454-3484.
42. Ji YB, Gao SY, Ji CF, Zou X. Induction of apoptosis in HepG2 cells by solanine and Bcl-2 protein. *J Ethnopharmacol.* 2008;115:194-202.
43. Xu Y, Du Y. Effect of molecular structure of chitosan on protein delivery properties of chitosan nanoparticles. *Int J Pharm.* 2003;250:215-226.
44. Qi L, Xu Z, Jiang X, Hu C, Zou X. Preparation and antibacterial activity of chitosan nanoparticles. *Carbohydr Res.* 2004;339:2693-2700.
45. Artursson P, Lindmark T, Davis SS, Illum L. Effect of chitosan on the permeability of monolayers of intestinal epithelial cells (Caco-2). *Pharm Res.* 1994;11:1358-1361.
46. Fernández-Urrusuno R, Calvo P, Remuñán-López C, Vila-Jato JL, Alonso MJ. Enhancement of nasal absorption of insulin using chitosan nanoparticles. *Pharm Res.* 1999;16:1576-1581.
47. Vårum KM, Myhr MM, Hjerde RJ, Smidsrød O. *In vitro* degradation rates of partially *N*-acetylated chitosans in human serum. *Carbohydr Res.* 1997;299:99-101.
48. Yuan B, Byrnes DR, Dinssa FF, Simon JE, Wu Q. Identification of polyphenols, glycoalkaloids, and saponins in *Solanum scabrum* berries using HPLC-UV/Vis-MS. *J Food Sci.* 2019;84:235-243.
49. Niknejad H, Mahmoudzadeh R. Comparison of different crosslinking methods for preparation of docetaxel-loaded albumin nanoparticles. *Iran J Pharm Res.* 2015;14:385-394.
50. Siddique AB, Brunton N. Food Glycoalkaloids: distribution, structure, cytotoxicity, extraction, and biological activity. In: *Alkaloids* (Kurek J, Ed.), Ebook, IntechOpen, 2019.
51. Vane JR, Botting RM. Anti-inflammatory drugs and their mechanism of action. *Inflamm Res.* 1998;(Suppl 2):S78-S87.
52. Porter AG, Jänicke RU. Emerging roles of caspase-3 in apoptosis. *Cell Death Differ.* 1999;6:99-104.
53. Ordóñez- Vásquez A, Aguirre-Arzola V, De la Garza-Ramos MA, Urrutia-Baca VH, Suárez-Obando F. Toxicity, teratogenicity and anti-cancer activity of  $\alpha$ -solanine: a perspective on anti-cancer potential. *Int J Pharmacol.* 2019;15:301-310.
54. Crnkovic-Mertens I, Hoppe-Seyler F, Butz K. Induction of apoptosis in tumor cells by siRNA-mediated silencing of the *livin/ML-IAP/KIAP* gene. *Oncogene.* 2003;22:8330-8336.
55. Mao S, Sun W, Kissel T. Chitosan-based formulations for delivery of DNA and siRNA. *Adv Drug Deliv Rev.* 2010;62:12-27.



# Evaluation of Marketed Rosemary Essential Oils (*Rosmarinus officinalis* L.) in Terms of European Pharmacopoeia 10.0 Criteria

Timur Hakan BARAK<sup>1\*</sup>, Elif BÖLÜKBAŞ<sup>2</sup>, Hilal BARDAKCI<sup>1</sup>

<sup>1</sup>Acıbadem Mehmet Ali Aydınlar University, Faculty of Pharmacy, Department of Pharmacognosy, İstanbul, Türkiye

<sup>2</sup>Acıbadem Mehmet Ali Aydınlar University, Faculty of Pharmacy, İstanbul, Türkiye

## ABSTRACT

**Objectives:** Various pure rosemary essential oil containing commercial products are in demand for their health-promoting and cosmetic claims in Türkiye. Although they are natural and harmless, they should be in compliance with European Pharmacopoeia (EP) criteria. Therefore, in this study, 15 rosemary oil samples sold in pharmacies, herbal shops, and online platforms in Türkiye were investigated in terms of "Rosemary Oil" EP 10.0 monograph criteria. In the current study, we aimed to evaluate the current quality status of rosemary essential oils in the Turkish market.

**Materials and Methods:** Appearance, fatty oils and resinified essential oils, relative density, refractive index, optical rotation, and acid value tests were performed according to EP 10.0 and compared with the given standards. In addition, thin layer chromatography (TLC) and gas chromatography-mass spectrometry (GC-MS) analysis were conducted on all samples for advanced understanding of their phytochemical profile and harmony with EP standards.

**Results:** Fifteen pure rosemary oil-containing products from the Turkish market were evaluated. All of the samples were licensed as cosmetic products in Türkiye via the Ministry of Health. 83.1 to 96.9% of the ingredients of all samples were determined via GC-MS analysis. Results demonstrated that none of the samples from the Turkish rosemary essential oil market fully complied with the EP rosemary oil monograph standards.

**Conclusion:** Considering our data, it was revealed that enhanced regulations and auditing mechanisms are needed to improve the quality of products. When the difference between the sources of purchase is assessed, pharmacies are still better locations to obtain such products.

**Keywords:** *Rosmarinus officinalis* L., rosemary oil, European Pharmacopoeia, GC-MS, essential oil

## INTRODUCTION

With the increasing interest in natural-based therapies, use of essential oils for medical and cosmetic purposes is accordingly accumulating. Essential oils have various biological activities, thus scientific studies investigating aromatherapy are growing.<sup>1</sup> *Rosmarinus officinalis* L. is a member of Lamiaceae family, grown naturally and widely cultivated in the Mediterranean region, particularly for culinary purposes. The aerial parts have distinct characteristic fragrance and flavor.<sup>2</sup> In traditional medicinal systems, aerial parts of *R. officinalis* are used as tea or tinctures against gastrointestinal system (GIS) disorders

and inflammatory diseases. In addition to crude herbal preparations, essential oil of *R. officinalis* has also significant biological activities, thus, popularity of use in aromatherapy is escalating.<sup>3</sup> Previous studies demonstrated that essential oil of *R. officinalis* may be used against circulatory problems, GIS disorders, muscular pain, and inflammations.<sup>4</sup> Reported biological properties of the essential oil is attributed to several ingredients, primarily monoterpenes, such as 1,8-cineole, borneol, and limonene.<sup>4</sup> Therefore, it is crucial to evaluate the phytochemical profile of an essential oil before its use for medical and cosmetic purposes.

March 7, 8 2022, online 2<sup>th</sup> International Aegean Health Areas Symposium (IAHAS'22).

\*Correspondence: thakanbarak@gmail.com, Phone: +90 216 500 44 44, ORCID-ID: orcid.org/0000-0002-7434-3175

Received: 29.07.2022, Accepted: 20.11.2022



©2023 The Author. Published by Galenos Publishing House on behalf of Turkish Pharmacists' Association.

This is an open access article under the Creative Commons Attribution-NonCommercial-NoDerivatives 4.0 (CC BY-NC-ND) International License.

Pharmacopoeias are official publications that establish necessary quality requirements for both synthetic and natural based medical products aiming to promote and protect public health. The Republic of Türkiye is legally bound (or responsible or have to obey the rules of) to the European Pharmacopoeia (EP), which contains more than 200 herbal drug monographs. Products claiming to contain pure *R. officinalis* essential oil are readily available in Turkish market and most of them are licensed as cosmetic products *via* the Ministry of Health. It may be beneficial to evaluate marketed products in terms of EP 10.0, which is the most up to date version, for better understanding the current situation of the essential oil market in terms of quality that strongly affects public health. Yet, a literature survey revealed that there is a lack of studies investigating quality situation of *R. officinalis* products on the market based on the rosemary oil monograph in the EP. For this reason, in this study, 15 samples that were sold as pure rosemary oil were investigated, 5 of them were purchased in pharmacies, while 10 of them were purchased from other sales channels such as herbalists and online platforms. Relative density, refractive index, optical rotation, and acid value of the samples were calculated through assays given in pharmacopeia. Similarly, appearance and thin layer chromatography (TLC) results were visually investigated based on the given criteria. Furthermore, chromatographic profiles of the samples are given in the monograph for two different chemotypes of rosemary oil. For determining the correspondence of the samples with the monograph, gas chromatography-mass spectrometry (GC-MS) analysis was conducted. Twelve different components were given in the monograph for both chemotypes and with different ranges. Results of GC-MS analysis were compared and analyzed with the required ranges stated in the monograph. In the current study, it was aimed to evaluate current quality status of rosemary essential oils in the Turkish market for creating a plain picture. It is an essential public health requirement for products that claim to have health benefits to contain the specified international standards.

## MATERIALS AND METHODS

### Materials

Products containing pure rosemary essential oil were procured from herbalists, online shopping platforms, and pharmacies in the Istanbul region. All products are registered as cosmetics by the Turkish Ministry of Health. In addition, labels of all oil samples claim to contain pure rosemary oil. Until the experiments, products were maintained at room temperature in tightly closed containers and protected from sunlight. All products were coded indicating their source (P: pharmacy, A: other sources). All standards and solvents (1,8-cineole, borneol, bornyl acetate, hexane, toluene, ethyl acetate, *etc.*) were purchased from Sigma-Aldrich.

*Appearance, labelling, and fatty oils and resinified essential oils*  
All tests were applied as stated in EP with small modifications.<sup>5</sup> All samples were dripped on the filter paper as a drop and the filter paper was kept in an oven at 80 °C for 30 minutes for the

fatty oils and resinified essential oils tests. The samples were filled in a glass tube and photographed for evaluation of their appearance. Labels of the samples were checked for presence of knowledge of chemotype.

### *Relative density, refractive index, optical rotation, and acid value*

Relative density, refractive index, optical rotation, and acid value assays were conducted according to the methods given in EP 10.0. Relative density results were evaluated using a pycnometer and volume of the essential oil samples with an equivalent volume of water at 20 °C was measured. For refractive index analysis, Anton Paar-Abbemat 3100 device and Anton Paar-MCP 150 device for optical rotation assay were used. The acid values of the samples were determined by the titrimetric method described in EP. All experiments were conducted in triplicate and results were given with average and standard deviation (SD).<sup>5</sup>

### *TLC analysis*

TLC analyses were conducted according to indications given in rosemary monograph in EP. Standards of borneol, bornyl acetate, and cineole were dissolved in toluene and used as reference solutions. 0.5 mL of samples were also dissolved in same solvent as test solutions. Ethyl acetate and toluene mixture (5:95, v/v) was used as mobile phase. Detections were completed with vanillin reagent application and immediately heating the plate in an oven at 100-105 °C for 10 min.<sup>5</sup>

### *GC-MS analysis*

Qualitative and quantitative analyses were performed using GC-MS. Agilent Technologies 7890 A GC system equipped with a DP-5 MS column (30 m x 0.25 mm x 0.25 µm) was used. The oven temperature was started at 60 °C and, then, steadily increased to 246 °C with 3 °C increase *per* minute. Helium was used as the mobile phase with 0.9 mL/min flow rate. Split mode was used with 50:1 ratio with 1 µL sample volume. Relative retention index (RRI) was calculated *via* comparison with (C<sub>4</sub>-C<sub>40</sub>) standards. Identification of the essential oil components was completed by comparison of their RRI calculated against *n*-alkanes and relative retention times with those of authentic samples and mass spectra obtained from NIST14 and Wiley7 mass spectra libraries as well as MS literature data was used for the identification.<sup>6</sup>

## RESULTS

### *Appearance, labelling, and fatty oils and resinified essential oils*

EP 10.0 states that rosemary oil should be clear, mobile, colorless or pale-yellow liquid with characteristic odor. EP 10.0 states that all of the rosemary oil samples should indicate the chemotype of the ingredient on the labels. Conformance of the samples to EP criteria is evaluated in Figure 1. Results exhibited that appearance properties of all the samples were compatible with EP; however, only samples P4 and P5 indicated the chemotype of the oil in the label. Fatty oils and resinified essential oils were conducted to reveal possible adulteration of oils with non-volatile materials. After drying in the incubator,

Experiment	Reference interval	P1	P2	P3	P4	P5	A1	A2	A3	A4	A5	A6	A7	A8	A9	A10
Fatty oils and resinified essential oils		✓	✓	X	✓	✓	X	X	✓	X	✓	✓	✓	✓	✓	✓
Appearance		✓	✓	✓	✓	✓	✓	✓	✓	✓	✓	✓	✓	✓	✓	✓
Relative density	0.895 - 0.920	0.893	0.876	0.900	0.919	0.945	0.893	0.903	0.901	0.888	0.880	0.920	0.890	0.886	0.889	0.889
Refractive index	1.464 - 1.473	1.467	1.469	1.473	1.471	1.469	1.474	1.473	1.466	1.474	1.472	1.467	1.471	1.467	1.475	1.471
Optical rotation	-5, 8	3.73	5.86	6.71	6.2	23.88	-2.92	1	5.88	-2.79	5.71	0.2	5.97	2.3	4.3	-0.33
Acidity index	Maximum 1	1.40	2.16	1.43	0.45	1.6	1.12	0.45	0.62	0.51	0.34	0.45	0.28	0.69	1.46	0.55
TLC		✓	✓	✓	✓	✓	✓	X	X	✓	✓	✓	X	X	✓	✓
Labelling		X	X	X	✓	✓	X	X	X	X	X	X	X	X	X	X

**Figure 1.** General evaluation of EP tests

\*Green boxes show suitability, red boxes are indicative of inconvenience with ranges indicated in EP

EP: European Pharmacopoeia, TLC: Thin layer chromatography

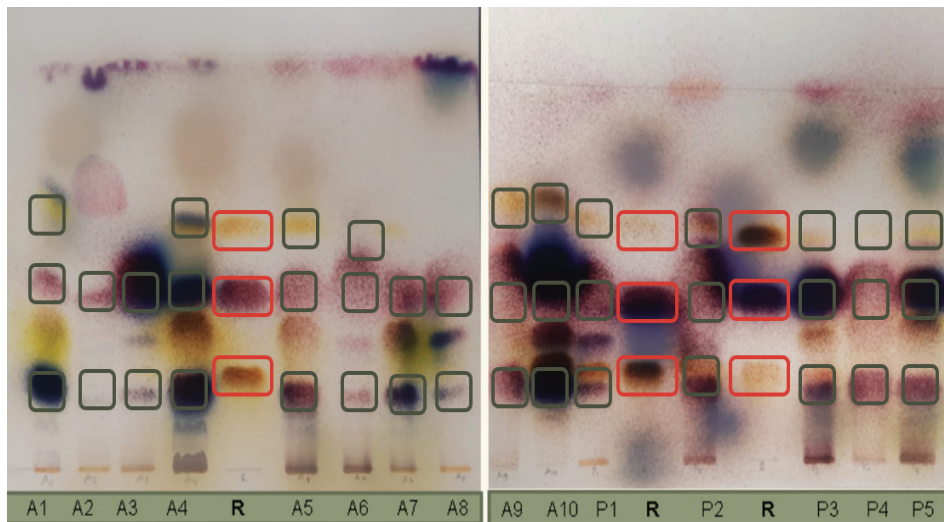


**Figure 2.** TLC chromatograms of all samples. R: Reference mixture; bornyl acetate, cineole, and borneol from top to bottom. Mobile phase; ethyl acetate:toluene (5:95, v/v), TLC: Thin layer chromatography

P3, A1, A2, and A4 samples exhibited a remaining spot in the filter paper, which indicates the presence of non-volatile ingredients Figure 1.

#### *Relative density, refractive index, optical rotation, and acid value*

The relative density, refractive index, optical rotation, and acid value results of 15 essential oil samples are given in Table 1. According to EP 10.0 standards, the relative density value for rosemary oil should be between 0.895 and 0.920, 1.464 and 1.473 for refractive index,  $-5^\circ$  and  $8^\circ$  for optical rotation, and the acid value must be lower than 1.0. Compatibility of samples with EP 10.0 standards was evaluated and summarized in Figure 1.

#### *TLC analysis*

According to EP 10.0, bornyl acetate should appear as a bluish-gray zone of low intensity (top), cineole as an intense blue zone (midline), and borneol as a violet-blue zone of medium intensity (bottom). All of the samples were evaluated with TLC method; the images of the plaques and coherence of all ingredients with the monograph are given in Figures 1 and 2, respectively.

#### *GC-MS analysis*

EP 10.0 mentions two different chemotypes of rosemary oil. Results of GC-MS analyses conducted on all samples are given in Table 2, where 83.1 to 96.9% of the ingredients were determined for all samples. Chromatograms that indicate the ingredients specified in EP are given in Figure 3. GC-MS results were evaluated in accordance with the most proximate chemotype and coherence of all ingredients with the monograph is given in Figure 4.

## DISCUSSION

EP contains specific individual monographs for some essential oils, which are widely used in pharmacy and have medicinal or cosmetic utilization. Thus, it is crucial for a product that contains pure essential oil to meet the criteria stated in monographs to ensure its scientific basis for aforementioned utilizations.<sup>7</sup> Importance of quality standards of herbal products in the market is increasing because public attention to complementary therapies and natural cosmetics is growing and amplified competition between producers creates possible

Table 1. Results of relative density, refractive index, optical rotation, and acid value of the tested samples

	P1	P2	P3	P4	P5	A1	A2	A3	A4	A5	A6	A7	A8	A9	A10
<b>Relative density</b>	0.89 ± 0.02	0.79 ± 0.16	0.90 ± 0.02	0.92 ± 0.03	0.95 ± 0.10	0.74 ± 0.26	0.90 ± 0.05	0.80 ± 0.17	0.89 ± 0.01	0.79 ± 0.15	0.92 ± 0.03	0.89 ± 0.01	0.89 ± 0.01	0.89 ± 0.01	0.89 ± 0.01
<b>Refractive index</b>	1.47 ± 0.001	1.47 ± 0.000	1.47 ± 0.000	1.47 ± 0.001	1.47 ± 0.000	1.47 ± 0.000	1.47 ± 0.001	1.47 ± 0.000	1.47 ± 0.000	1.47 ± 0.000	1.47 ± 0.000	1.47 ± 0.000	1.47 ± 0.000	1.48 ± 0.003	1.47 ± 0.001
<b>Optical rotation</b>	3.76° ± 0.11	5.90° ± 0.14	6.71° ± 1.82	6.20° ± 0.11	23.82° ± 0.59	-2.92° ± 0.07	1.00° ± 0.46	5.88° ± 0.30	-2.79° ± 0.02	5.71° ± 0.44	0.20° ± 0.11	5.97° ± 0.12	2.33° ± 1.15	4.33° ± 0.58	-0.33° ± 4.04
<b>Acid value</b>	1.40 ± 0.08	2.16 ± 0.20	1.43 ± 0.36	0.45 ± 0.16	1.60 ± 0.12	1.12 ± 0.00	0.45 ± 0.01	0.62 ± 0.08	0.50 ± 0.08	0.34 ± 0.00	0.45 ± 0.00	0.28 ± 0.08	0.69 ± 0.14	1.46 ± 0.00	0.55 ± 0.06

All test were done in triplicate and results were given in average ± standard deviation (SD)

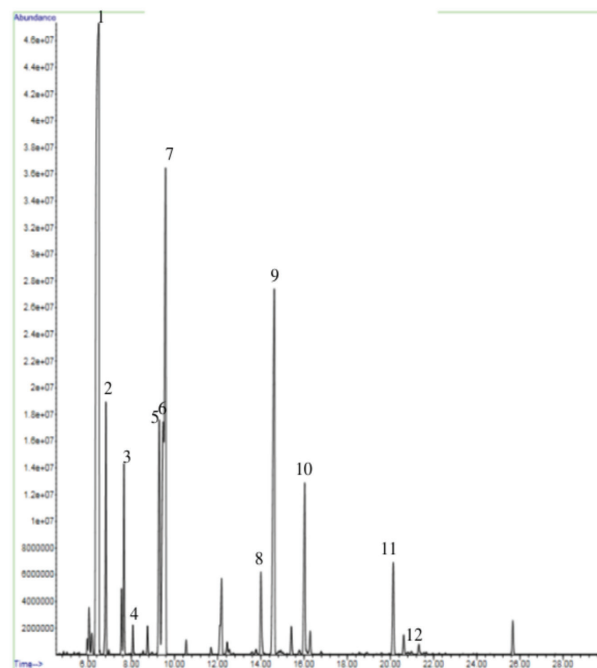


**Figure 3.** GC-MS chromatograms of P5 sample showing the chemical components given in pharmacopoeia: 1:  $\alpha$ -pinene, 2: camphene, 3:  $\beta$ -pinene, 4:  $\beta$ -myrcene, 5: limonene, 6: cineole, 7: *p*-cymene, 8: camphor, 9: borneol, 10:  $\alpha$ -terpineol, 11: bornyl acetate, and 12: verbenone

GC-MS: Gas chromatography-mass spectrometry

exploitation environment in conjunction with insufficient regulations and low knowledge level of the public. Thus, conducting regular scientific market analysis may create a clear understanding of the current status and may lead both public authorities, healthcare professionals, and the public to be deliberate against such products. There are several studies conducted in Türkiye that evaluate herbal drugs from Turkish market for their compliance with EP. Previous studies on the evaluation of *Hibiscus sabdariffa* L., *Eucalyptus* L'Her, and *Alchemilla* L. samples collected from the Turkish market for their consistency with EP are examples on that manner.<sup>8-10</sup> All studies demonstrated complications on the quality of the drugs that are freely sold in the market for medicinal purposes. In addition, two recent studies evaluated fixed oils sold on the Turkish market. Nearly all of the almond and safflower oil samples from the Turkish market were reported as lacking quality in terms of EP criteria.<sup>11,12</sup> Previous studies noticeably demonstrated the importance of such studies, when considering increasing public attention to natural based products for various medicinal purposes. Similarly, public demand for aromatherapy that uses essential oils for medicinal purposes is increasing.<sup>13</sup> Nonetheless, there is an obvious scarcity of studies assessing essential oil-containing products in the Turkish market for their compliance with EP. Basic objective of EP is ensuring the standards of products, so consumers can purchase any product without being anxious about its quality. In this context, for this study, 15 commercial products (5 from pharmacies and 10 from other sources) that claimed to contain pure rosemary oil were

Components	P1	P2	P3	P4	P5	A1	A2	A3	A4	A5	A6	A7	A8	A9	A10
$\alpha$ -Pinene	10.75	11.64	13.50	14.51	33.33	21.9	11.19	10.2	20.3	11.56	10.2	14.6	14.7	6.6	4.58
Camphene	5.1	5.88	3.66	5.53	4.159	3.109	3.06	6.35	3.26	4.89	5.18	5.3	8.7	2.3	3.04
$\beta$ -Pinene	6.41	7.77	2.58	2.91	3.24	3.03	1.54	8.21	3.12	3.01	8.98	2.8	5.6	1.4	2.48
$\beta$ -Myrcene	1.34	1.56	0.55	0.51	0.49	0.18	2.47	1.79	0.19	0.82	1.61	0.56	2.5	0.25	1.25
Limonene	-	-	-	-	6.91	3.04	3.17	-	2.99	11.1	-	-	-	-	19.82
1,8-Cineole	33.4	31.7	24.3	22.6	13.4	9.5	44.7	36.2	9.3	4.8	35.1	23.9	31.1	21.5	8.4
<i>p</i> -Cymene	3.45	2.28	6.67	6.67	6.18	1.62	3.95	5.02	1.7	9.51	2.57	6.28	1.97	6.6	4.9
Camphor	15.6	16.3	10.9	2.82	2.06	1.50	5.49	17.50	1.38	3.70	12.11	3.86	15.2	4.62	18.4
Bornyl acetate	1.92	1.22	2.00	3.20	2.18	1.12	2.26	1.62	1.22	4.01	1.81	3.13	2.6	5.3	1.8
$\alpha$ -Terpineol	2.5	2.4	3.3	6.7	4.5	16.3	2.4	2.9	16.4	7.7	2.4	6.4	1.8	9.2	3.9
Borneol	4.8	5.4	7.5	19.2	12.8	28.3	2.6	6.4	27.6	19.1	4.1	17.9	3.8	25.3	2.4
Verbenone	0.03	0.04	0.29	0.04	0.27	-	-	-	-	0.07	-	-	-	0.21	-

**Figure 4.** Comparison of GC-MS results with EP criteria

\*Green boxes show suitability, red boxes are indicative of inconvenience with ranges indicated in EP

GC-MS: Gas chromatography-mass spectrometry, EP: European Pharmacopoeia

purchased and evaluated in terms of standards stated in EP 10.0 “rosemary oil” monograph. Before the pharmacopoeia tests, simple fatty oils and resinified essential oil tests were applied to the products. Pure essential oils must be entirely composed of volatile features; therefore, when they are dripped onto filter paper and kept in an oven at high temperature, observing a significant stain on the paper is unexpected. Evident remaining stains may indicate a possible adulteration or a deficiency that causes a decrease in quality in production procedure, hence it is accepted as a parameter for this study. Results of the fatty oils and resinified essential oils assay are given in Figure 1. Four of the samples left clear stains in the filter paper (P3, A1, A2, and A4), which indicate that non-volatile principles are present in products and therefore failed to fulfill the parameter. Characters section in the monograph requires specific appearance and color for rosemary oil; clear, mobile colorless or pale yellow liquid with characteristic odor. Results displayed that all the samples were coherent with the properties stated in the monograph. TLC assay is required in the monograph as an identification test. Test solutions obtained from samples must correspond with the reference solution on the TLC plate according to monograph. TLC analysis was conducted on all samples and pictures of TLC plates are given in Figure 2. Results of the TLC test indicate that all the samples from pharmacies passed the test; in contrast, four of ten samples obtained from sales sources other than pharmacies (A2, A3, A7, and A8) failed to compensate for the TLC test requirements stated in EP. In the tests section of the monograph, necessities for refractive index, optical rotation, acid value, relative density, and chromatographic profile were stated. Refractive index can be defined as the ratio of the sine of the refraction angle, when light is passing from different mediums and represents a characteristic physical constant of an oil. Three decimals are mandatory for the definitive result and for rosemary oil, while the monograph indicates that the refractive index of rosemary

oil must be between 1.464 and 1.473. Refractive indices were conducted on all samples as explained in the pharmacopoeia in triplicate and results of the average measurements and standard deviations are given in Table 1. All samples from pharmacies displayed refractive index in the accepted range; however, three samples from other sources (A1, A4, and A9) were found to be out of range. Optical rotation is the feature exhibited by chiral substances rotating the linearly polarized light. In the monograph, it was specified that, optical rotation value must be between  $-5^\circ$  and  $+8^\circ$  for rosemary oil. In Table 1, average results and standard deviations were given for optical rotation tests of all samples. Results indicated that only one sample (P5) was out of the range and all other samples fulfilled the requirements of the pharmacopoeia. Relative density and acid value tests exhibited the most improper results amongst others. Relative density can be defined as the relation between the mass of a definite volume of the studied substance at  $20^\circ\text{C}$  and the mass of an equivalent volume of water at the identical temperature. Pharmacopoeia stated the relative density range for rosemary oil as 0.895 to 0.920 and only three of the studied samples (P3, A6, and A8) were measured in the specified range. Acid value ( $I_A$ ) shows the amount of mg of KOH required to neutralize all free acids in one gram of EO. For rosemary oil,  $I_A$  is limited to maximum 1. Parallel to relative density results, only three samples calculated (P4, A5, and A10) were in acceptable range after triple measurement.

Chromatographic profile can be considered as the most important feature of essential oils since biological activities occurring due to their volatile ingredients. Thus, their phytochemical profile determines the bioactivity.<sup>14</sup> However, some plant species are known for their rich chemotypes, which lead to massive variations in their chemical ingredients. *R. officinalis* is one of these species that has been detected for several different chemotypes highly affected from geographical impacts.<sup>15</sup> In relevant EP 10.0 monograph, there are two defined



Table 2. Chemical composition of the tested samples

Components	RI	R <sub>t</sub>	Identification	P1	P2	P3	P4	P5	A1	A2	A3	A4	A5	A6	A7	A8	A9	A10
<b>Monoterpene hydrocarbons</b>																		
$\alpha$ -Pinene	932	6.3	a, b, c	10.8	11.6	13.5	14.5	33.3	21.9	11.2	10.2	20.3	11.6	10.2	14.6	14.7	6.6	4.58
Camphene	949	6.8	b, c	5.1	5.9	3.7	5.5	4.2	3.1	3.1	6.3	3.3	4.9	5.2	5.3	8.8	2.3	3.04
$\beta$ -Phellandrene	974	7.53	b, c	0.07	0.03	0.17	1.32	1.13	0.03	-	0.04	0.03	1.82	0.18	2.00	-	-	-
$\beta$ -Pinene	978	7.65	b, c	6.41	7.77	2.58	2.91	3.24	3.03	1.54	8.21	3.17	3.01	8.98	2.84	5.55	1.38	2.48
$\beta$ -Myrcene	992	8.06	b, c	1.34	1.56	0.55	0.51	0.49	0.18	2.47	1.79	0.19	0.82	1.61	0.56	2.54	0.25	1.25
<i>p</i> -Cymene	1027	9.32	b, c	3.45	2.28	6.67	6.67	6.18	1.62	3.95	5.02	1.71	9.51	2.57	6.28	1.97	6.56	4.88
$\alpha$ -Phellandrene	1006	8.53	b, c	0.12	0.27	0.07	0.25	0.08	0.07	0.19	0.58	0.09	0.32	0.23	0.27	0.36	-	0.54
Limonene	1031	9.4	a, b, c	-	-	-	-	6.91	3.04	3.17	-	2.99	11.1	-	-	-	-	19.8
$\gamma$ -Terpinene	1059	10.54	b, c	0.37	0.37	0.03	3.00	0.27	0.51	0.34	0.55	0.58	2.51	1.17	2.99	1.01	-	9.93
$\beta$ -Ocimene	1048	10.12	b, c	0.05	-	-	-	-	-	-	0.02	-	0.01	0.06	-	0.06	-	0.60
3-Carene	1102	12.16	c	0.03	0.21	1.35	2.49	2.15	1.07	0.41	0.17	1.20	-	-	-	-	-	-
Bornyl acetate	1.288	20.11	a, b, c	1.92	1.22	2.00	3.20	2.18	1.12	2.26	1.62	1.22	4.01	1.81	3.13	2.59	5.31	1.83
<b>Oxygenated monoterpenes</b>																		
1,8-Cineole	1035	9.6	a, b, c	33.4	31.7	24.3	22.6	13.4	9.5	44.7	36.2	9.3	4.8	35.1	23.9	31.1	21.5	8.4
Linalool	1103	12.2	a, b, c	-	-	-	-	-	-	-	-	-	3.1	1.08	2.34	2.01	3.7	1.8
Fenchol	1116	12.8	b, c	0.08	0.12	0.09	0.03	-	0.17	-	-	0.21	0.04	0.04	0.06	0.05	0.04	0.08
Camphor	1146	14.10	a, b, c	15.6	16.3	10.9	2.8	2.1	1.50	5.49	17.5	1.38	3.70	12.1	3.86	15.2	4.62	18.4
Borneol	1163	14.73	a, b, c	4.8	5.4	7.5	19.2	12.8	28.3	2.6	6.4	27.6	19.1	4.1	17.9	3.8	25.3	2.4
4-Terpineol	1179	15.41	c	-	0.3	-	-	-	0.7	0.8	-	-	-	-	0.8	0.7	1.0	0.1
$\alpha$ -Terpineol	1194	16.10	a, b, c	2.5	2.4	3.3	6.7	4.5	16.3	2.4	2.9	16.4	7.7	2.4	6.4	1.8	9.2	3.9
<b>Sesquiterpene hydrocarbons</b>																		
Verbenone	1302	20.73	b, c	0.03	0.04	0.29	0.04	0.27	-	-	-	-	0.07	-	-	-	0.21	-
Caryophyllene	1420	25.68	b, c	5.2	0.8	3.0	1.7	0.8	0.5	10.1	1.0	0.6	2.1	6.0	1.9	3.6	1.2	2.8
Humulene	1454	27.05	b, c	0.55	0.11	0.80	-	-	0.06	1.63	0.10	0.07	0.02	0.64	0.04	0.41	0.13	0.04
$\gamma$ -Muuroleone	1486	28.37	b, c	0.41	0.09	0.05	-	-	-	0.25	0.05	-	-	0.28	-	0.15	-	-
$\alpha$ -Muuroleone	1500	28.93	b, c	0.12	-	0.04	-	-	-	-	-	-	-	0.09	-	-	-	-
<b>Oxygenated sesquiterpenes</b>																		
$\alpha$ -Copaene	1376	23.83	b, c	0.52	0.07	-	-	-	-	0.22	0.05	-	0.04	0.42	-	0.24	-	-
$\beta$ -Copaene	1429	26.05	c	0.10	-	-	-	-	-	-	-	-	-	0.08	-	0.04	-	-
Caryophyllene oxide	1584	32.16	b, c	0.45	-	2.19	-	0.24	-	0.47	-	-	0.17	0.3	0.1	0.1	1.44	-
<b>Others</b>																		
3-Octanone	985	7.857	c	0.06	-	0.06	-	-	-	-	-	-	-	0.06	-	0.03	-	-
Ylangene	1372	23.667	c	0.14	0.05	0.26	-	-	-	-	-	-	-	0.12	-	0.08	-	-
$\alpha$ -Guaiene	1487	28.385	c	0.04	0.07	-	-	-	0.04	-	-	-	-	-	-	-	-	-
Isolodene	1499	28.854	c	0.14	0.39	-	-	-	-	-	0.07	-	-	0.12	-	0.06	-	-
Total (%)				83.1	89.1	83.3	93.6	94.1	92.8	97.3	98.7	90.3	90.4	94.9	95.2	96.9	90.6	86.8

a: Identification based on comparison of retention time with standard compounds, b: Identification based on retention index; c: Identification based on library, RI: Retention index, Rt: Retention time

chemotypes, which are recorded as Spanish and Moroccan/Tunisian types. It is also crucial for producer to indicate the chemotype on the label so it is possible for consumers and healthcare professionals to select the product accordingly. As a result, in the monograph labeling is a necessity for rosemary oil. Nevertheless, only two of the evaluated products (P4 and P5) contain a label that indicates the chemotype of the ingredient (Figure 1). In the monograph, chromatographic profile diversifies according to the chemotype (*i.e.* Spanish type contains a lower amount of cineole and higher amount of camphor). For this study, chromatographic profiles were analyzed with a GC-MS method and results were evaluated according to the most consistent chemotype, which is proximate to the products that contain labels that do not remark the chemotype. There are 12 monoterpenoid compounds that were mentioned and indicated as a requirement in the pharmacopeia for the Spanish type.  $\alpha$ -Pinene and cineole are determined as major components with the range of 18–26% and 16–25%, respectively. For the Moroccan/Tunisian type, cineole is determined as the dominant major ingredient in the range between 38 and 55%, while  $\alpha$ -pinene content was determined between 9 and 14%. However, chemotype information was mentioned only two of the samples, whereas other samples were evaluated according to most proximate one in the pharmacopeia. All 15 samples were analyzed with GC-MS method and results are given in Table 2. GC-MS results were also compared with the monograph and results are given in Figure 4. None of the samples was entirely fitting with the monograph requirements. A6 was determined as the most coherent sample with GC profile given in monograph for Moroccan/Tunisian type, 9 of the ingredients out of 12 requirements for these samples were consistent with the monograph.

Cineole content of A6 sample is slightly lower than expected, while *p*-cymene content is slightly higher. However, limonene is absent in the oil, which is required to contain a minimum of 1.5% according to EP.<sup>5</sup> Limonene is known for its various beneficial bioactivities such as antioxidant, anti-inflammatory, and gastroprotective effects.<sup>16</sup> Absence of limonene may reduce possible health benefits of *R. officinalis* essential oil. A2 followed A6 with 8 positive results and P1, P2, and A8 were measured with 7 positive results. Limonene content is suitable for A2, however it is also absent in P1, P2, and A8 samples. For A2 samples there are slight differences for  $\beta$ -pinene,  $\beta$ -myrcene, *p*-cymene, and bornyl acetate. In contrast, A9 was designated as most out of spec sample consistent with only one ingredient of the GC profile requirements. It is followed by P4 and A7, which are congruent with only two components (Figure 3). Cineole is the major ingredient of both chemotypes; however, only A2 sample was measured to contain sufficient cineole to meet the criteria of Moroccan/Tunisian type with 44.7%, all other samples had cineole content between 8.4 and 36.2%. Previous studies also reported a great variation. For instance, Ozcan and Chalcha<sup>16</sup> calculated cineole content of *R. officinalis* essential oil from Türkiye as 2.64%, while Daferera et al.<sup>17</sup> found that 88.9% of the rosemary oil from Greece was cineole.  $\alpha$ -pinene is another major ingredient of rosemary oil according

to monograph. Results of the GC-MS analysis similarly demonstrated that  $\alpha$ -pinene contents of the samples are highly varied, between 4.58–33.3%. Previous literature exhibited considerable diversion between  $\alpha$ -pinene content of different rosemary oil samples. Sharma et al.<sup>18</sup> calculated  $\alpha$ -pinene content of French rosemary oil as 37.5%, while Tunisian counterpart only had 1.2%.<sup>19</sup> Even though there is a significant variation between samples, 10 of 15 were concordant with the pharmacopeia criteria. Limonene contents of the samples were most out of reach parameter, only 3 of the samples fitted with EP requirement; Spanish and Moroccan/Tunisian types need to be 2.5–5% and 1.5–4%, respectively. Results showed that 9 of the samples do not contain limonene at all, while 3 of the samples contain greater than the upper limit. A1, A2, and A4-coded samples were found convenient with limits, 3, 3.17, and 2.99%, respectively. Variations in limonene contents were also suitable with previous results since Sharma et al.<sup>18</sup> measured limonene content of French and Italian rosemary oils as 5.35 and 3.06%, respectively. However, some researchers determined absence of limonene in rosemary oil samples from different locations.<sup>18,19</sup>

#### Study limitations

Although there are many more commercial products of rosemary essential oil in the Turkish market, 15 samples were studied to have adequate number. Even more accurate results could be achieved, if all relevant products on the market were studied.

## CONCLUSION

Essential oils are marketed with notable health-promoting statements. Amongst, rosemary oil is also claimed to have health and cosmetic benefits and sold without any control and restriction in several channels such as herbalists, websites, and pharmacies. Any product claiming any health benefits should meet the criteria of EP monograph, even if they are synthetic medicines, natural products, excipients in medicines or essential oils. Basic mission of any pharmacopeia is to prevent health hazards due to lack of quality of products. For these reasons, it is important to assess the quality of the rosemary oil-containing products in the market to determine the current status and level of quality of commercial products in the market. In this study, 15 products from the Turkish market were evaluated according to EP 10.0 and results revealed that none of the samples was in full compliance with the monograph. When the compliance rate was compared with purchase location, products from pharmacies were found to be slightly better than those from other sales channels. Ultimately, it was clearly revealed that quality standards or rosemary essential oils in the Turkish market need to be increased. Higher demands and improved auditing mechanisms from public authorities should be the initial step for increasing the quality of products.

#### Ethics

**Ethics Committee Approval:** Ethical approval is not necessary for this study.

**Informed Consent:** Not applicable.

**Peer-review:** Externally peer-reviewed.

#### Authorship Contributions

Concept: T.H.B., Design: T.H.B., E.B., H.B., Data Collection or Processing: T.H.B., E.B., Analysis or Interpretation: T.H.B., E.B., Literature Search: T.H.B., H.B., Writing: T.H.B., H.B.

**Conflict of Interest:** No conflict of interest was declared by the authors

**Financial Disclosure:** This study was supported by a grant (2209-A) from the Scientific and Technological Research Council of Türkiye (TÜBİTAK).

## REFERENCES

- Tang Y, Gong M, Qin X, Su H, Wang Z, Dong H. The therapeutic effect of aromatherapy on insomnia: a meta-analysis. *J Affect Disord.* 2021;288:1-9.
- Hudaib MM, Abu Hajal AF, Sakkal MM. Chemical composition of the volatile oil from aerial parts of *Rosmarinus officinalis* L. growing in UAE. *J Essent Oil Bear Plants.* 2022;25:282-289.
- Zeghib F, Tine-Djebbar F, Zeghib A, Bachari K, Sifi K, Soltani N. Chemical composition and larvicidal activity of *Rosmarinus officinalis* essential oil against west Nile vector mosquito *Culex pipiens* (L.). *J Essent Oil Bear Plants.* 2020;23:1463-1474.
- Rašković A, Milanović I, Pavlović N, Čebović T, Vukmirović S, Mikov M. Antioxidant activity of rosemary (*Rosmarinus officinalis* L.) essential oil and its hepatoprotective potential. *BMC Complement Altern Med.* 2014;14:225.
- EDQM. European Pharmacopoeia, 10<sup>th</sup> ed.; EDQM: Strasbourg, France, 2019.
- Abu Zarga MH, Al-Jaber HI, Baba Amer ZY, Sakhrif L, Al-Qudah MA, Al-humaidi JY, Abaza IF, Afifi, FU. Chemical composition, antimicrobial and antitumor activities of essential oil of *Ammodaucus leucotrichus* growing in Algeria. *J Biol Act Prod Nat.* 2013;3:224-231.
- Bouin AS, Wierer M. Quality standards of the European Pharmacopoeia. *J Ethnopharmacol.* 2014;158:454-457.
- Pesen Özdoğan F, Orhan N, Ergun F. Studies on the conformity of *Hibiscus sabdariffa* L. samples from Turkish market to European Pharmacopoeia. *FABAD J Pharm Sci.* 2011;36:25-32.
- Tombul AG, Orhan N, Sezik E, Ergun F. Morphologic, anatomical, and chromatographic studies on *Eucalyptus* (L'Hér.) samples from the market. *FABAD J Pharm Sci.* 2012;37:79-87.
- Renda G, Tevek F, Korkmaz B, Yaylı N. Comparison of the *Alchemilla* L. samples from Turkish Herbal Market with the European Pharmacopoeia 8.0. *Fabad J Pharm Sci.* 2017;42:167-177.
- Berkkan A, Dede Türk BN, Pekacar S, Ulutaş OK, Deliorman Orhan D. Evaluation of marketed almond oils [*Prunus dulcis* (Mill.) D.A. Webb] in terms of European Pharmacopoeia Criteria. *Turk J Pharm Sci.* 2022;19:322-329.
- Deliorman Orhan D, Pekacar S, Ulutaş OK, Özüpek B, Sümmeoğlu D, Berkkan A. Assessment of commercially safflower oils (Carthami Oleum Raffinatum) in terms of European Pharmacopoeia Criteria and their weight control potentials. *Turk J Pharm Sci.* 2022;19:273-279.
- Ueki S, Niinomi K, Takashima Y, Kimura R, Komai K, Murakami K, Fujiwara C. Effectiveness of aromatherapy in decreasing maternal anxiety for a sick child undergoing infusion in a paediatric clinic. *Complement Ther Med.* 2014;22:1019-1026.
- Karadag AE, Demirci B, Kultur S, Demirci F, Baser KHC. Antimicrobial, anticholinesterase evaluation and chemical characterization of essential oil *Phlomis kurdica* Rech. fil. growing in Turkey. *J Essent Oil Res.* 2020;32:242-246.
- Chalchat, JC, Garry RP, Michet A, Benjlilali B, Chabart JL. Essential oils of rosemary (*Rosmarinus officinalis* L.). The chemical composition of oils of various origins (Morocco, Spain, France). *J Essent Oil Res.* 1993;5:613-618.
- Ozcan MM, Chalchat JC. Chemical composition and antifungal activity of rosemary (*Rosmarinus officinalis* L.) oil from Turkey. *Int J Food Sci Nutr.* 2008;59:691-698.
- Daferera DJ, Ziogas BN, Polissiou MG. GC-MS analysis of essential oils from some Greek aromatic plants and their fungitoxicity on *Penicillium digitatum*. *J Agric Food Chem.* 2000;48:2576-2581.
- Sharma Y, Schaefer J, Streicher C, Stimson J, Fagan J. Qualitative analysis of essential oil from French and Italian varieties of rosemary (*Rosmarinus officinalis* L.) grown in the Midwestern United States. *Anal Chem Lett.* 2020;10:104-112.
- Jardak M, Elloumi-Mseddi J, Aifa S, Mnif S. Chemical composition, anti-biofilm activity and potential cytotoxic effect on cancer cells of *Rosmarinus officinalis* L. essential oil from Tunisia. *Lipids Health Dis.* 2017;16:190.



# Formulation, Characterization, and Optimization of a Topical Gel Containing Tranexamic Acid to Prevent Superficial Bleeding: *In Vivo* and *In Vitro* Evaluations

Farideh SHIEHZADEH<sup>1</sup>, Daryosh MOHEBI<sup>1</sup>, Omid CHAVOSHIAN<sup>2\*</sup>, Sara DANESHMAND<sup>1\*\*</sup>

<sup>1</sup>Zabol University of Medical Sciences, Faculty of Pharmacy, Department of Pharmaceutics, Zabol, Iran

<sup>2</sup>Mashhad University of Medical Sciences, Pharmaceutical Technology Institute, Nanotechnology Research Center, Mashhad, Iran

## ABSTRACT

**Objectives:** Tranexamic acid (TXA) is used systemically to stop bleeding, but it can lead to thromboembolism. Trials have revealed the efficacy of topical TXA on local hemorrhages. However, there is a need for an efficient delivery system that can keep the drug at the site of action.

**Materials and Methods:** To develop a gel containing TXA (3%) optimized in terms of viscosity and dispersibility, the central composite design based on two factors-three levels [carbopol 940 and hydroxypropyl methylcellulose (HPMC), 1-1.5% and 1-2%, respectively] was applied. The spreadability and viscosity were assessed using glass slide and rheometer, respectively. To confirm the compatibility of TXA with the gel, fourier transform-infrared (FTIR) spectroscopy was performed. Drug content uniformity was analyzed by a spectroscopy method. An *ex vivo* mice model using Franz cells was applied to evaluate the permeation of TXA through the skin. To investigate the effect of topical TXA gel on bleeding time, IVY human method was performed.

**Results:** HPMC/carbopol 940 (1:1, w/w) gel showed the highest quality in terms of viscosity and dispersibility ( $3.982 \pm 17.6$  and  $6.052 \pm 3.562$ , respectively). FTIR absorption spectrum showed that all the TXA index peaks appeared without displacement. The complete-encapsulated TXA content was uniformly dispersed throughout the gel. *In vitro* TXA cumulative release reached 90% in 4 h. The bleeding time determined *in vivo* for TXA gel was significantly lower than that for TXA solution and control.

**Conclusion:** The results confirm the importance of further studies on this formulation as a potential medication to stop acute superficial bleeding.

**Key words:** Tranexamic acid, hydroxypropyl methylcellulose, gel

## INTRODUCTION

In recent years, due to the difficulty, significant costs, and slow pace of discovery and development of new active ingredients, a major part of pharmaceutical science has focused on repositioning or in other words repurposing Food and Drug Administration (FDA)-approved drugs for human use to treat diseases.<sup>1</sup> One type of repositioning is to replace systemically

administered formulations with topical ones to cure local pathologic conditions. If this formulation can display acceptable effects on the site of action, while carrying fewer risks than systemic administration due to reduced systemic exposure to the drug, it could find a new position in the treatment schedule.<sup>2</sup> Tranexamic acid (TXA) was one of these studied medicines. It has a structure similar to amino acid lysine and inhibits

\*Correspondence: \*dr.chavoshian.omid@gmail.com, \*\*sdmehrpooaya@gmail.com, Phone: \*+985432225402, \*\*+989155079029

ORCID-ID: orcid.org/0000-0002-7635-8952 - 0000-0001-7474-0157

Received: 27.07.2022, Accepted: 30.11.2022



©2023 The Author. Published by Galenos Publishing House on behalf of Turkish Pharmacists' Association.

This is an open access article under the Creative Commons Attribution-NonCommercial-NoDerivatives 4.0 (CC BY-NC-ND) International License.

bleeding by fibrinolysis inhibition mechanism. This drug is used systemically to stop various types of bleedings, but its systemic use can lead to risks such as thromboembolism and *etc.*<sup>3</sup> The topical anti-inflammatory and anti-melanin-producing properties of tranexamic acid have led it to be extensively considered and commercially available in the field of dermatology as an off-label topical treatment for rosacea, urticaria, and post-inflammatory hyperpigmentation. However, randomized controlled trials have shown the positive effects of TXA topical administration on local hemorrhages, including post-surgery or traumatic mucosal (*e.g.* epistaxis)<sup>4</sup> or cutaneous hemorrhages.<sup>5,6</sup>

In these studies, TXA solution is often used, and sterile gauze is impregnated by it and placed at the site of bleeding.<sup>7</sup> However, there is still a need for a safer and more efficient drug delivery system than the method used, which can keep the drug at the site of action for a certain period and help it to be better absorbed.

Recently, in some studies, nasal spray formulations containing TXA in the form of powder mixed with hyaluronic acid<sup>8</sup> or *in situ* gel forming chitosan<sup>9</sup> have been considered for epistaxis treatment.

Gels composed of polymers such as poly (acrylic acid) (Carbopol®) and cellulose derivatives are one of suitable bases for prolonged delivery of water-soluble drugs to the dermal and mucosal areas, and their effectiveness for this purpose has been proven in the previous studies.<sup>10</sup>

Therefore, in this study, using the response surface method (RSM), an ideal carbopol 940/hydroxypropyl methylcellulose (HPMC) gel formulation containing TXA 3% was developed in terms of appearance, spreadability, and acidity. Then the uniformity of drug loading, interactions with, and release from the gel base in *ex vivo* environment was evaluated. Finally, *in vitro* efficacy of the formulation was evaluated by examining bleeding time in healthy volunteers.

To the best of our knowledge, this is the first HPMC/carbopol-based gel formulation containing TXA developed for topical application as anticoagulant agent, while *in vitro/in vivo* assessments were performed.

## MATERIALS AND METHODS

### Materials

TXA, Carbopol® 940, HPMC, ninhydrin, and triethanolamine were purchased from Sigma Aldrich (Germany). Deionized distilled water was freshly prepared. In this study, all solvents and chemicals were of analytical grade.

### Methods

#### Preparation of TXA containing carbopol 940/HPMC gel formulation

To achieve the topical drug-loaded gel formulation, an aqueous solution of carbopol 940 and HPMC with known concentration of each polymer (Table 1) was prepared by dissolving the polymers powder in 100 mL of deionized distilled water under 1100 rpm stirring for 2 hours at room temperature (RT) to

completely dissolve and hydrate. A constant volume (0.23 mL) of triethanolamine aqueous solution was then slowly added, while stirring continued. Following the gel base formation, 3% (w/w) of TXA was added and the gel formulation was stirred at 200 rpm overnight to load the drug efficiently. Finally, the volume of final gel formulation was brought up to 100 mL by deionized distilled water. Prepared gel formulations were preserved from air and direct light in sealed amber glass containers and kept at 4 °C before further analysis.<sup>11</sup>

#### Optimization of the carbopol/HPMC gel formulation by central composite design (CCD)

To develop an optimized gel base in terms of viscosity and dispersibility, CCD-based on two factors-three levels using Design Expert® software (version: DX7 trial) was applied. Carbopol 940 and HPMC concentrations were considered as independent variables while keeping triethanolamine volume constant (0.23 mL). The influence of independent factors on Y1 (spreadability) and Y2 (viscosity) as dependent variables was evaluated by RSM. By analyzing the obtained data, the formulation showing ideal spreadability and viscosity was chosen for further evaluation.

#### Rheological evaluations

##### Spreadability

The investigation of spreadability potential of the prepared gels was performed on the basis of a published study<sup>11</sup> with some slight modifications.

In this method, 2 g of gel was placed on a standard glass slide in the center between two lines with a distance of 4 cm. Then, the second glass slide weighing 110 g was gently placed on the gel. The dispersion time was calculated from the moment the second glass slide was placed until the gel was completely dispersed between the two lines. The experiment was repeated three times, and the meantime was calculated. The following equation (Equation 1) was used to calculate the dispersibility:

$$S = m \times l/t \text{ (Equation 1)}$$

Where, S= spreadability, m= weight of the upper slide (110 g), l- the distance of two lines (4 cm), t- time is taken in sec.

##### Viscosity

Viscosity of the prepared gel formulations was measured using a rheometer (AMETEK Brookfield R/S plus, USA) using a CC3-14 spindle. While the sample holder was filled with the gel, the spindle was inserted into the sample and rotated at a speed of 1/min. Rheological evaluations were performed at RT (n: 3).<sup>12</sup>

##### pH evaluation

To ensure acidity of the gel bases place in the standard range of 4.5-5.5, 1 g of each gel was diluted in 100 mL of double distilled water, and pH of the prepared solution was assessed using a calibrated pHmeter at RT (827 PH Lab, Metrohm, Switzerland).

##### Visual inspection

To evaluate the relative apparent transparency, suspended particles, and uniformity of the gel structures as a common

method of gel base quality control, each gel base was visually inspected by the naked eye using an illuminated dark background.

To assess the physical stability of the gel after 6 months of preparation, all the above items and pH were re-examined in the final optimized gel. The gel was preserved in an opaque sealed bottle at ambient temperature.

#### *Fourier transform-infrared spectroscopy (FTIR)*

FTIR spectroscopy was performed to confirm the compatibility of the active ingredient with the gel base chemical structure. Carbopol/HPMC (1:1 w/w) gel (run 13), TXA 3%-containing HPMC/carbopol 940 (1:1 w/w) gel, and TXA powder were analyzed by FTIR spectroscopy (IRAffinity SHIMADZU, Japan) to clarify the molecular interactions. Each sample was prepared as individual KBr disk and was scanned in the range of 400–4000  $\text{cm}^{-1}$ .

#### *The TXA quantification method*

To 1 mL of different dilutions of the drug solution (10–100  $\mu\text{g/mL}$ ), 1 mL of phosphate buffer (pH: 8) and 2 mL of the methanolic solution of 0.2% ninhydrin as the reagent were added (derivatization process). The samples were then heated with liquid paraffin oil at 90 °C for 20 min. After cooling to RT using 10 mL of double distilled water, the samples were brought to a volume of 10 mL. Finally, using an ultraviolet/visible spectrophotometer (CE1021, CECIL, England) the absorbance of the samples was read against a blank solution at 565 nm.<sup>13</sup>

#### *Drug encapsulation efficiency (EE) of gel preparation*

To measure the drug EE, 1 g of gel formulation was carefully weighed using deionized distilled water made up to 100 mL. Then, following the dilution up to 1:5 and filtration with a 0.45  $\mu\text{m}$  filter, the derivatization process was performed according to standard samples (mentioned earlier) and its absorption was read against a blank at 565 nm (n: 3).<sup>14</sup> EE percentage was calculated using the following equation (Equation 2):

$$EE\% = 100 \times (\text{detected drug content in gel}) / (\text{primary drug content added into the gel (Equation 2)})$$

#### *TXA content uniformity of gel formulation*

To check the uniformity of the content of the gel formulation, 72 hours after preparation, samples were taken from five different points of HPMC/carbopol 940 (1:1, w/w) gel and the amount of drug was determined according to the quantification method.

#### *Ex vivo permeation study*

An *ex vivo* animal model evaluating permeation of TXA through natural skin following topical application of the prepared gel formulation (run 13) using Franz cells was applied. All experiments were performed according to the Ethics Committee Acts (approval code: IR.ZBMU.REC.1397.085, date: 20.11.2018) of Zabol University of Medical Sciences, Iran and complied with the ARRIVE guidelines and in accordance with the guide for the care and use of laboratory animals proposed by the National Institutes of Health (NIH).

#### *Skin preparation*

To obtain a suitable skin to cover each Franze cell, the shaved abdominal BALB/c mice skin was excited under systemic ether-induced anesthesia. The subcutaneous appendices were eliminated from the skin by soaking the dermal side in normal saline for 1 h.

#### *Process of the release test*

Each donor compartment was covered by 16  $\text{cm}^2$  skin for the dermal side faced the receiver compartment. This later compartment was filled with well-stirred 29 mL phosphate buffer pH 7.4 and the entire system was circulated by a 37 °C water jacket.

Drug-loaded gel formulation and respective blank gel bases were applied on the skins of separated cells, while control cell remained untreated. The donor compartment was sealed by parafilm during the process. The samples were taken from the receiver compartment at 0.5, 1, 2, 4, and 5 h and replaced with the fresh PBS, which had been maintained at 37 °C. Finally, the drug content of each sample was analyzed using the aforementioned spectrophotometric method and the release profile was determined in terms of the cumulative release percentage of TXA (n: 3).<sup>15</sup>

#### *In vivo bleeding time assessment*

The time taken for a standard small wound to heal is called bleeding time. To investigate the effect of topical TXA gel on bleeding time compared with TXA topical solution, a known *in vivo* assessment called IVY method was performed on 10 healthy men aged 25 to 45 years on the same health conditions. All experiments were performed according to the Ethics Committee Acts (approval code: IR.ZBMU.REC.1397.085) of Zabol University of Medical Sciences, Iran.

#### *The intervention process*

Control and treatment interventions were applied to the same volunteers at a sufficiently separated period. In the control group, no treatment was applied, while for the topical gel group, TXA 3%-containing HPMC/carbopol 940 (1:1 w/w) gel and for the solution group, a TXA 3% aqueous solution (a gas was soaked by and placed on the site of the action) was topically applied on the volar aspect of the arm.

#### *IVY procedure*

After 5 h of applying the topical interventions, a cuff was inflated on the upper arm to 40 mmHg. Three stab wounds (3 mm deep) were made using a sterile lancet on the volar aspect of the forearm. The blood was removed every 30 seconds by filter paper until no blood residue remained on the filter paper. The times were recorded and the average time of the 3 incisions was reported. The statistical analysis was done to clarify the significance of treatment influence on reducing bleeding time.<sup>16</sup>

#### *Statistical analysis*

Data are presented as mean  $\pm$  standard deviation. The statistical analysis was performed using Prism 6.0 software. Statistical significance was evaluated by one-way ANOVA followed by

Tukey-Kramer as a *post hoc*-test. A *p* value equal to or less than 0.05 was considered statistically significant. RSM was used to optimize the formulations *via* Design-Expert software (version: DX7Trial).

## RESULTS AND DISCUSSION

### *Gel formulation design*

Due to the increasing need for efficient drug formulations and the cost-effectiveness of changing and optimizing the formulations of drugs available in the pharmaceutical market instead of discovering new drugs, in the present study, a new topical gel formulation of TXA was developed.

To best of our knowledge, this is the first study on topical TXA gel formulation to prevent superficial dermal and mucosal bleeding. Topical TXA formulations have been previously developed to treat melasma.<sup>17</sup>

In a limited number of studies, nasal spray powder formulations containing TXA mixed with hyaluronic acid or *in situ* gel forming chitosan have been considered for epistaxis treatment. While they have shown promising *in vitro* results, extensive *in vivo* and human assessments are still lacking.<sup>8,9</sup>

Based on previous studies,<sup>18</sup> carbopol 940 (as the gelling agent) in combination with HPMC (as a viscosity enhancer) were considered to form the gel matrix. The formulations were prepared using various concentrations of carbopol 940 and HPMC.

The formulation was first designed using experimental design method. RSM based on CCD was used to evaluate and optimize the effect of carbopol 940 and HPMC concentrations as independent variables on viscosity and spreadability as response functions. According to the literature, the concentration ranges

of 1-1.5% and 1-2% were considered for carbopol 940 and HPMC, respectively. Experiments (13 in total) designed by the software are presented in Table 1.

In this study, 5 runs (runs 2, 3, 5, 6, and 12) were carried out as center points. The experiment runs, in which repetitions in the independent parameters occurred, are center points. The values of each factor are the medians of the values used in the factorial portion. These points are replicated to improve the precision of the experiment.<sup>11</sup>

### *Rheological characterizations*

Due to the importance of viscosity of topical pharmaceutical products in their ease of use and patient compliance (difficulty of handling, application, and delayed drug release in case of high viscosity and quick removal from the application site in case of low viscosity) the viscosity of the gel should be within the appropriate range. In previous studies, viscosities lower than 4000 centipoises (Cps) have been considered suitable for topical gel products.<sup>19</sup> As can be seen in Table 1, only the viscosities of runs 8 and 13 showed viscosities lower than the upper limit, while they were not too low.

According to the three-dimensional plot obtained from the data analysis (Figure 1) by Design-Expert software, viscosity change is proportional to the concentration of polymers used, which has also been reported in previous studies.<sup>19,20</sup>

A similar pattern can be seen between the dispersibility factor of gels and the concentration of polymers used in their matrix (Figure 2), which is consistent with previous studies.<sup>21</sup>

In the dispersibility calculation, weight and distance parameters are constant, so, the quicker the gel dispersion at the specified distance takes place, the better the dispersibility and consequently the higher the quality of the gel would obtain.

**Table 1. Independent variables (carbopol 940 and HPMC concentrations) and their respective responses (viscosity and spreadability) for different runs of carbopol 940/HPMC gel preparation containing tranexamic acid 3%, (mean  $\pm$  SD, n: 3)**

Run	Factor 1 carbopol 940 (% w/w)	Factor 2 HPMC (% w/w)	Response 1 viscosity Cps	Response 2 spreadability g.cm/sec
1	1.00	2.00	4.800 $\pm$ 6.341	10 $\pm$ 2.946
2	1.25	1.50	4.305 $\pm$ 7.253	11.28 $\pm$ 2.203
3	1.25	1.50	4.289 $\pm$ 6.579	11.89 $\pm$ 3.018
4	1.25	2.00	4.965 $\pm$ 6.922	9.77 $\pm$ 2.839
5	1.25	1.50	4.350 $\pm$ 7.417	11.57 $\pm$ 2.582
6	1.25	1.50	4.245 $\pm$ 7.883	11.89 $\pm$ 2.290
7	1.50	2.00	4.980 $\pm$ 7.421	8.98 $\pm$ 2.713
8	1.25	1.00	3.836 $\pm$ 7.585	16.92 $\pm$ 3.374
9	1.00	1.50	4.040 $\pm$ 8.257	14.19 $\pm$ 3.596
10	1.50	1.00	4.100 $\pm$ 7.433	15.17 $\pm$ 2.924
11	1.50	1.50	4.270 $\pm$ 7.269	10.73 $\pm$ 2.561
12	1.25	1.50	4.136 $\pm$ 6.970	11.28 $\pm$ 3.459
13	1.00	1.00	3.562 $\pm$ 6.052	17.6 $\pm$ 3.982

HPMC: Hydroxypropyl methylcellulose, SD: Standard deviation, Cps: Centipoise

Based on this, run 13 [HPMC/carbopol 940 (1:1, w/w)] gel has shown the highest quality in terms of dispersibility of the gel.

The statistical studies revealed that the change in the concentration of HPMC had a more significant effect on the viscosity than the change in the concentration of carbopol 940. In general, the variation in the concentration of the polymers had a more significant effect on the viscosity than on the spreadability.

The results disclosed that the gel prepared in run 13 possessed the optimized viscosity and dispersibility,  $3.982 \pm 17.6$  and  $6.052 \pm 3.562$ , respectively (Table 1). This was designed by Design-Expert software with 0.981 desirability.

The gel composition predicted by mathematical model was prepared in triplicate to validate the prediction. The predicted theoretical values were very close to the responses produced by the experiments, indicating that the experimental design employed in the current study was robust (Table 2).

#### Visual inspection and determination of pH

The above factors were considered determining responses to choose the ideal formulation. However, due to easiness of evaluating the apparent clarity and acidity and their important role in the apparent quality of the gel, these two parameters were also analyzed for all the runs.

Uniformity, transparency, and being free of suspended particles determine the obvious quality of topical gels. The relative clarity

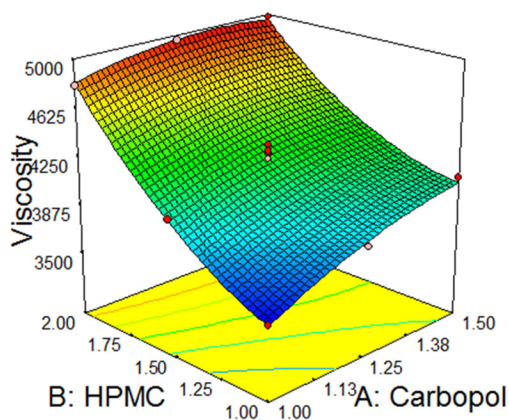


**Figure 1.** 3D response surface plot showing the influence of HPMC and carbopol 940 concentrations on tranexamic acid 3% gels viscosity  
HPMC: Hydroxypropyl methylcellulose

**Table 2.** Comparison between predicted and experimental values in the formulation prepared under predicted optimum conditions

Response	Experimental values	Predicted values	% Bias*
Viscosity (Cps)	3562	3607.85	1.271
Spreadability (g.cm/sec)	17.6	18.15	3.04

\*% Bias: (predicted value-experimental value)/predicted value 100, Cps: Centipoise

of the prepared gel formulations was visually inspected. Out of 13 runs, gels of runs 1, 2, 3, 4, 5, 6, 10, 12, and 13 showed higher transparency than the rest. Run 13 gel is presented in Figure 3.

Another factor to consider when preparing topical gel products is their acidity. If that exceeds the normal pH of the skin (4.1-5.8) and mucosal membrane (5.5-6.5), it will lead to local irritation. In addition, extreme pHs can cause gel formulation instability.<sup>22</sup> Investigations showed that the prepared gels were in this acidity range, Table 3.

Finally, according to the data analysis performed using Design-Expert software, the formulation of run 13 [HPMC/carbopol 940 (1:1, w/w)] was considered the best gel formulation both in terms of viscosity and dispersibility and was subjected to further analysis.

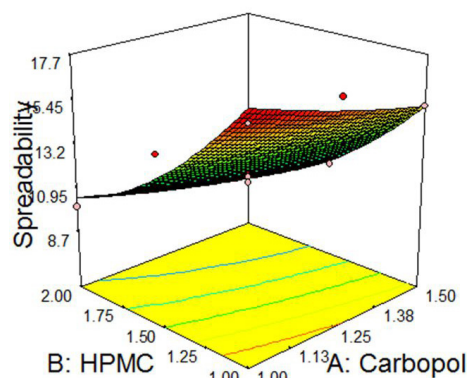


**Figure 2.** 3D response surface plot showing the influence of HPMC and carbopol 940 on tranexamic acid 3% gels spreadability  
HPMC: Hydroxypropyl methylcellulose

**Table 3.** Acidity of the carbopol 940/HPMC gels containing tranexamic acid (3%) prepared based on response surface method, runs 1-13 (mean  $\pm$  SD, n: 3)

Run	pH
1	5.42 $\pm$ 1.231
2	5.44 $\pm$ 2.455
3	5.45 $\pm$ 1.783
4	5.41 $\pm$ 2.359
5	5.43 $\pm$ 1.561
6	5.46 $\pm$ 2.213
7	5.30 $\pm$ 1.954
8	5.32 $\pm$ 2.323
9	5.46 $\pm$ 2.586
10	5.40 $\pm$ 1.440
11	5.37 $\pm$ 1.575
12	5.47 $\pm$ 2.691
13	5.39 $\pm$ 1.876

HPMC: Hydroxypropyl methylcellulose, SD: Standard deviation



The visual inspection and pH determination of optimized gel (run 13) 6 months after preparation showed no significant change indicating desirable stability in storage conditions.

#### FTIR spectroscopy

The possible interactions among polymers and active ingredients were investigated by FTIR spectroscopy. The IR spectra of pure TXA (Figure 4) showed the distinguished, strong, wide bands of carbonyl stretch (C=O) and the O-H stretch of the carboxylic acid at 1543  $\text{cm}^{-1}$  and 3200-2500  $\text{cm}^{-1}$  respectively. CH<sub>2</sub>-N and NH stretch appeared at 1396  $\text{cm}^{-1}$  and 1533  $\text{cm}^{-1}$ , respectively.

In the IR spectrum of carbopol 940/HPMC gel (Figure 5), C-O of secondary alcohol stretch is recognized at 1100  $\text{cm}^{-1}$ . CH<sub>3</sub> presented a stretch peak at 1381  $\text{cm}^{-1}$  and the broad absorptive peak fell in 3250-3000  $\text{cm}^{-1}$ , which was attributed to O-H stretch.

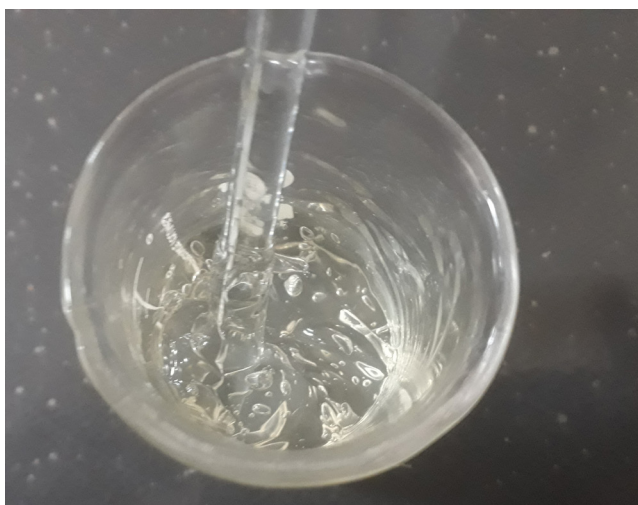


Figure 3. Carbopol 940/HPMC (1:1, w/w) gel

IR absorption spectrum of TXA (3%)-containing carbopol 940/HPMC (1:1, w/w) gel (Figure 6) exhibited that all of the drug index peaks discussed earlier appeared without displacement. This indicates that the drug did not chemically interfere with the structure of gel and could be entirely released once applied.<sup>23</sup> It also indicated that the gel base functional groups were free to establish electrostatic bands with the site of action and show mucoadhesive characteristics.<sup>24</sup>

#### Drug content uniformity

Resistance to phase separation is one of the important features of ideal pharmaceutical gels. Phase separation in addition to the obvious quality of the gel will change the consistency of the drug throughout the gel. Therefore, to evaluate the content uniformity of the TXA (3%)-containing carbopol 940/HPMC (1:1, w/w) gel, 5 different samples were taken from different parts of the gel and TXA content was quantified. The obtained results indicated that the TXA content of all the samples falls into the range of 97.3-102.6% (Table 4) of the expected drug content, which implied drug content uniformity and phase consistency of the gel.<sup>22</sup>

Table 4. Percentage of tranexamic acid content measured in 5 different zones of tranexamic acid (3%)-containing carbopol 940/HPMC (1:1, w/w) gel, run 13, (mean  $\pm$  SD, n: 3)

	Drug content %
1	97.324 $\pm$ 2.237
2	98.394 $\pm$ 2.668
3	99.158 $\pm$ 2.924
4	101.6 $\pm$ 3.421
5	102.675 $\pm$ 2.806

HPMC: Hydroxypropyl methylcellulose, SD: Standard deviation

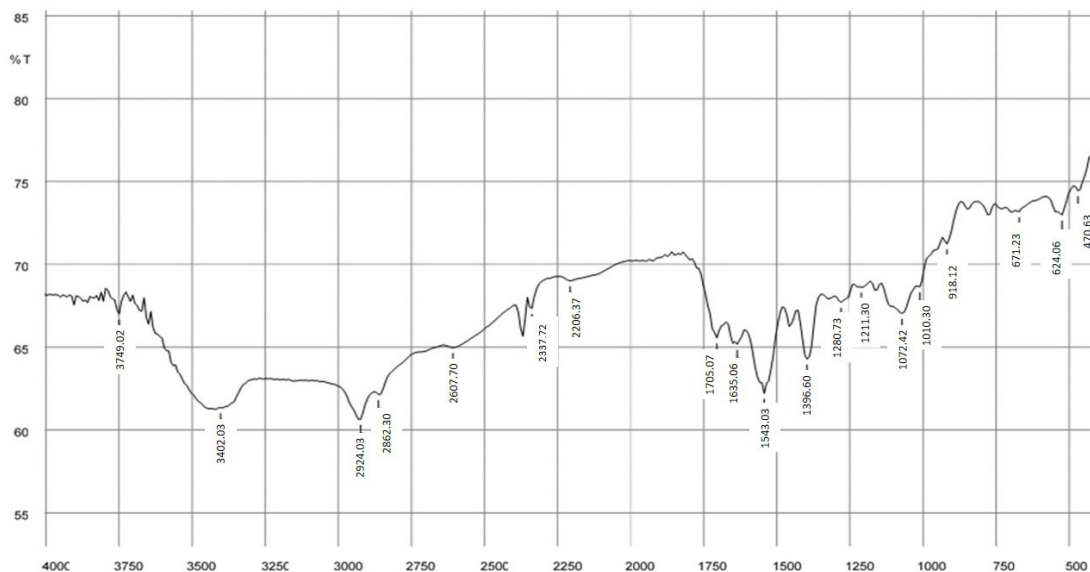


Figure 4. Fourier transform-infrared spectroscopy pattern: pure tranexamic acid

### Ex vivo permeation study

In order to evaluate the release of TXA from TXA (3%)-containing carbopol 940/HPMC (1:1, w/w) gel and its permeation through the skin, Franz cells covered by animal skin were used. This method was used to correlate an *in vitro* environment with an *in vivo* environment. With all their limitations and sometimes poor correlation to *in vivo* results, *in vitro* permeation experiments and animal models still provide important options for evaluating drug delivery systems.<sup>25</sup> The plot of cumulative drug release within 5 h is presented in Figure 7. As can be seen, the drug was released and penetrated through the skin model uniformly and cumulative release reached 90% in 4 h and 97% in 5 h. This indicates ability of the gel to completely release the drug

and let it permeate through the skin in relatively short time, when applied topically. This result is in correlation with the FTIR absorptive spectrum, which showed no strong interaction between TXA and the gel base, which led to complete drug release.

### Bleeding time assessment

In this study, we focused on the preparation of topical formulations containing TXA, an anticoagulant medicine. In order to check its efficiency in stopping bleeding, a common fast screening method without the need for paraclinical evaluation called IVY method<sup>16</sup> was used to evaluate the efficacy of topical TXA (3%)-containing carbopol 940/HPMC (1:1, w/w) gel on reducing the bleeding time in healthy volunteer individuals.

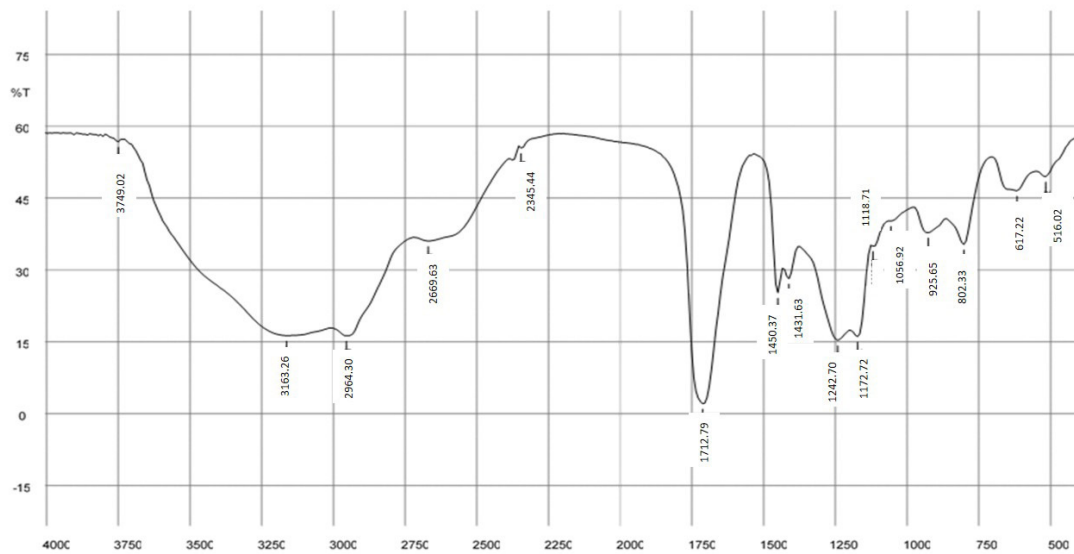


Figure 5. Fourier transform-infrared spectroscopy pattern: carbopol 940/ HPMC (1:1, w/w) gel

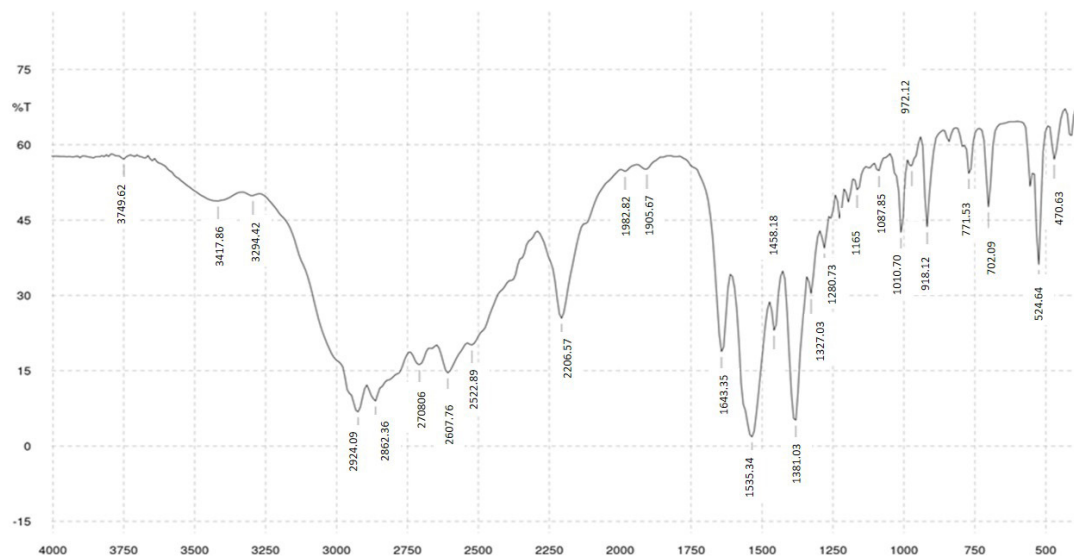
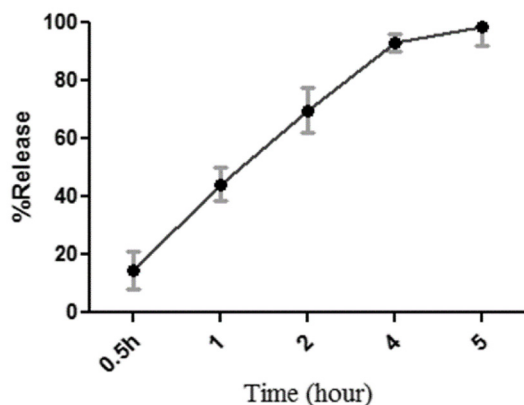


Figure 6. Fourier transform-infrared spectroscopy pattern: tranexamic acid 3%-containing carbopol 940/HPMC (1:1, w/w) gel, run 13  
HPMC: Hydroxypropyl methylcellulose

The process of coagulation has different stages and different methods have been developed to evaluate the status of each of these stages in hemostasis. The choice of each of these methods to evaluate blood coagulation depends on various factors, including the mechanism considered in the coagulation process, the speed of operation, and the cost. IVY method has been widely used to evaluate coagulation status and platelet function in various conditions such as pathologic conditions, drug-induced or presurgery evaluations. Although more sophisticated and accurate tests have been applied for this purpose recently, the bleeding time test is still used both in animal studies and in human studies, especially in the early stages of evaluation.<sup>26</sup>

Based on the bleeding times of groups presented in Figure 8, bleeding time in the control group was significantly higher than the other two groups ( $p < 0.001$ ). Similarly, bleeding time in the TXA solution treated group was significantly higher than in the



**Figure 7.** Plot of cumulative tranexamic acid release percentage from tranexamic acid 3%-containing carbopol 940/HPMC (1:1, w/w) gel within 5 hours evaluated by an *ex vivo* permeation study using Franz cell (mean  $\pm$  SD, n: 3)

HPMC: Hydroxypropyl methylcellulose, SD: Standard deviation

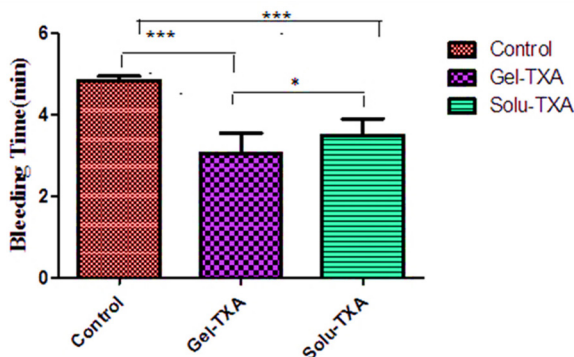


**Figure 8.** Bleeding time (minutes) measured in healthy volunteers receiving control, tranexamic acid (3%)-containing carbopol 940/ HPMC (1:1 w/w) gel and topical aqueous tranexamic acid solution, \* $p < 0.05$  and \*\*\* $p < 0.001$ , (mean  $\pm$  SD, n: 3)

HPMC: Hydroxypropyl methylcellulose, SD: Standard deviation

TXA gel group ( $p < 0.05$ ). All subjects even in the TXA gel-treated group displayed normal bleeding times (4-10 minutes).<sup>27</sup>

The results can be explained by the ability of the gel to remain in the site of application and complete release of the drug, which led to higher efficacy in reducing bleeding time compared with the free drug solution. This result has been in line with other studies on topical gels containing anticoagulants in reducing bleeding time in animal models.<sup>28</sup>

The absence of abnormal bleeding time in all three groups indicates the safety of topical use of TXA and topical products containing it. Meanwhile, the decrease in the bleeding time of the gel group compared to the soluble drug indicates the short-term and transient effects of this drug in reducing the bleeding time, which can find its place in cases such as acute nosebleeds.<sup>29</sup>

#### Study limitations

In this study, the impact of topical use of TXA gel on plasma coagulation factors has not been evaluated.

## CONCLUSION

In this study, an optimal carbopol 940/HPMC gel formulation containing TXA (3%) was designed and fabricated using the experimental design method. *In vitro* studies showed desirable physical quality of this gel and non-chemical interactions with the loaded drug. In the *ex vivo* permeation test, it was shown that the gel was capable to completely release its loaded drug and drug permeate through the skin within 5 h. The results of *in vitro* evaluation of the gel on reducing bleeding time led to promising results that could confirm the importance of further studies on this formulation as a potential medication to stop acute superficial bleeding.

#### Ethics

**Ethics Committee Approval:** This study has been registered in the Ethics Committee of Zabol University of Medical Sciences and the code of ethics is the same as the study registration code given in the text of the manuscript (approval code. IR.ZBMU.REC.1397.085, date: 20.11.2018).

**Informed Consent:** The informed consent form was signed by all participants.

**Peer-review:** Externally peer-reviewed.

#### Authorship Contributions

Surgical and Medical Practices: D.M., Concept: O.C., S.D., F.S., Design: O.C., S.D., Data Collection or Processing: D.M., S.D., O.C., Analysis or Interpretation: S.D., F.S., Literature Search: F.S., Writing: F.S., S.D., O.C.

**Conflict of Interest:** No conflict of interest was declared by the authors.

**Financial Disclosure:** This study was supported financially by a research grant from Zabol University of Medical Sciences, Zabol, Iran, as a part of the Pharm.D. thesis.

## REFERENCES

1. Pushpakom S, Iorio F, Eyers PA, Escott KJ, Hopper S, Wells A, Doig A, Williams T, Latimer J, McNamee C, Norris A, Sanseau P, Cavalla D, Pirmohamed M. Drug repurposing: progress, challenges and recommendations. *Nat Rev Drug Discov*. 2019;18:41-58.
2. Sharadha M, Gowda DV, Vishal Gupta N, Akhila AR. An overview on topical drug delivery system – updated review. *Int J Res Pharm Sci*. 2020;11:368-385.
3. Sun X, Dong Q, Zhang YG. Intravenous *versus* topical tranexamic acid in primary total hip replacement: a systemic review and meta-analysis. *Int J Surg*. 2016;32:10-18.
4. Gottlieb M, Koifman A, Long B. Tranexamic acid (TXA) for the treatment of epistaxis. *Acad Emerg Med*. 2019;11:1207-1305.
5. Montroy J, Hutton B, Moodley P, Fergusson NA, Cheng W, Tinmouth A, Lavallée LT, Fergusson DA, Breau RH. The efficacy and safety of topical tranexamic acid: a systematic review and meta-analysis. *Transfus Med Rev*. 2018;S0887-7963:30151-7.
6. Hosseinalhashemi M, Jahangiri R, Faramarzi A, Asmarian N, Sajedianfard S, Kherad M, Soltaniesmaeili A, Babaei A. Intranasal topical application of tranexamic acid in atraumatic anterior epistaxis: a double-blind randomized clinical trial. *Ann Emerg Med*. 2022;80:182-188.
7. Soares EC, Costa FW, Bezerra TP, Nogueira CB, de Barros Silva PG, Batista SH, Sousa FB, Sá Roriz Fonteles C. Postoperative hemostatic efficacy of gauze soaked in tranexamic acid, fibrin sponge, and dry gauze compression following dental extractions in anticoagulated patients with cardiovascular disease: a prospective, randomized study. *Oral Maxillofac Surg*. 2015;19:209-216.
8. Gomes Dos Reis L, Ghadiri M, Young P, Traini D. Nasal powder formulation of tranexamic acid and hyaluronic acid for the treatment of epistaxis. *Pharm Res*. 2020;37:186.
9. Gholizadeh H, Messerotti E, Pozzoli M, Cheng S, Traini D, Young P, Kourmatzis A, Caramella C, Ong HX. Application of a Thermosensitive *in situ* gel of chitosan-based nasal spray loaded with tranexamic acid for localised treatment of nasal wounds. *AAPS PharmSciTech*. 2019;20:299.
10. Najafabadi AR, Moslemi P, Tajerzadeh H. Intranasal bioavailability of insulin from carbopol-based gel spray in rabbits. *Drug Deliv*. 2004;11:295-300.
11. Aiyalu R, Govindarjan A, Ramasamy A. Formulation and evaluation of topical herbal gel for the treatment of arthritis in animal model. *Braz J Pharm Sci*. 2016;52:493-507.
12. Gaikwad L, Yadav V, Dhavale P, Choudhari B, Jadhav S. Effect of carbopol 934 and 940 on fluconazole release from topical gel formulation: a factorial approach. *Int J Curr Pharm Res*. 2012;2:487-493.
13. Ansari TM, Raza A, Rehman AU. Spectrophotometric determination of tranexamic acid in pharmaceutical bulk and dosage forms. *Anal Sci*. 2005;21:1133-1135.
14. Tas C, Ozkan Y, Savaser A, Baykara T. *In vitro* release studies of chlorpheniramine maleate from gels prepared by different cellulose derivatives. *Farmaco*. 2003;58:605-611.
15. Daneshmand S, Jaafari MR, Movaffagh J, Malaekheh-Nikouei B, Iranshahi M, Seyedian Moghaddam A, Tayarani Najaran Z, Golmohammadzadeh S. Preparation, characterization, and optimization of auraptene-loaded solid lipid nanoparticles as a natural anti-inflammatory agent: *in vivo* and *in vitro* evaluations. *Colloids Surf B Biointerfaces*. 2018;164:332-339.
16. Janzarik H, Heinrich D, Bödeker RH, Lasch HG. "Haemostasis time", a modified bleeding time test and its comparison with the Duke and Ivy/template bleeding times. II. application in bleeding disorders. *Blut*. 1988;57:111-116.
17. Kanechorn Na Ayuthaya P, Niumphradit N, Manosroi A, Nakakes A. Topical 5% tranexamic acid for the treatment of melasma in Asians: a double-blind randomized controlled clinical trial. *J Cosmet Laser Ther*. 2012;14:150-154.
18. Kouchak M, Mahmoodzadeh M, Farrahi F. Designing of a pH-Triggered Carbopol®/HPMC *in situ* gel for ocular delivery of dorzolamide HCl: *in vitro*, *in vivo*, and *ex vivo* evaluation. *AAPS PharmSciTech*. 2019;20:210.
19. Kim JY, Song JY, Lee EJ, Park SK. Rheological properties and microstructures of carbopol gel network system. *Colloid Polym Sci*. 2003;281:614-623.
20. Ferry, John D. Viscoelastic properties of polymers. New York: Wiley 1980.
21. Helal DA, El-Rhman DA, Abdel-Halim SA, El-Nabarawi MA. Formulation and evaluation of fluconazole topical gel. *Int J Pharm Pharm Sci*. 2012;4:176-183.
22. Chang RK, Raw A, Lionberger R, Yu L. Generic development of topical dermatologic products: formulation development, process development, and testing of topical dermatologic products. *AAPS J*. 2013;15:41-52. Erratum in: *AAPS J*. 2015;17:1522.
23. Shiehazadeh F, Hadizadeh F, Mohammadpour A, Aryan E, Gholami L, Tafaghodi M. Streptomycin sulfate dry powder inhalers for the new tuberculosis treatment schedule. *J Drug Deliv Sci Technol*. 2019;52:957-967.
24. Uthaiwat P, Priprem A, Puthongking P, Daduang J, Nukulkit C, Chio-Srichan S, Boonsiri P, Thapphasaraphong S. Characteristic evaluation of gel formulation containing niosomes of melatonin or its derivative and mucoadhesive properties using ATR-FTIR spectroscopy. *Polymers (Basel)*. 2021;13:1142.
25. Godin B, Touitou E. Transdermal skin delivery: predictions for humans from *in vivo*, *ex vivo* and animal models. *Adv Drug Deliv Rev*. 2007;59:1152-1161.
26. Thiruvankatarajan V, Pruett A, Adhikary SD. Coagulation testing in the perioperative period. *Indian J Anaesth*. 2014;58:565-572.
27. Shore-Lesserson L. Chapter 12 - coagulation monitoring. In: Kaplan JA, eds. *Essentials of cardiac anesthesia*. Philadelphia: W.B. Saunders; 2008;264-290.
28. Ebrahimi F, Mahmoudi J, Torbati M, Karimi P, Valizadeh H. Hemostatic activity of aqueous extract of *Myrtus communis* L. leaf in topical formulation: *in vivo* and *in vitro* evaluations. *J Ethnopharmacol*. 2020;249:112398.
29. Joseph J, Martinez-Devesa P, Bellorini J, Burton MJ. Tranexamic acid for patients with nasal haemorrhage (epistaxis). *Cochrane Database Syst Rev*. 2018;12:CD004328.



# Exploration of Structure-Activity Relationship Using Integrated Structure and Ligand Based Approach: Hydroxamic Acid-Based HDAC Inhibitors and Cytotoxic Agents

Ekta SHIRBHATE<sup>1</sup>, Jaiprakash PANDEY<sup>1</sup>, Vijay Kumar PATEL<sup>1</sup>, Ravichandran VEERASAMY<sup>2</sup>, Harish RAJAK<sup>1\*</sup>

<sup>1</sup>Guru Ghasidas University, Department of Pharmacy, Bilaspur, India

<sup>2</sup>AIMST University, Faculty of Pharmacy, Department of Pharmaceutical Chemistry, Kedah, Malaysia

## ABSTRACT

The present study aimed to establish significant and validated quantitative structure-activity relationship (QSAR) models for histone deacetylase (HDAC) inhibitors and correlate their physicochemical, steric, and electrostatic properties with their anticancer activity. We have selected a dataset from earlier research findings. The target and ligand molecules were procured from recognized databases and incorporated into pivotal findings such as molecular docking (XP glide), e-pharmacophore study and 3D QSAR model designing study (phase). Docking revealed molecule 39 with better docking score and well binding contact with the protein. 3D QSAR analysis, which was performed for partial least squares factor 5 reported good 0.9877 and 0.7142 as R<sup>2</sup> and Q<sup>2</sup> values and low standard of deviation: 0.1049 for hypothesis AADRR.139. Based on the computational outcome, it has been concluded that molecule 39 is an effective and relevant candidate for inhibition of HDAC activity. Moreover, these computational approaches motivate to discover novel drug candidates in pharmacological and healthcare sectors.

**Key words:** HDAC inhibitors, QSAR, e-pharmacophore, molecular docking, structure and ligand based approach

## INTRODUCTION

The growth and division of cancer cells are usually faster than normal cells. Chemotherapy is an effective way to treat tumor cells. However, chemotherapeutic drugs are powerful and principally cause impairment to healthy cells<sup>1</sup> leading to subside in their usage. This predicament has created a medical urge to flourish effective antitumor agents with heightened safety outline.<sup>2,3</sup> As clinically proven cancer targets, histone deacetylase (HDAC) inhibitors have been established as a flourishing tactic for the progress of new anticancer agents.<sup>2-4</sup>

Acetylation and deacetylation of histone proteins play an essential role in transcription and regulation of genes

in eukaryotic organisms. The enzymes *viz.*, histone acetyltransferase and HDACs, play an influential role behind this.<sup>5,6</sup> The imbalance of any of them may result hindrance in differentiation and proliferation of typical cells and conduct start of tumor cells. Overexpressed HDAC effectuates the eviction of acetyl groups from histones, leading to compression of chromatin and downregulation of tumor suppressor genes.<sup>7-10</sup> Cell cycle arrest, chemosensitization, apoptosis induction, and overexpression of tumor suppressors are some of the primary mechanisms controlled by HDAC inhibitors.<sup>11</sup> To date, 18 members are present in the mammalian HDAC family, which are classified into four classes; class I-IV, on the basis of their sequence homology with the yeast protein. Class I enclose

\*Correspondence: harishdops@yahoo.co.in, Phone: +91 9827911824, ORCID-ID: orcid.org/0000-0003-2008-2827

Received: 25.04.2021, Accepted: 05.05.2022



©2023 The Author. Published by Galenos Publishing House on behalf of Turkish Pharmacists' Association.

This is an open access article under the Creative Commons Attribution-NonCommercial-NoDerivatives 4.0 (CC BY-NC-ND) International License.

1, 2, 3, and 8 isoforms promoting cellular proliferation and hindering apoptosis. Class II is further classified into class IIa with isoforms 4, 5, 7, and 9 and class IIb consist of 6 and 10. Class I and II forbid the cellular differentiation. Some class II isoforms (HDACs 4, 6, 7, and 10) boost cellular migration and angiogenesis, which are two crucial means for cancer metastasis. Class IV is with a lone member of HDAC 11. Classes I, II and IV act by  $Zn^{2+}$  reliant mechanism, while class III shows homology with silent information regulator 2, needing  $NAD^+$  as cofactor for catalysis.<sup>10-12</sup>

Five HDAC inhibitors have been approved to date for the treatment of different types of cancers. Vorinostat [suberoylanilide hydroxamic acid (SAHA)] and romidepsin (FK228) have been approved for the treatment of cutaneous T-cell lymphoma, while belinostat (PXD101) and tucidinostat (chidamide) (CS055) have been approved for peripheral T-cell lymphoma. Panobinostat (LBH589) finds application in the treatment of multiple myeloma. Besides this, several HDAC inhibitors are currently under different phases of clinical trials, *i.e.*, rocilinostat (multiple myeloma), entinostat (breast cancer), and tacedinaline (lung cancer) are in phase I, II, and

III, respectively, as represented in Figure 1. HDAC inhibitors are also structurally classified as hydroxamic acids, benzamides, cyclic tetrapeptides, short chain fatty acids, electrophilic ketones, *etc.*<sup>10,13</sup>

Remarkably, because these medications are mostly pan-HDAC inhibitors or target many HDAC isoforms, they have a lot of negative effects. Because of their low toxicity and limited off-target effects, isoform-selective HDAC inhibitors may provide therapeutic benefits. As a result, in recent years, investigations on HDAC inhibitors have focused on isoform- or class-specific inhibition.<sup>14,15</sup>

Although all these types bear a resembling core structure comprising of three key components, *i.e.* (i) zinc binding group (ZBG) responsible for chelation of zinc ion at active site; (ii) cap group (a hydrophobic or aromatic or heteroaromatic moiety) accounts for interaction with residues of HDACs external pocket, and (iii) a linker (with optimal length) accounts for joining the ZBG and cap group. The latter two components, *i.e.* cap group and linker, are being employed for structural modification to obtain compounds with selective and optimum anticancer activity.<sup>13</sup>

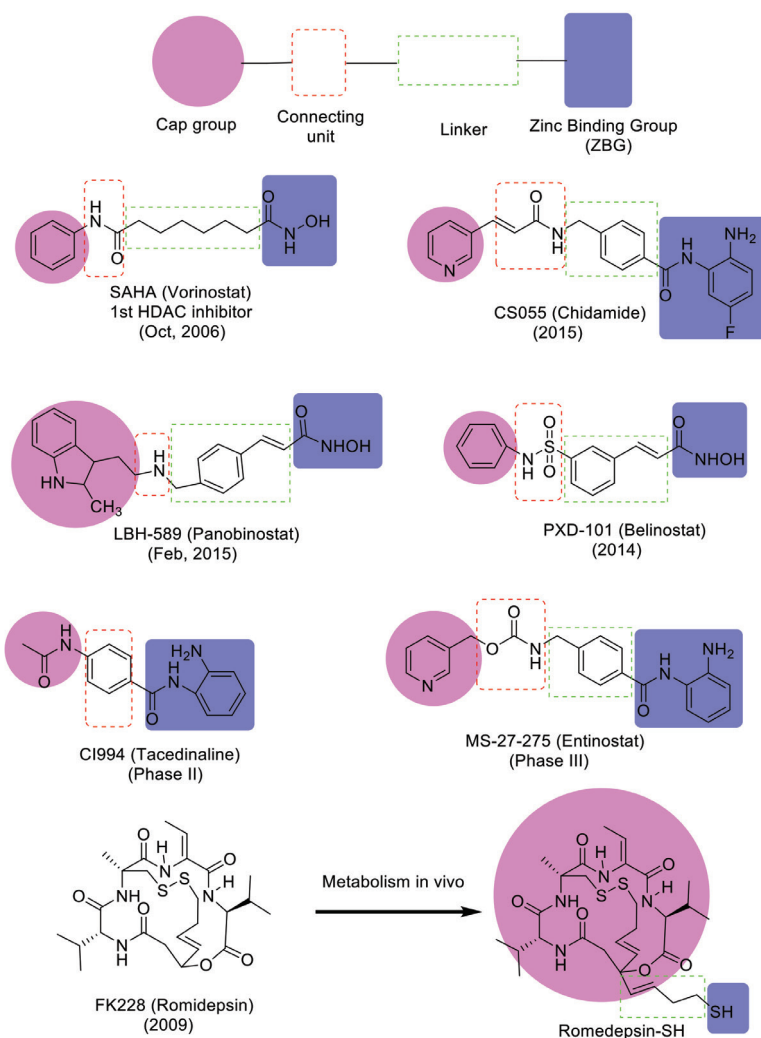


**Figure 1.** Chemical structures of some FDA-approved HDAC inhibitors

FDA: Food and Drug Administration, HDAC: Histone deacetylase

Computer-aided molecular drug design plays an important role in design and discovery of novel chemical entities. The role of computational study of HDAC enzymes is evolving nowadays, with particular emphasis on molecular modeling for the development of HDAC inhibitors with enhanced selectivity and effectiveness. Generally, 3D quantitative structure-activity relationship (QSAR) studies are complemented by docking studies.<sup>16</sup>

Various studies have been reported by many scientists for studying and developing HDAC inhibitors using computational tools and techniques.<sup>16</sup> Kim *et al.*<sup>17</sup> synthesized many  $\delta$ -lactam-based HDAC inhibitors containing modified cap groups. Hamblett *et al.*<sup>18</sup>, employed MS-275 as the lead moiety and modified it around pyridine ring for designing novel HDAC inhibitors with enhanced class I selectivity. Estiu *et al.*<sup>19</sup> studied the structural basis for the selectivity of class II-selective HDAC inhibitors SAHA, turacin, and NK308 using molecular dynamics simulations approach. Huhtiniemi *et al.*<sup>20</sup> disclosed a relative modeling of human SIRT1. Xie *et al.*<sup>21</sup> reported a QSAR study on HDACi for the identification of structural features responsible for anticancer activity. Chen *et al.*<sup>22</sup> selected around 30 known HDAC inhibitors for designing 3D QSAR pharmacophore model to recognize critical ligand features for HDAC inhibition activity. Ragno *et al.*<sup>23</sup> accomplished 3D QSAR studies for their newly designed class II selective HDAC inhibitor (APHAs) against maize HD1-A and HD1-B with acceptable selectivity.

The upregulation of the HDAC enzyme has been linked to a variety of cancers, making it a possible therapeutic target. The research found possible inhibitors of human HDAC enzyme by screening several biologically active molecules from several databases.<sup>24</sup> Various bioinformatics tools can be used to screen prospective drugs before moving forward with wet-lab research.<sup>25</sup> As a result, computer-aided drug design has been shown to be extremely useful in lowering drug development costs and risks, while also increasing speed and accuracy of drug discovery.<sup>26</sup> Molecular docking, binding mode and energy, and hydrogen bond interactions aid in the identification of a possible inhibitor in the active site of the HDAC target protein from a dataset. In other words, the ligand-receptor interaction is predicted by molecular docking.<sup>27</sup> In addition, QSAR model assesses the biological activity of experimental data by comparing it with chemical descriptors of known training set substances. The application domain and appropriate validation approaches were used to determine the reliability and robustness of the developed QSAR models.<sup>28</sup> Nonetheless, the study discusses the creation of an atom-based 3D QSAR model that specifies molecular level comprehension and structure-activity relationship regions for a dataset of chemicals. The created QSAR model considers essential pharmacophoric properties such as average shape, hydrophobic/non-polar areas, electrostatic (positive ionic and negative ionic), electron withdrawing, and electron donating for their respective positive and negative coefficient patterns. Different metrics of QSAR models from partial least squares (PLS) statistical analysis, such as  $Q^2$ ,  $R^2$ , standard deviation (SD), stability, F, and root mean squared error values, also show that the model has strong predictive capacity. As a

result, the research above aims to provide useful information for designing innovative and effective HDAC inhibitors using computational and bioinformatic approaches.

## MATERIALS AND METHODS

The present work comprises computer-aided drug design studies. Thus, it does not require ethics committee approval and patient consent for its accomplishment.

The computational analysis was performed employing the Schrodinger suite (Maestro v 9.3, LLC, New York) including protein prep wizard, ligprep, grid generation, glide XP dock, and 3D QSAR model designing.

### Biological dataset

The data resources were collected from the research papers.<sup>29-32</sup> The literature review clearly exhibited that the heterocyclic linker in hydroxamic acid-based HDAC inhibitors improves activity by facilitating ligand receptor binding. The selected compounds have similar skeletons and biological assay methods. A data set of 57 compounds was chosen for the study along with inhibitory concentration 50 ( $IC_{50}$ ) values in  $\mu$ M against human carcinoma cancer cell lines as shown in Table 1.  $IC_{50}$  value was used as a dependent variable in the QSAR study.  $IC_{50}$  values of all compounds for different pharmacophore studies were changed into negative logarithm of  $IC_{50}$  ( $pIC_{50}$ ).<sup>33</sup> These data are critical for constructing good 3D QSAR models for investigating structure-activity relationships.

### Protein preparation

The protein preparation wizard in Maestro v. 9.3 was practiced to organize the receptor in order for docking studies.<sup>34</sup> The binding region of HDAC inhibitor was initially studied by complexed crystal structure of SAHA (proto type HDAC inhibitor) with HDAC protein (PDB ID: 1ZZ1).<sup>35</sup> This task was carried out in three steps, (i) importing the protein from PDB followed by processing to fix its structure, (ii) reviewing chemical correctness of structure and its modification by adding missing hydrogen atoms and neutralizing the remotely situated side chain from binding sites, (iii) refining the orientation of optimized H-bound groups and geometric minimizing the structure by OPLS\_2005 force field by facilitating the realignment of hydroxyl groups of side chains.<sup>35,36</sup>

### Ligand preparation

Lig prep version 2.5 (Schrodinger, LLC, NY) was employed for constructing and processing the selected ligands.<sup>37</sup> Initially, the structures of all these ligands were drawn in ChemDraw Professional version 16.0 and saved in mol format. In lig prep, the ligands were picked from their mol files and proceeded through several steps, like generation of 3D structures from their 2D structures, removal of low energy conformers, formation of stereoisomers and ionization state of ligands, addition and elimination of hydrogen atoms and counter ions, respectively, and lastly energy minimization using OPLS\_2005 force field. The ligands were geometrically optimized through Optimized Potentials Liquid Simulations 2005 (OPLS\_2005) force field.<sup>38</sup> The partial atomic charges were figured out employing the OPLS\_2005 force field.<sup>39</sup>

Table 1. Chemical structures and  $pIC_{50}$  values of the selected compounds for the dataset

Compound	R	R'	n	HDAC ( $IC_{50}$ $\mu$ M)	$pIC_{50}$
1	-CH <sub>3</sub>	-	-	0.062	7.208
2	-CH <sub>2</sub> CH <sub>3</sub>	-	-	0.055	7.260
3	-CH <sub>2</sub> CH <sub>2</sub> CH <sub>3</sub>	-	-	0.132	6.879
4	-CH <sub>2</sub> CH <sub>2</sub> CH <sub>2</sub> CH <sub>3</sub>	-	-	0.137	6.863
5		-	-	0.022	7.658
6		-	-	0.018	7.745
7		-	-	0.838	6.077
8		-	-	0.054	7.268
9		-	-	0.115	6.939
10		-	-	0.09	7.046
11		-	-	0.077	7.114
12		-	-	0.171	6.767
13		-	-	0.403	6.395
14		-	-	0.51	6.292
15		-	-	0.111	6.955



Table 1. continued

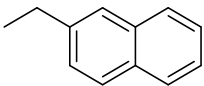
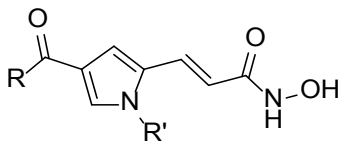
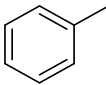
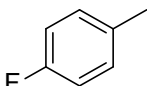
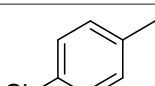
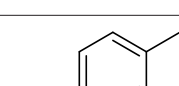
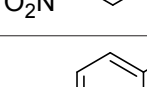
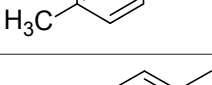
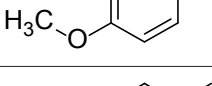
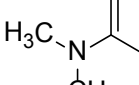
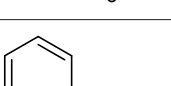
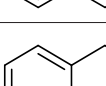
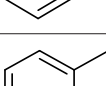
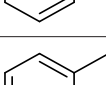
Compound	R	R'	n	HDAC (IC <sub>50</sub> μM)	pIC <sub>50</sub>
16		-	-	0.094	7.027
					
17		CH <sub>3</sub>	-	3.8	5.420
18		CH <sub>3</sub>	-	3.8	5.420
19		CH <sub>3</sub>	-	2.4	5.620
20		CH <sub>3</sub>	-	3.9	5.409
21		CH <sub>3</sub>	-	1.9	5.721
22		CH <sub>3</sub>	-	2.9	5.538
23		CH <sub>3</sub>	-	2.4	5.620
24		CH <sub>3</sub>	-	0.1	7.000
25		CH <sub>3</sub>	-	1	6.000
26		H	-	5	5.301
27		i-propyl	-	53	4.276
28		Phenyl	-	110	3.959

Table 1. continued

Compound	R	R'	n	HDAC (IC <sub>50</sub> μM)	pIC <sub>50</sub>
29		-	-	0.172	6.764
30		-	-	0.205	6.688
31		-	-	0.37	6.432
32		-	-	0.941	6.026
33		-	-	0.569	6.245
34		-	1	0.03	7.523
35		-	1	0.066	7.180
36		-	1	0.023	7.638

Table 1. continued

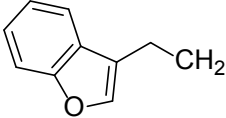
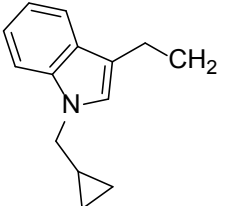
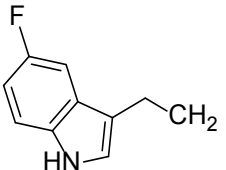
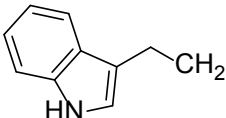
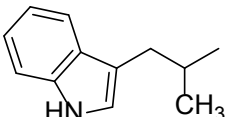
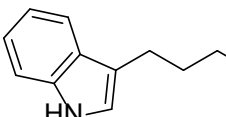
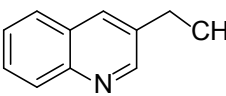
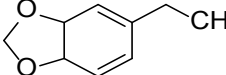
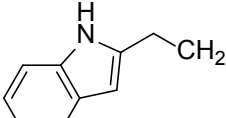
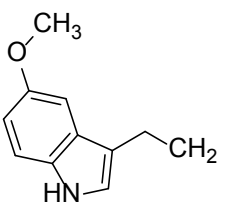
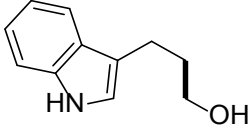
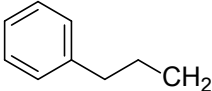
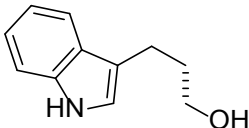
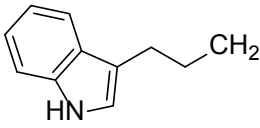
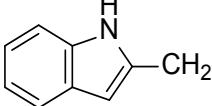
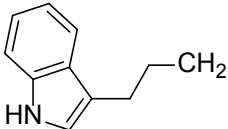
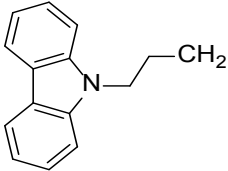
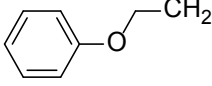
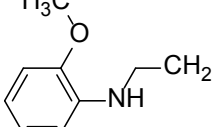
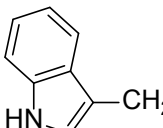
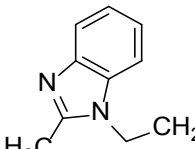
Compound	R	R'	n	HDAC (IC <sub>50</sub> μM)	pIC <sub>50</sub>
37		-	1	0.016	7.796
38		-	1	0.084	7.076
39		-	1	0.014	7.854
40		-	1	0.063	7.201
41		-	1	0.024	7.620
42		-	1	0.037	7.432
43		-	1	0.067	7.174
44		-	1	0.03	7.523
45		-	1	0.046	7.337
46		-	1	0.014	7.854

Table 1. continued

Compound	R	R'	n	HDAC (IC <sub>50</sub> μM)	pIC <sub>50</sub>
47		-	1	0.04	7.398
48		-	1	0.15	6.824
49		-	1	0.027	7.569
50		-	0	0.262	6.582
51		-	1	0.051	7.292
52		-	1	0.053	7.276
53		-	1	0.079	7.102
54		-	1	0.069	7.161
55		-	1	0.111	6.955
56		-	1	0.059	7.229
57		-	1	0.038	7.420

HDAC: Histone deacetylase, pIC<sub>50</sub>: Negative logarithmic concentration of 50% inhibition

### Docking studies

Glide version 5.8 (Schrodinger, LLC, NY) molecular docking tool was used for docking studies.<sup>40</sup> An effective interaction of hydroxamate derivatives with the target protein (PDB ID: 1ZZ1) to estimate the potential response against tumor cells can be predicted by this study. 1ZZ1, the target protein, was acquired from the protein data bank (PDB)<sup>39</sup> and was prepared for the docking task by working on “protein preparation wizard” in Maestro version 9.3. The selected ligands were prepared by lig prep in Maestro version 9.3. Low energy conformers of ligands were screened. The grid was generated on the receptor protein by following receptor generation module in glide and finally the screened ligands were docked into the receptor grid containing protein exercising XP and SP docking approaches.<sup>41-44</sup>

### Energetic (e)-pharmacophore hypothesis generation

Both ligand and structure based techniques are combined in energetic (e)-pharmacophore approach. The e-pharmacophore script feature permitting docking post processing option in Maestro v. 9.3 was accomplished for e-pharmacophore hypothesis study.<sup>5,33,45</sup> The module uses energetic tenets of the XP glide scoring function for mapping and creating energy-adjusted pharmacophores, *i.e.*, e-pharmacophores. Thereafter, phase version 3.4 (Schrodinger, LLC, NY) application generates pharmacophore sites using a default set of six chemical attributes: hydrogen bond acceptor (A), hydrogen bond donor (D), hydrophobic group (H), positive ionizable (P), negative ionizable (N), and aromatic ring (R). The glide XP energies of each atom were summed to constitute each pharmacophore site. These sites were then ordered as *per* their energy and the most affirmative site was picked for pharmacophore generation.

### Pharmacophore hypothesis generation

Phase version 3.4 (Schrodinger, LLC, NY) was engaged for the pharmacophore model (hypotheses) generation.<sup>46</sup> It is a commonly used system-based method for recognizing common pharmacophores and developing 3D QSAR models. Pharmacophore modeling is a ligand-based method for identifying new lead moieties.

The process gets initiated with cleaning of all 57 selected ligands. The conformers of these ligands were created by a macromodel search approach in which maximum number of conformers was 1000 *per* structure and minimization steps as 100 was set as default. Conformers were minimized using OPLS\_2005.<sup>47</sup> Later, sites were created for all the ligands depending on the values set for activity threshold, which progressively generated common pharmacophore hypothesis (CPHs). The CPHs are based upon the activity threshold of active and inactive molecules. A maximum of six feature sites was present in each hypotheses, namely, hydrogen bond donor (D), hydrogen bond acceptor (A), hydrophobic group (H), positively charged group (P), negatively charged group (N), and aromatic ring (R). These generated hypotheses were monitored on the basis of survival, survival-inactive, and *post-hoc* scores. The hypotheses possessing lowest relative conformational energy and highest adjusted survival score were selected for building the QSAR model.<sup>48</sup>

### 3D QSAR model development

The dataset was efficiently segregated into training (38) and test (19) sets for analysis using a random and rational division method. In the phase module, pharmacophore and atom-based alignments are available to orient 3D structures of compounds. In this study, an atom-based QSAR model was used, which explained the better structure-activity relationship. Initially, the overall dataset was segregated into a modeling set (80% compounds) and an external evaluation set (20% compounds) employing random division approach. The modeling set was further sectioned into a training set (comprising of 80% of the modeling set) and a test set (comprising of 20% of the modeling set) again using the rational division method. The best fitting model was generated through a random division. The atom-based QSAR model was generated for ligands by selecting the best fit hypothesis with good scoring value, keeping 1 Å as grid spacing and maximum PLS factor as 5. The QSAR results were later visualized, which ultimately helped in the optimization of the thrust structure of dataset.<sup>49-51</sup>

### Validation of the pharmacophore model

The primary goal of QSAR model is to estimate biological activity of novel molecules. Internally and externally, the model developed would sound. A training set and a test set were created from the data. With 38 compounds in the training set, atom-based 3D-QSAR models were created for hypotheses. By estimating the activities of 19 test molecules, top QSAR model was externally validated.

### Statistical analysis

Statistical criteria such as squared correlation coefficient ( $R^2$ ),  $q^2$  ( $R^2$  for test set), SD of regression, Pearson's correlation coefficient (pearson's  $r$ ), statistical significance ( $P$ ), and variance ratio were used to internally validate the developed pharmacophore hypotheses ( $F$ ). The anticipated  $pIC_{50}$  was calculated using the 5<sup>th</sup> PLS factor. An increase in the number of PLS factors has no effect on the model's statistics or prediction ability.

## RESULTS AND DISCUSSION

### Molecular docking study

The result of docking studies shown in Figure 2 indicated the probable interaction of ligands containing hydroxamate groups with the receptor 1ZZ1. Compound 39 from the dataset exhibits maximum structural alignment with that of SAHA in protein 1ZZ1. 2D interaction diagram of compound 39 docked with 1ZZ1 revealed metallic bond interaction with zinc (Zn2451) of receptor 1ZZ1 and keto group of ligand, hydrogen bond formation between NH- moiety of hydroxamic acid group of the ligand with GLY151 and TYR312 amino acids, and hydrogen bond formation between NH- moiety of hydroxamic acid group of the ligand with GLY151 and TYR312 amino acids. Hydrogen bonding is also obvious between the NH- moiety of indole ring and the ASP98 amino acid. The hydrophobic interaction of PHE208 with five-membered ring B of indole and benzene ring of compound 39 was also found in the diagram.

### Energetic (e)-pharmacophore study

An energetic (e)-pharmacophore study displayed its result for compound 45 with protein 1ZZ1. A maximum of seven pharmacophore attributes were taken as default, but five pharmacophore sites were recorded. The created hypothesis presented one hydrogen bond acceptor, two hydrogen bond donors, and two aromatic rings, as presented in Figure 3b. Its ranking order and scoring value as represented in Table 2 clearly indicate that the two aromatic rings R10 and R11 create a hydrophobic environment and acceptor A2 and donor D4 and D6 groups participate in hydrogen bonding.

### Pharmacophore generation and 3D QSAR model analysis and validation

Phase version 3.4 presented the outcome for pharmacophore generation and atom-based 3D QSAR modelling. The activity

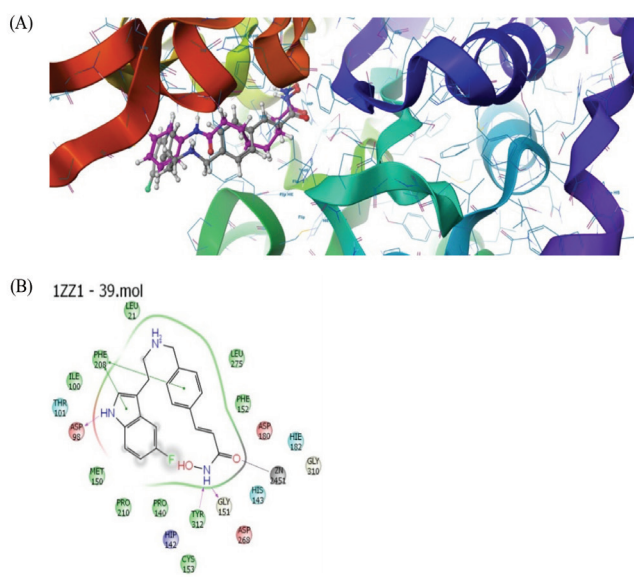


**Figure 2.** Docking pose of compound 39 complexing with 1ZZ1 protein (A) docking pose alignment showing crystal ligand SAHA (magenta) and docked ligand (white) (B) 2D interaction pattern of ligand with protein SAHA: Suberoylanilide hydroxamic acid

threshold was maintained at a range of 7.6 to 6.9, which divided the dataset into active, moderately active and inactive range. The dataset was further partitioned into training (38 molecules) and test (19 molecules) sets based on structural features and the range of biological activity. The five features containing CPHs were selected based on their high survival score to define the entire binding arena of the molecule as displayed in Figure 3a. The suitable 10 CPHs (Table 3) representing good scores (survival-inactive) were considered for 3D QSAR model design using 5 PLS factors.

**Table 2. Score of pharmacophoric features based on energetic terms of XP docking**

Feature label	Score (kcal/mol)	Score source
R12	-1.86	Ring chemscoreHPhobe
A3	-0.65	H-bond
D4	-0.51	H-bond
D5	-0.43	H-bond
R11	-0.65	Ring chemscoreHPhobe

XP: Extra precision

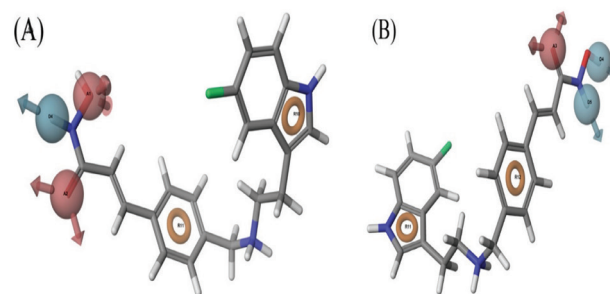


**Figure 3.** Pharmacophore hypothesis. Pharmacophore features elucidating hydrogen bond acceptor (A, pink), hydrogen bond donor (D, blue), and aromatic rings (R, brown) (A). Pharmacophore model AADRR.139 developed using the phase module (ligand-based approach). (B) Pharmacophore model ADDRR was developed using the e-pharmacophore script (ligand and structure based approaches)

**Table 3. Hypothesis score generated by phase**

Serial no.	Hypothesis	Survival	Survival-inactive	Post-hoc	Site	Vector	Volume	Matches
1	AADRR.139	3.44	1.546	3.44	0.79	0.946	0.704	7
2	ADRR.202	3.307	1.471	3.307	0.76	0.917	0.628	7
3	AADDR.209	3.435	1.601	3.435	0.76	0.934	0.743	7
4	AAAAR.175	3.521	1.67	3.521	0.83	0.921	0.786	7
5	AAADR.210	3.402	1.559	3.402	0.80	0.919	0.678	7
6	AADHR.205	3.450	1.566	3.450	0.78	0.944	0.721	7
7	AAADH.201	3.451	1.585	3.451	0.81	0.941	0.699	7
8	AADDH.192	3.41	1.644	3.41	0.78	0.935	0.695	7
9	AAARR.81	3.307	1.471	3.307	0.76	0.917	0.628	7
10	ADRR.207	3.518	1.694	3.518	0.82	0.934	0.762	7

CPH AADRR.139 executed best statistical conclusion for PLS factor 5, revealing  $Q^2$  (0.7142),  $R^2$  (0.9877), SD (0.1049), F (531.1), P (1.627e-030), root mean square deviation (RMSD) (0.4435), stability (0.4939), and pearson-r (0.8478) (Table 4). The scatter plots of actual vs predicted activity for training and test set compounds were plotted (Figure 4). The results showing comparison of predicted activity with their actual experimental activity was studied and is mentioned in Table 5.

The statistics and predictive ability ( $q^2$ ) of the model did not improve with an increase in the digit of PLS factors. The regression is carried out by creating a series of models with progressively more PLS components. When the number of PLS factors is increased, the model's accuracy improves until overfitting occurs. Although there is no limit to the number of PLS factors that can be added, in general, adding factors should be halted when the SD of the regression is roughly equivalent to the experimental error. This problem began to appear on models generated after PLS 5. At 5<sup>th</sup> PLS factor with the smallest SD of regression, statistical measures like  $R^2$  and  $q^2$  were also high (0.9877 and 0.7142, respectively). As a result, for the construction of our atom-based three-dimensional quantitative structure-activity relationship model, 5<sup>th</sup> SD of regression component was chosen.

### 3D QSAR model visualization

There are some essential features in the form of different colored cubes for each feature observed in QSAR visualization maps highlighting an active ligand-receptor interaction. These

features indicate the type and position of the attachment of functional groups for showing specific pharmacological activity. They also throw light on toxicity statement of ligands. The ligand 40 from the dataset, more specific from the training set, was carefully chosen as the template molecule for improved understanding of the study. The QSAR model made between hypothesis AADRR.139 and compound 40 is visualized in Figure 5.

The substitution of hydrogen atom of NH- and its adjacent  $-CH_2$  group by a hydrogen bond donating moiety increases the activity; similarly, replacement of hydrogen atom of OH of hydroxamic acid also displays an elevation in activity. Replacement of oxygen of hydroxamic acid by any H-bond donor leads to decrease in activity. The attachment of the hydrophobic group rather than H present at 4<sup>th</sup> position of the indoline ring leads to rise in activity. In addition, the substitution of hydrogen atoms of the ethylene moiety present in the linker also escalates the activity. Attachment of the hydrophobic group and an electron withdrawing group in the phenyl ring of linker causes a decline in activity. Substitution of the hydrogen of indoline nitrogen with electron withdrawing moiety increases the activity.

The outcome of these computational studies clearly indicate that among all compounds, higher fitness value and docking score, lesser toxicity, and superior drug properties and more complimentary conformation as compared to the original ligand has been shown by compound 39. Thus, ligand 39 can be considered as a possible lead moiety for the development of newer HDAC inhibitors.

**Table 4. Statistical result of the developed 3D QSAR model using AADRR.139 CPHs**

ID	PLS fact.	SD	R2	F	P	Stability	RMSE	Q2	Pearson-r
AADRR.139	1	0.4577	0.7381	104.3	2.578e-012	0.8691	0.3095	0.8609	0.9294
	2	0.2661	0.9139	191.1	6.764e-020	0.6313	0.3984	0.7694	0.8779
	3	0.1807	0.9614	290.5	8776e-025	0.5401	0.4271	0.7349	0.8601
	4	0.1372	0.9784	384.4	8.771e-028	0.5275	0.4596	0.6931	0.8337
	5	0.1049	0.9877	531.1	1.627e-030	0.4939	0.4435	0.7142	0.8478

QSAR: Quantitative structure activity relationship, CPH: Common pharmacophore hypothesis, PLS fact: Partial least squares factor, SD: Standard deviation,  $R^2$ : Multiple correlation coefficient between dependent and independent variable, F: Aromatic substituents electronic inductive effect, P: Partition coefficient, RMSE: Root mean squared error,  $Q^2$ : Predictive squared correlation coefficient, Pearson-r: Pearson correlation matrix

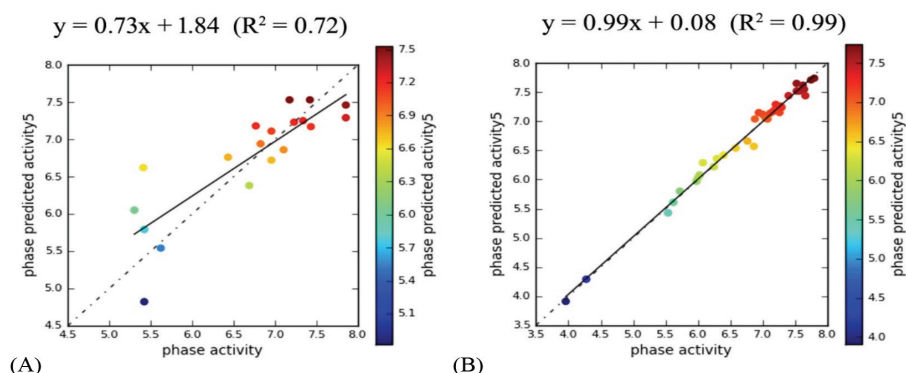


**Figure 4.** Test (A) and training (B) plots showing the observed activity versus the predicted activity for 3D QSAR models generated using AADRR.139 QSAR: Quantitative structure-activity relationship

**Table 5. Comparison between experimental and predicted activity along with fitness values of dataset ligands, which are obtained from the best generated atom based 3D-QSAR models AADRR.139**

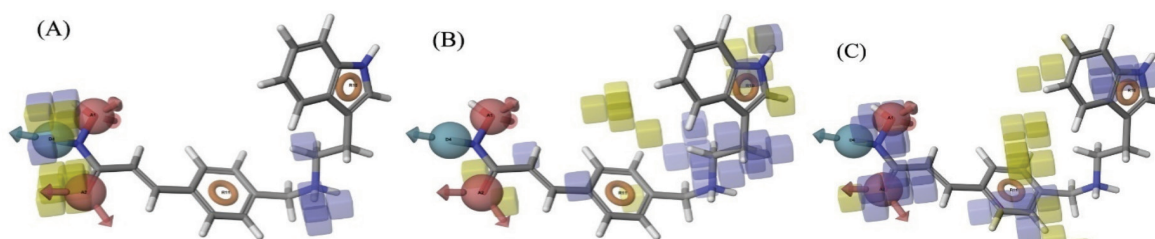
Lig. name	QSAR set	Experimental activity	Predicted activity 3D QSAR AADRR.139	Residual	Fitness	Pharma set
1	Training	7.208	7.04	0.168	1.94	+
2	Training	7.26	7.32	-0.06	1.87	+
3	Training	6.879	6.81	0.069	1.85	Inactive
4	Training	6.863	6.89	-0.027	2.24	Inactive
5	Training	7.658	7.50	0.158	1.98	Active
6	Training	7.745	7.86	-0.115	1.91	Active
7	Training	6.077	6.42	-0.343	1.8	Inactive
8	Training	7.268	7.18	0.088	1.85	+
9	Training	6.939	7.01	-0.071	1.91	+
10	Training	7.046	7.19	-0.144	2.39	+
11	Training	7.114	7.03	0.084	1.91	+
12	Test	6.767	7.05	-0.283	2.29	Inactive
13	Training	6.395	6.43	-0.035	1.87	Inactive
14	Training	6.292	6.31	-0.018	1.8	Inactive
15	Test	6.955	6.77	0.185	1.81	+
16	Training	7.027	7.11	-0.083	2.17	+
17	Test	5.42	5.26	0.16	1.38	Inactive
18	Test	5.42	5.33	0.09	1.39	Inactive
19	Training	5.62	5.88	-0.26	1.67	Inactive
20	Test	5.409	5.84	-0.431	1.66	Inactive
21	Training	5.721	5.43	.0291	1.38	Inactive
22	Training	5.538	5.51	0.028	1.38	Inactive
23	Test	5.62	5.52	0.10	1.37	Inactive
24	Training	7	7.16	-0.16	1.43	+
25	Training	6	6.03	-0.03	1.47	Inactive
26	Test	5.301	5.79	-0.489	1.13	Inactive
27	Training	4.276	4.37	-0.094	1.37	Inactive
28	Training	3.959	4.00	-0.041	1.32	Inactive
29	Training	6.764	6.57	0.194	1.62	Inactive
30	Test	6.688	6.47	0.218	1.78	Inactive
31	Test	6.432	6.27	0.162	1.67	Inactive
32	Training	6.026	6.05	-0.024	1.76	Inactive
33	Training	6.245	6.14	0.105	1.68	Inactive
34	Training	7.523	7.43	0.093	2.3	+
35	Training	7.18	7.20	-0.02	2.83	+
36	Training	7.638	7.44	0.198	2.93	Active
37	Training	7.796	7.80	-0.004	2.73	Active



Table 5. continued

Lig. name	QSAR set	Experimental activity	Predicted activity	Residual	Fitness	Pharma set
			3D QSAR AADRR.139			
38	Training	7.076	7.23	-0.154	2.84	+
39	Test	7.854	7.47	0.384	3.00	Active
40	Training	7.201	7.44	-0.239	2.94	+
41	Training	7.62	7.56	0.06	2.43	Active
42	Test	7.432	7.23	0.202	1.75	+
43	Test	7.174	7.11	0.064	2.4	+
44	Training	7.523	7.58	-0.057	2.31	+
45	Test	7.337	7.26	0.077	2.27	+
46	Test	7.854	7.48	0.374	2.78	Active
47	Training	7.398	7.48	-0.082	2.64	+
48	Test	6.824	7.19	-0.366	2.13	Inactive
49	Training	7.569	7.54	0.029	2.13	+
50	Training	6.582	6.53	0.052	1.97	Inactive
51	Training	7.292	7.27	0.022	1.72	+
52	Training	7.276	7.12	0.156	2.19	+
53	Test	7.102	6.90	0.202	2.04	+
54	Training	7.161	7.07	0.091	2.41	+
55	Test	6.955	7.16	-0.205	2.41	+
56	Test	7.229	7.15	0.079	2.33	+
57	Test	7.42	7.50	-0.08	2.87	+

+ represents moderately active compounds, QSAR: Quantitative structure-activity relationship



**Figure 5.** Visualization of QSAR models generated using hypotheses AADRR.139 for various substituent groups (A) H-bond donor (B) hydrophobic/non-polar (C) electron withdrawing. Blue cubes indicate favorable regions, whereas yellow cubes indicate unfavorable regions for the activity

QSAR: Quantitative structure-activity relationship

## CONCLUSION

HDAC inhibitors, a newer addition to chemotherapy, have been found to play a crucial role in the treatment of cancer. HDAC inhibitors are scarcely available on the market. The computational study performed on hydroxamic acid-based derivatives of the dataset exhibited a convincing outcome.

The various computational studies such as pharmacophore and atom-based 3D-QSAR, molecular docking (XP and SP),

and energetic-based pharmacophore mapping effectively established a correlation between the structure of ligands with their predicted biological activity. Both ligand- and structure-based pharmacophore mapping approaches in combination efficiently forecasted this correlation and would be helpful in the design and development of novel HDAC inhibitors as anticancer agents. Moreover, they may also help in designing novel ligands more accurately. The molecular docking study showed maximum

structural similarity of compound 39 with that of reference HDAC inhibitor (SAHA). It revealed the crucial intermolecular interactions between the ligand moieties and amino acids in the target protein. The created 3D QSAR pharmacophore model exhibited exceptional regression coefficient standards for the training set, with  $Q^2$ : 0.7142,  $R^2$ : 0.9877, and low RMSD: 0.4435. It is expected that the findings of these investigations will be used to develop new structural analogs of substituted phenyl hydroxamide derivatives with anticancer activity.

#### Ethics

**Ethics Committee Approval:** Not applicable.

**Informed Consent:** Not applicable.

**Peer-review:** Externally peer-reviewed.

#### Authorship Contributions

Concept: E.S., H.R., Design: E.S., R.V., H.R., Data Collection or Processing: E.S., Analysis or Interpretation: E.S., V.K.P., R.V., H. R., Literature Search: E.S., J.P., Writing: E.S.

**Conflict of Interest:** No conflict of interest was declared by the authors.

**Financial Disclosure:** The first author is grateful to DST, New Delhi for providing financial assistance to the author through Inspire Fellowship Program (IF210097). The corresponding author is thankful to the Indian Council of Medical Research (ICMR, New Delhi) for providing financial support in the form of Extra-Mural research project (grant no: 58/33/2020/PHA/BMS).

## REFERENCES

- Understanding chemotherapy. Accessed: 19 November 2021. Available from: [http://www.cancer.net/navigating-cancer-care/how-cancer-treated/chemotherapy/understanding-chemotherapy&sa=U&ved\\_](http://www.cancer.net/navigating-cancer-care/how-cancer-treated/chemotherapy/understanding-chemotherapy&sa=U&ved_)
- Wu Q, Yang Z, Nie Y, Shi Y, Fan D. Multi-drug resistance in cancer chemotherapeutics: mechanisms and lab approaches. *Cancer Lett.* 2014;347:159-166.
- Lu W, Wang F, Zhang T, Dong J, Gao H, Su P, Shi Y, Zhang J. Search for novel histone deacetylase inhibitors. Part II: design and synthesis of novel isoferulic acid derivatives. *Bioorg Med Chem.* 2014;22:2707-2713.
- Mohamed MFA, Shaykoon MSA, Abdelrahman MH, Elsadek BEM, Aboaraia AS, Abuo-Rahma GEAA. Design, synthesis, docking studies and biological evaluation of novel chalcone derivatives as potential histone deacetylase inhibitors. *Bioorg Chem.* 2017;72:32-41.
- Rajak H, Singh A, Raghuvanshi K, Kumar R, Dewangan PK, Veerasamy R, Sharma PC, Dixit A, Mishra P. A structural insight into hydroxamic acid based histone deacetylase inhibitors for the presence of anticancer activity. *Curr Med Chem.* 2014;21:2642-2664.
- Patel P, Singh A, Patel VK, Jain DK, Veerasamy R, Rajak H. Pharmacophore based 3D-QSAR, virtual screening and docking studies on novel series of HDAC inhibitors with thiophen linker as anticancer agents. *Comb Chem High Throughput Screen.* 2016;19:735-751.
- Witt O, Deubzer HE, Milde T, Oehme I. HDAC family: What are the cancer relevant targets? *Cancer Lett.* 2009;277:8-21.
- Haberland M, Montgomery RL, Olson EN. The many roles of histone deacetylases in development and physiology: implications for disease and therapy. *Nat Rev Genet.* 2009;10:32-42.
- Dawson MA, Kouzarides T. Cancer epigenetics: from mechanism to therapy. *Cell.* 2012;150:12-27.
- Xie R, Li Y, Tang P, Yuan Q. Design, synthesis and biological evaluation of novel 2-aminobenzamides containing dithiocarbamate moiety as histone deacetylase inhibitors and potent antitumor agents. *Eur J Med Chem.* 2018;143:320-333.
- Ramaiah MJ, Tangatur AD, Manyam RR. Epigenetic modulation and understanding of HDAC inhibitors in cancer therapy. *Life Sci.* 2021;277:119504.
- Hieu DT, Anh DT, Tuan NM, Hai PT, Huong LT, Kim J, Kang JS, Vu TK, Dung PTP, Han SB, Nam NH, Hoa ND. Design, synthesis and evaluation of novel *N*-hydroxybenzamides/*N*-hydroxypropenamides incorporating quinazolin-4(3H)-ones as histone deacetylase inhibitors and antitumor agents. *Bioorg Chem.* 2018;76:258-267.
- Yu C, He F, Qu Y, Zhang Q, Lv J, Zhang X, Xu A, Miao P, Wu J. Structure optimization and preliminary bioactivity evaluation of *N*-hydroxybenzamide-based HDAC inhibitors with Y-shaped cap. *Bioorg Med Chem.* 2018;26:1859-1868.
- Brindisi M, Senger J, Cavella C, Grillo A, Chemi G, Gemma S, Cucinella DM, Lamponi S, Sarno F, Iside C, Nebbioso A, Novellino E, Shaik TB, Romier C, Herp D, Jung M, Butini S, Campiani G, Altucci L, Brogi S. Novel spiroindoline HDAC inhibitors: synthesis, molecular modelling and biological studies. *Eur J Med Chem.* 2018;157:127-138.
- Guha M. HDAC inhibitors still need a home run, despite recent approval. *Nat Rev Drug Discov.* 2015;14:225-226. Erratum in: *Nat Rev Drug Discov.* 2015;14:365.
- Wang D. Computational studies on the histone deacetylases and the design of selective histone deacetylase inhibitors. *Curr Top Med Chem.* 2009;9:241-256.
- Kim HM, Hong SH, Kim MS, Lee CW, Kang JS, Lee K, Park SK, Han JW, Lee HY, Choi Y, Kwon HJ, Han G. Modification of cap group in delta-lactam-based histone deacetylase (HDAC) inhibitors. *Bioorg Med Chem Lett.* 2007;17:6234-6238.
- Hamblett CL, Methot JL, Mampreian DM, Sloman DL, Stanton MG, Kral AM, Fleming JC, Cruz JC, Chenard M, Ozerova N, Hitz AM, Wang H, Deshmukh SV, Nazef N, Harsch A, Hughes B, Dahlberg WK, Szewczak AA, Middleton RE, Mosley RT, Secrist JP, Miller TA. The discovery of 6-amino nicotinamides as potent and selective histone deacetylase inhibitors. *Bioorg Med Chem Lett.* 2007;17:5300-5309.
- Estiu G, Greenberg E, Harrison CB, Kwiatkowski NP, Mazitschek R, Bradner JE, Wiest O. Structural origin of selectivity in class II-selective histone deacetylase inhibitors. *J Med Chem.* 2008;51:2898-2906.
- Huhtiniemi T, Wittekindt C, Laitinen T, Leppänen J, Salminen A, Poso A, Lahtela-Kakkonen M. Comparative and pharmacophore model for deacetylase SIRT1. *J Comput Aided Mol Des.* 2006;20:589-599.
- Xie A, Liao C, Li Z, Ning Z, Hu W, Lu X, Shi L, Zhou J. Quantitative structure-activity relationship study of histone deacetylase inhibitors. *Curr Med Chem Anticancer Agents.* 2004;4:273-299.
- Chen YD, Jiang YJ, Zhou JW, Yu QS, You QD. Identification of ligand features essential for HDACs inhibitors by pharmacophore modeling. *J Mol Graph Model.* 2008;26:1160-1168.
- Ragno R, Simeoni S, Rotili D, Caroli A, Botta G, Brosch G, Massa S, Mai A. Class II-selective histone deacetylase inhibitors. Part 2: alignment-independent GRIND 3-D QSAR, homology and docking studies. *Eur J Med Chem.* 2008;43:621-632.

24. Jayaraj JM, Krishnasamy G, Lee JK, Muthusamy K. *In silico* identification and screening of CYP24A1 inhibitors: 3D QSAR pharmacophore mapping and molecular dynamics analysis. *J Biomol Struct Dyn*. 2019;37:1700-1714.
25. Vora J, Patel S, Sinha S, Sharma S, Srivastava A, Chhabria M, Shrivastava N. Structure based virtual screening, 3D-QSAR, molecular dynamics and ADMET studies for selection of natural inhibitors against structural and non-structural targets of Chikungunya. *J Biomol Struct Dyn*. 2019;37:3150-3161.
26. Gao Y, Wang H, Wang J, Cheng M. *In silico* studies on p21-activated kinase 4 inhibitors: comprehensive application of 3D-QSAR analysis, molecular docking, molecular dynamics simulations, and MM-GBSA calculation. *J Biomol Struct Dyn*. 2020;38:4119-4133.
27. Shirbhate E, Divya, Patel P, Patel VK, Veerasamy R, Sharma PC, Rajak H. Searching for potential HDAC2 inhibitors: structure-activity relationship studies on indole-based hydroxamic acids as an anticancer agent. *Lett Drug Des Discov*. 2020;19:905-917.
28. Roy K, Das RN, Ambure P, Aher RB. Be aware of error measures. Further studies on validation of predictive QSAR models. *Chemom Intell Lab Syst*. 2016;152:18-33.
29. Kim DK, Lee JY, Kim JS, Ryu JH, Choi JY, Lee JW, Im GJ, Kim TK, Seo JW, Park HJ, Yoo J, Park JH, Kim TY, Bang YJ. Synthesis and biological evaluation of 3-(4-substituted-phenyl)-*N*-hydroxy-2-propenamides, a new class of histone deacetylase inhibitors. *J Med Chem*. 2003;46:5745-5751.
30. Miller TA, Witter DJ, Belvedere S. Histone deacetylase inhibitors. *J Med Chem*. 2003;46:5097-5116.
31. Remiszewski SW, Sambucetti LC, Bair KW, Bontempo J, Cesarz D, Chandramouli N, Chen R, Cheung M, Cornell-Kennon S, Dean K, Diamantidis G, France D, Green MA, Howell KL, Kashi R, Kwon P, Lassota P, Martin MS, Mou Y, Perez LB, Sharma S, Smith T, Sorensen E, Taplin F, Trogani N, Versace R, Walker H, Weltchek-Engler S, Wood A, Wu A, Atadja P. *N*-Hydroxy-3-phenyl-2-propenamides as novel inhibitors of human histone deacetylase with *in vivo* antitumor activity: discovery of (2*E*)-*N*-hydroxy-3-[4-[(2-hydroxyethyl)[2-(1*H*-indol-3-yl)ethyl]amino]methyl]phenyl]-2-propenamide (NVP-LAQ824). *J Med Chem*. 2003;46:4609-4624.
32. Hou J, Feng C, Li Z, Fang Q, Wang H, Gu G, Shi Y, Liu P, Xu F, Yin Z, Shen J, Wang P. Structure-based optimization of click-based histone deacetylase inhibitors. *Eur J Med Chem*. 2011;46:3190-3200.
33. Patel P, Patel VK, Singh A, Jawaid T, Kamal M, Rajak H. Identification of hydroxamic acid based selective HDAC1 inhibitors: computer aided drug design studies. *Curr Comput Aided Drug Des*. 2019;15:145-166.
34. Protein preparation wizard, Schrodinger, 2012, LLC, New York. Accessed: 19 November, 2021. Available from: <https://www.schrodinger.com/science-articles/protein-preparation-wizard>
35. Patel VK, Chouhan KS, Singh A, Jain DK, Veerasamy R, Singour PK, Pawar RS, Rajak H. Development of structure activity correlation model on azetidine-2-ones as tubulin polymerization inhibitors. *Lett Drug Des Discov*. 2015;12:351-365.
36. Jorgensen WL, Maxwell DS, Tirado-Rives J. Development and testing of the OPLS all-atom force field on conformational energetics and properties of organic liquids. *J Am Chem Soc*. 1996;118:11225-11236.
37. Ligprep v 2.5, Schrodinger, 2012, LLC, New York. Accessed: 19 November, 2021. Available from: <https://www.schrodinger.com/products/ligprep>
38. Kakarala KK, Jamil K, Devaraji V. Structure and putative signaling mechanism of protease activated receptor 2 (PAR2) - a promising target for breast cancer. *J Mol Graph Model*. 2014;53:179-199.
39. Vijayakumar S, Manogar P, Prabhu S, Pugazhenthii M, Praseetha PK. A pharmacoinformatic approach on cannabinoid receptor 2 (CB2) and different small molecules: homology modelling, molecular docking, MD simulations, drug designing and ADME analysis. *Comput Biol Chem*. 2019;78:95-107.
40. Glide, version 5.8, Schrodinger, 2016, LLC, New York. Accessed: 19 November, 2021. Available from: <https://www.schrodinger.com/products/gleide>
41. Liu J, Zhu Y, He Y, Zhu H, Gao Y, Li Z, Zhu J, Sun X, Fang F, Wen H, Li W. Combined pharmacophore modeling, 3D-QSAR and docking studies to identify novel HDAC inhibitors using drug repurposing. *J Biomol Struct Dyn*. 2020;38:533-547.
42. Scafuri B, Bontempo P, Altucci L, De Masi L, Facchiano A. Molecular docking simulations on histone deacetylases (HDAC)-1 and -2 to investigate the flavone binding. *Biomedicines*. 2020;8:568.
43. Ukey S, Choudhury C, Sharma P. Identification of unique subtype-specific interaction features in class II zinc-dependent HDAC subtype binding pockets: a computational study. *J Biosci*. 2021;46:71.
44. Liu J, Zhou J, He F, Gao L, Wen Y, Gao L, Wang P, Kang D, Hu L. Design, synthesis and biological evaluation of novel indazole-based derivatives as potent HDAC inhibitors *via* fragment-based virtual screening. *Eur J Med Chem*. 2020;192:112189.
45. Salam NK, Nuti R, Sherman W. Novel method for generating structure-based pharmacophores using energetic analysis. *J Chem Inf Model*. 2009;49:2356-2368.
46. Dixon SL, Smondryev AM, Rao SN. PHASE: a novel approach to pharmacophore modeling and 3D database searching. *Chem Biol Drug Des*. 2006;67:370-372.
47. Watts KS, Dalal P, Murphy RB, Sherman W, Friesner RA, Shelley JC. ConfGen: a conformational search method for efficient generation of bioactive conformers. *J Chem Inf Model*. 2010;50:534-546.
48. Dixon SL, Smondryev AM, Knoll EH, Rao SN, Shaw DE, Friesner RA. PHASE: a new engine for pharmacophore perception, 3D QSAR model development, and 3D database screening: 1. Methodology and preliminary results. *J Comput Aided Mol Des*. 2006;20:647-671.
49. Golbraikh A, Tropsha A. Predictive QSAR modeling based on diversity sampling of experimental datasets for the training and test set selection. *J Comput Aided Mol Des*. 2002;16:357-369.
50. Ruzic D, Djokovic N, Nikolic K. Fragment-based drug design of selective HDAC6 inhibitors. *Methods Mol Biol*. 2021;2266:155-170.
51. Abdizadeh R, Hadizadeh F, Abdizadeh T. QSAR analysis of coumarin-based benzamides as histone deacetylase inhibitors using CoMFA, CoMSIA and HQSAR methods. *J Mol Struct*. 2019;1199:126961.